THE REGULATORS AND BIOLOGICAL ROLES OF THE UNFOLDED PROTEIN RESPONSE IN *ARABIDOPSIS THALIANA*

By

YA-NI CHEN

A DISSERTATION

Submitted to
Michigan State University
in partial fulfillment of requirements
for the degree of

Plant Biology – Doctor of Philosophy

2013

ABSTRACT

THE REGULATORS AND BIOLOGICAL ROLES OF THE UNFOLDED PROTEIN RESPONSE IN *ARABIDOPSIS THALIANA*

By

YA-NI CHEN

The secretory pathway is fundamental for majority of cellular responses in eukaryotes. Most secretory proteins are folded and modified in the endoplasmic reticulum (ER). Thus, the ER is critical for operation of the secretory pathway. To adjust protein-folding capacity in the ER, eukaryotic cells activate intra-cellular signaling pathways termed the unfolded protein response (UPR). The UPR is triggered by stress sensors to respond the accumulation of unfolded proteins in the ER, a cellular condition referring to ER stress. To identify the plant UPR regulators, I performed mutant analyses of a conserved ER stress sensor IRE1 in *Arabidopsis*. I established that IRE1 is a functional ER stress sensor in plants. By showing that an *ire1* mutant displays a short-root phenotype under normal growth conditions, I revealed a biological function of plant IRE1 in multicellular organisms. In addition, I found that a mutant of a component of G-protein complex, AGB1, enhances both the ER stress-sensitive and the short-root phenotype in *ire1*, suggesting that regulation of AGB1 on the UPR does not completely rely on IRE1. I further investigated regulatory relationship between the UPR and other cellular processes. Auxin is a major phytohormone essential for plant physiology. I found that ER stress down-regulates the transcription of auxin receptors and transporters, suggesting that ER stress represses the auxin response to coordinate stress adaption and growth regulation. By establishing that ER-localized auxin transporters and regulators are required for optimal UPR activation, I uncovered a

previously unknown cellular function of ER-based auxin biology. The results also support the suggestion that regulation on auxin homeostasis is a plant-specific strategy to cope with ER stress. Moreover, I showed that *ire1* displays a compromised root-inhibition phenotype under exogenous auxin treatment, indicating that IRE1 is required for the auxin response. The free auxin level is lower in *ire1*, supporting a role of IRE1 in regulation of the auxin homeostasis. I further examined the functional relationship between IRE1 and an ER-localized auxin transporter, PIN5. I found that *pin5* enhances the defects of both the auxin response and the UPR activation in *ire1*. Together, my results have established the inter-regulation of the UPR and auxin signaling. In summary, my work has identified a conserved ER stress sensor IRE1 and previously unknown UPR mediators, ER-localized auxin regulators. By examination of the regulatory relationship between IRE1 and AGB1 or PIN5, my results contribute to important understanding of the plant UPR signaling network. I have also uncovered biological roles of plant IRE1 in primary root growth and auxin homeostasis. Thus, I have provided significant insights into regulators and physiological significance of the plant UPR.

DEDICATION

To my parents and my husband, Kyaw Aung,
whose love and support sustained me through this journey.

ACKNOWLEDGMENTS

I would like to thank my mentor, Dr. Federica Brandizzi, for her tremendous support over the years. Federica provided me so many wonderful opportunities and trainings to become a better researcher. Right at the beginning, she gave me full trust and generous resources to explore my projects independently. Whenever I need her advices, she is always happy to help with full patience as well as passion. Because of her faith in me, I started to believe in myself. I am extremely grateful for such a valuable journey in her lab.

I would also like to thank my committee, Dr. Gregg Howe, Dr. Rob Last, and Dr. Shin-Han Shiu for their constructive advices and encouraging guidance. Whenever there is challenge in my research life, I always look up to them to retain my original intention to be a scientist. I especially like to thank Shin-Han and his wife, Melissa Lehti-Shiu, for their continual support and encouragement.

I would like to acknowledge current and past members of the Brandizzi lab. I have learned incredibly by working with each of them. It is truly an influential and important experience for me. I especially like to thank Giovanni Stefano and Kathryn Walicki for their wonderful help in my research projects.

I am also very grateful for pursuit of my graduate study at MUS especially the Plant Research Laboratory. It is such a fantastic and cooperative research environment. I am truly honored to be a part of this community. I would like to thank all the friends and colleagues for their helpfulness and support.

Most importantly, if I have conquered any challenge in this journey, it is all because I have my families and my husband, who always watch over me. I could never ever thank them enough for what they have given to me.

TABLE OF CONTENTS

LIST OF TABLES

LIST OF FIGURES

KEY TO ABBREVIATIONS

35S	Cauliflower Mosaic Virus 35S promoter
ABA	Abscisic acid
ABRC	*Arabidopsis* Biological Resource Center
ACC	1-aminocyclopropane-1-carboxylic acid
AGB1	Guanine nucleotide-binding protein subunit beta
At	*Arabidopsis thaliana*
ATF4	Activating transcription factor 4
ATF6	Activating transcription factor 6
BiP	Immunoglobulin binding protein
bZIP	Basic leucine zipper
CASP2	Caspase-2
C.elegans	*Caenorhabditis elegans*
CHOP	CCAAT enhancer-binding protein homology protein
Col-0	Columbia-0
CRT	Calreticulin
C-terminus	Carboxyl-terminus
DNA	Deoxyribonucleic acid
DR5	Auxin responsive element
DTT	Dithiothreitol
eIF2α	Eukaryotic initiation factor 2α
ER	Endoplasmic reticulum

GFP	Green fluorescent protein
G-protein	GTP-binding protein
GTP	Guanosine-5’-triphosphate
H	Hours
IAA	Indole-3-acetic acid
IRE1	Inositol-requiring enzyme 1
JA	Jasmonic acid
JNK	C-Jun N-terminal kinase
MEFs	Mouse embryonic fibroblasts
MiRs	MicroRNAs
mRNA	Messenger RNA
MUC2	Mucin2
N-linked	Asparagine-linked
N-terminus	Amine-terminus
PCR	Polymerase chain reaction
PERK	Protein kinase R-like ER kinase
qRT-PCR	Quantitative reverse transcriptase PCR
RIDD	Regulated IRE1-Dependent Decay
RNA	Ribonucelic acid
RNase	Ribonuclease
SDS	Sodium dodecyl sulfate
SDS-PAGE	SDS-polyacrylamide gel electrophoresis
TIR1	Transport inhibitor response 1

TXNIP	Thioredoxin interacting protein
UBQ	Ubiquitin
UPR	Unfolded protein response
XBP-1	X-box binding protein 1
YFP	Yellow fluorescent protein

CHAPTER 1

Literature review

The unfolded protein response

Introduction

Approximately one-third of the eukaryotic proteome is synthesized in the secretory pathway. Most secretory proteins first enter the endoplasmic reticulum (ER) for folding and maturation. The ER can sense an imbalance between demand and capacity of secretory protein synthesis. To increase protein-folding capacity in the ER, cells invoke protective signaling pathways known as the unfolded protein response (UPR) [1, 2]. The UPR is triggered by stress sensors to respond the accumulation of unfolded proteins in the ER, a cellular condition referring to ER stress. The initial response of the UPR aims to rebalance the protein-folding homeostasis in the ER. If cells fail to recover from ER stress, the UPR triggers apoptosis on irremediable ER stress [3-8].

The ER quality control system

The ER is a specialized sub-cellular compartment for protein folding and modification. Because the ER has many unique features, including an oxidizing environment and abundance of protein-folding enzymes, certain important protein modifications only occur at the ER. The fidelity of protein functions relies on the precise protein modifications and conformation. Unfolded or misfolded proteins are not only nonfunctional, but they could be harmful for cells. To ensure that only properly modified and folded proteins exit from the ER, eukaryotic cells operate a robust system termed the ER quality control to scrutinize processes of protein maturation and transportation [6,

7, 9-12]. One major component of the ER quality control system is molecular chaperones. Molecular chaperones not only contribute to protein folding; they are also important in recognition of proteins that fail to be folded or modified. Once proteins are recognized for degradation, they are relocated back to the cytosol, tagged with ubiquitin, and degraded by an ER-associated degradation system [6, 7, 9-12].

Activation of the UPR

If the ER quality control system is sufficient to support the demand of protein folding in the ER, activation status of the UPR is relatively low. By contrast, certain physiological or environmental conditions can overwhelm the ER quality control system. To rebalance the protein-folding homeostasis, eukaryotic cells activate the UPR to increase the capacity of the ER quality control system. The UPR is triggered by an overload of unfolded proteins in the ER mediated by ER stress sensors [7, 9, 10, 13-15]. ER stress sensors are ER transmembrane proteins with a stress-sensing domain facing the ER lumen and enzymatic domains facing the cytosol. When levels of unfolded proteins are relatively low at the ER, the activity of ER stress sensors is restricted through physical association with BiP, the most abundant ER-resident chaperone. Dissociation with BiP or interaction with unfolded proteins is an important mechanism to activate ER stress sensors [16].

ER stress sensors

Inositol-requiring enzyme 1 (IRE1) is the most conserved ER stress sensor in eukaryotes [17, 18]. IRE1 is a type I membrane protein, consisting of a stress-sensing domain at the N-terminus as well as a kinase and an endoribonuclease domain at the C-terminus. Upon sensing an accumulation of unfolded proteins in the ER, the endoribonuclease domain of IRE1 is activated through trans-autophosphorylation and oligomerization. Active IRE1 unconventionally splices an intron of a transcription factor, *HAC1* in yeast [19] and *XBP-1* in animals [20]. To recover protein-folding capacity in the ER, the spliced transcription factors induce the expression of UPR target genes, which encode protein involved in assisting protein folding and degrading misfolded protein [19, 21]. To manage more complex UPR signaling, animal cells adopt the IRE1, the PKR-like ER kinase (PERK), and the activating transcription factor 6 (ATF6) regulatory pathways [22]. Like IRE1, PERK and ATF6 have a luminal stress-sensing domain and a cytosolic enzymatic domain that initiates downstream responses. PERK mediates the UPR by repression of protein synthesis through phosphorylation of eukaryotic initiation factor 2α (eIF2α) [23]. ATF6 is a membrane-tethered transcription factor. To activate the UPR, ATF6 is translocated to the Golgi and its transcriptional activation domain is released from the membrane by proteolytic cleavage. The released domain enters the nucleus to regulate UPR target genes [24]. It is undetermined that PERK homologs or inhibition of protein synthesis on ER stress exist in plants. By contrast, *Arabidopsis* genome encodes two sequence homologs of IRE1, IRE1A (At2g17520) and IRE1B (At5g24360) [25]. It was reported that the stress-sensing domain of *Arabidopsis* IRE1A or IRE1B functionally replaces that of yeast IRE1 to activate the UPR in yeast [25]. Also,

auto-phosphorylation activity of IRE1A was shown *in vitro* [26]. These observations hint that plant IRE1 also regulates UPR signaling. Furthermore, bZIP17 and bZIP28 are two functional homologs of AFT6 in plants. In addition of UPR, bZIP17 and bZIP28 regulate salt stress and heat stress [27].

Biological roles of the UPR

The UPR is essential for stress adaption and physiological regulation. The mammalian UPR is required for many fundamental biological processes. One of the most intensively studied fields is contribution of the UPR in professional secretory cells. In mammalian cells, individual UPR arm plays specific roles in regulation of professional secretory cells [28]. The IRE1α-XBP-1 UPR arm supports the high demand of secretory protein production when B lymphocytes differentiated into plasma cells [29]. IRE1β regulates the expression of Mucin2 (MUC2), the most prominent protein secreted from goblet cells [30]. These observations indicate the significance of mammalian IRE1-dependent UPR in professional secretory cells. In addition, PERK is important for proinsulin synthesis and insulin secretion [31]. The mammalian UPR is also essential for regulation of metabolism, cardiovascular development, immune responses, and sterol homeostasis By contrast, our knowledge of the plant UPR has relatively more restricted to stress adaption [27]. Biological roles of the plant UPR are still largely unexplored. The further characterization of regulatory relationships between the plant UPR and other cellular processes will not only uncover plant-specific features of the UPR, but also reveal the evolutional significance of the UPR in multicellular organisms.

Significance of the plant UPR

Yeast**,** plants, and animals share conserved components of the UPR. Compared to the UPR studies in yeast and animals, our knowledge of the plant UPR is still in its infants. Nevertheless, *Arabidopsis* is one of idealist model systems to enable *in vivo* UPR studies using intact organisms. Also, functional relationships between UPR transducers are more easily examined under physiological conditions in plants. Thus, the plant UPR research is valuable for understanding of essential regulation on the secretory pathway in eukaryotes. Moreover, organism-specific features of secretory pathway also exist in plants. Plants have evolved unique molecular mechanisms to coordinate the UPR signaling network. Thus, to gain more comprehensive understanding of the plant UPR, it is necessary to explore the molecular mechanisms and biological roles of the UPR using plants as a model system.

CHAPTER 2

Literature review

IRE1: ER stress sensor and cell fate executor

This section has been previously published in *Trends in Cell Biology*

YA-NI CHEN and FEDERICA BRANDIZZI (2013)

Trends in Cell Biology **23**:2547-555

Introduction

Cells operate a signaling network termed the unfolded protein response (UPR) to monitor protein-folding capacity in the endoplasmic reticulum (ER). IRE1 is an ER transmembrane sensor that activates the UPR to maintain ER and cellular function. Inositol-requiring enzyme (IRE1) is the only identified ER stress sensor in yeast and essential for the UPR in animals and plants [37-40] (Figure 2.1). As an ER transmembrane protein, IRE1 monitors ER homeostasis through an ER luminal stress-sensing domain and triggers the UPR through a cytoplasmic kinase domain and an RNase domain [37, 38]. On ER stress, IRE1 RNase is activated through conformational change, autophosphorylation, and higher order oligomerization [41-43]. Mammalian IRE1 initiates diverse downstream signaling of the UPR either through unconventional splicing of the transcription factor *Xbp-1* or and through posttranscriptional modifications via Regulated IRE1-Dependent Decay (RIDD) of multiple substrates [37, 38, 44-47]. In addition, PERK and ATF6 function as two distinct mammalian ER stress sensors to cope with complex UPR scenarios [14, 48] (Figure 2.1). Similar to IRE1, PERK and ATF6 are ER transmembrane proteins that contain an ER luminal stress-sensing domain and a cytoplasmic enzymatic domain. To prevent a further increase in protein-folding demand in the ER, PERK transiently inhibits general protein translation through phosphorylation of eukaryotic initiation factor 2 alpha (eIF2α). Phosphorylated eIF2α can also selectively activate translation of mRNAs including ATF4 transcription factor to regulate UPR target genes [49]. ER stress triggers relocation of ATF6 from the ER to the Golgi where it undergoes proteolytic cleavage. The cleaved transcription factor domain of ATF6 enters the nucleus for UPR regulation [36, 50, 51] (Figure 2.1).

The main molecular mechanisms underlying IRE1 unconventional splicing are conserved in eukaryotes. In budding yeast, mammals, and plants, there is only one transcription factor identified as a splicing target of IRE1 (Figure 2.1). The stem-loop structure and cleavage site of the IRE1 splicing substrate are conserved among species. By contrast, RIDD appears more divergent in eukaryotes. Among yeast, RIDD operates in fission yeast *Schizosaccharomyces pombe*, but not in budding yeast *Saccharomyces cerevisiae* [52]. Intriguingly, RIDD-mediated decrease in protein-folding demand is the only identified mechanism of UPR in fission yeast [52]. Although plant RIDD may potentially degrade a significant portion of mRNAs encoding secretory proteins [53], it is undetermined whether plant RIDD processes various substrates to direct UPR outputs like mammalian RIDD. Unlike the mammalian UPR, plant PERK orthologs remain to be identified; however, two functional homologs of ATF6, bZIP28 and bZIP17, exist in plants [27] (Figure 2.1). Moreover, a component of G-protein complex, AGB1, is essential for the plant UPR [39] and an alternative G-protein-coupled receptor is involved in non-canonical UPR in *Caneorhabditis elegans* [54]. Due to the large number of members of the mammalian G-protein complex, its roles in the classical UPR may be more challenging to reveal. While the IRE1 and ATF6 arms are partially conserved between plants and animals, it will be interesting to establish the degree of UPR diversification between the two kingdoms.

This chapter presents the latest advances and viewpoints on IRE1-dependent UPR research. I focus on the recent groundbreaking discoveries that define IRE1 as a master regulator in cell fate determination on ER stress. IRE1 was long considered as a positive regulator of cell survival. Thus, the repression of IRE1 was believed to

potentiate apoptosis. The recent identification of novel IRE1 regulatory events reveals that IRE1 signaling is persistent during ER stress. Namely, IRE1 can no longer be considered simply as a driving force for cell survival, but rather as an administrator/executor of cell fate determination on ER stress. Through presentation of the recent evidence establishing that IRE1 triggers diverse signaling, we delineate current IRE1-signaling models. It has also become clear that IRE1 monitors cellular homeostasis beyond protein-folding status in the ER; therefore, the functional relevance of the UPR within physiological processes will be discussed. Finally, we compare convergent and divergent features of IRE1 between plants and mammals to provide an integrated view of IRE1 in multicellular eukaryotes.

IRE1 signaling in cell fate determination

Life-versus-death determination is constantly scrutinized and tightly controlled. The prevalence of malfunctioning cells due to irremediable ER stress contributes to significant diseases, including cancer and diabetes. Conversely, overcommitment to cell death may result in organ damage or cell-degenerative diseases [55-59]. To reach optimal fitness under ER stress, cell fates are determined through tight coordination of adaptive and apoptotic responses [57, 60, 61]. In mammals, PERK-eIF2α-ATF4 regulates the transcription factor CHOP to activate ER stress-triggered apoptosis. In parallel, IRE1 controls cell fate determination through mitogen protein kinase JNK on ER stress [7, 14, 62, 63] (Figure 2.1). By contrast, although ER stress plays a role in programmed cell death in plants [64], very little is known about ER stress-induced cell death in plants [39, 53, 65]. Furthermore, lack of sequence homologs of most

mammalian apoptosis regulators in plants hints that divergent mechanisms of ER stress-induced cell death exist among organisms.

Revised model of IRE1α signaling network in mammals

The mammalian genome encodes two isoforms of IRE1, IRE1α and IRE1β. IRE1α is expressed ubiquitously and IRE1α knockout mice exhibit embryonic lethality. By contrast, IRE1β expression is restricted and IRE1β knockout mice are viable [30, 66]; therefore, most mammalian UPR research conducts on IRE1α. IRE1α was identified as a positive regulator of cell survival. It was believed that IRE1α signaling was terminated during irremediable ER stress to enable apoptosis [6, 9, 14, 37, 67, 68]. Nevertheless, recent studies have challenged this concept by showing that IRE1α persistently adjusts protein-folding capacity, actively directs UPR signaling, and executes cell fate determination [69, 70] (Figure 2.2). IRE1α employs splicing and RIDD to direct cell fate throughout ER stress. Despite *Xbp-1* being the only identified IRE1α splicing target, numerous types of RNA are proven to be RIDD substrates [44, 69, 70]. Although the significance of RIDD targets is not completely understood, some RIDD events are critical for IRE1α-dependent cell fate determination. During the adaptive response, IRE1α conducts RIDD on mRNAs encoding ER-translocating proteins to prevent further increases in protein-folding demand in the ER [70]. To augment protein-folding capacity, IRE1α splices the transcription factor *Xbp-1* mRNA to induce the transcription of ER quality control components. If attempts to restore ER homeostasis fail, IRE1α ceases to splice *Xbp-1* mRNA. Alternatively, IRE1α represses adaptive responses and activates apoptosis through RIDD [69, 70]. During the transition phase,

occurring between the adaptive and apoptotic response, RIDD increases ER stress intensity through degradation of selective UPR target genes including ER protein chaperone BiP [70]. Once ER stress intensity reaches its threshold, RIDD initiates apoptosis through repression of antiapoptotic pre-miRNAs [69]. Caspase-2 (CASP2) is a proapoptotic protease essential for the execution of apoptosis [71]. Upregulation of CASP2 is an indicator of apoptotic initiation. Through decay of anti-*Casp2* pre-miRNAs, IRE1α activates apoptosis through upregulation of *Casp2* (Figure 2.2) [69]. A close association of IRE1α activity and cell fate determination has been proposed for years [6, 9, 14, 37, 67, 68]. These findings provide direct evidence that IRE1α is a molecular switch and apoptosis executioner during ER stress [69]. It was previously proposed that the attenuation of IRE1 activity allows cells to initiate apoptosis [6, 9, 14, 37, 67, 68]. The identification of the IRE1α-*Casp2* pathway elaborates an intriguing IRE1α signaling model: IRE1α-*Xbp-1* is active in the adaptive phase and attenuated in the apoptotic phase. In parallel, activation of IRE1α-*Casp2* event initiates cell death in the apoptotic phase (Figure 2.3).

Is mammalian IRE1α the only major trigger of ER stress-induced apoptosis?

IRE1α is necessary and sufficient to trigger apoptosis, whereas PERK and ATF6 are dispensable in the apoptosis activation [69]. Nonetheless, it cannot be excluded that distinct ER stress sensors may serve as major executioners of cell death in a context-specific manner. Using chemical genetic tools, the regulatory roles of the phosphor-transfer and RNase activity of IRE1α in the UPR can be examined separately. The phosphor-transfer function is dispensable for *Xbp-1* mRNA splicing and upregulation of

CASP2 expression; however, it is required for the subsequent CASP2 cleavage and apoptosis activation, indicating that IRE1α phosphor-transfer function is essential for cell fate switch during ER stress [69, 70]. Notably, the phosphor-transfer function is mostly studied through an *in vitro* conditional IRE1α induction that mimics ER stress. Although this experimental system is valuable to distinguish phosphor-transfer and RNase function of IRE1α, it is important to note that ATF6 and PERK are not activated through ER stress. A potentially compromised crosstalk among the UPR arms raises a possibility that the IRE1α induction system may not completely resemble a genuinely biological scenario of ER stress. Hence, careful data interpretation from the conditional induction system and integration of *in vivo* analyses are necessary to determine whether *IRE1α* is the master trigger in ER stress-induced apoptosis.

The substrate specificity of mammalian IRE1α

Although the four identified IRE1α-cleaved miRNAs, miR-17, miR-34a, miR-96, and miR-125b repress the common substrate *Casp2*, TXNIP is another target of miR-17 [72]. TXNIP is involved in β-cell death and was selected to potentially regulate ER stress-induced apoptosis based on its rapidly elevated expression under severe ER stress. Similar to the IRE1α mutation, TXNIP mutation leads to compromised apoptosis activation, indicating that TXNIP is essential for ER stress-induced apoptosis [72, 73]. Wheras PERK-eIF2α activates TXNIP transcription. IRE1α increases TXNIP expression by degradation of miR-17. Accordingly, it is conceivable that each of four IRE1α-cleaved miRNAs may have specific substrates such as TXNIP. Based on this scenario, IRE1α may differentially degrade its individual target miRNA for fine-tuning of the UPR.

Another interesting feature of mammalian RIDD is that distinct substrates have a degree of sequence similarity within the cleavage site, whereas the flanking sequences of the cleavage sites are relatively divergent [69, 74]. This suggests that the cleavage mechanisms are likely to be conserved, whereas the flanking sequence determines the specificity of substrate recognition. This scenario would support the hypothesis that IRE1α adjust its RNase substrate specificity to activate diverse UPRs. The flexibility of IRE1α to target different substrates may rely on combinations of phosphorylation status, conformational changes, and physical associations with IRE1α regulators. Because alterations of IRE1α substrate specificity lead to opposite cell fates [70], further understanding of IRE1α substrate preferences will reveal how IRE1α coordinates cellular homeostasis to determine cell fate under ER stress. Currently, target switching of RIDD has been reported only in animals. Therefore, to gain a deeper understanding of evolution of the UPR in eukaryotes, further studies are needed to determine whether similar mechanisms exist in yeast and plants.

Plant IRE1 in ER stress response and cell fate determination

Despite the conservation of IRE1 among eukaryotes, divergent IRE1-dependent regulatory events have also been observed between plants and mammals. These evolutionarily divergent mechanisms are likely the reason for different ER stress and cell fate phenotypes observed between plants and mammals. Unlike mammalian IRE1 isoforms, the two *Arabidopsis* IRE1 isoforms are expressed ubiquitously with a limited tissue-specific expression pattern [26, 75]. There is no significant defect of the UPR in single mutants of *Arabidopsis* IRE1A or IRE1B while *Arabidopsis ire1* double mutants

display compromised ER stress tolerance and a UPR activation phenotype [39, 40]. These observations indicate that the two *Arabidopsis* IRE1 homologues share partially overlapping function during the UPR. Evidence for established, dominant or specific roles of individual *Arabidopsis* IRE1 isoforms during the UPR and cell fate regulation need to be further elucidated. Notably, it is experimentally undetermined whether viable *Arabidopsis ire1b* are knockouts or partial loss-of-function mutants. Failure to recover a homozygous plant of putative IRE1B knockout hints that *Arabidopsis* IRE1B may be an essential gene similar to mammalian IRE1α [76]. Interestingly, although mammalian IRE1α is essential for the UPR in goblet cells, in other cell types, there is no detectable defect in UPR target gene induction in a mammalian *ire1* double mutant likely due to partially overlapping function with ATF6 and PERK [30, 77]. By contrast, although two functional homologs of ATF6, bZIP28 and bZIP17, exist in *Arabidopsis* [27] (Figure 2.1), *Arabidopsis ire1* double mutants exhibit dramatic reduction of UPR target gene activation [39, 40]. These data indicate that the UPR is partially diversified between mammals and plants. Nonetheless, similar IRE1 features are also observed between plants and mammals. For instance, *ire1* and *xbp1-1* mutants display differential phenotypes despite both being essential genes. Likewise, the mutant of *Arabidopsis* IRE1 splicing target bZIP60 shows comparable ER stress tolerance with wild type plants as opposed to *Arabidopsis ire1* double mutants [39], supporting the hypothesis that the function of *Arabidopsis* IRE1 is not restricted to unconventional splicing like mammalian IRE1.

Interestingly, mutations of IRE1 in plants and mammals lead to opposite effects in ER stress-induced cell death phenotypes [39, 40, 53]. *Ire1α*$^{-/-}$ mouse embryonic

fibroblasts (MEFs) exhibit a greater survival rate than *Ire1α*$^{+/+}$ MEFs on ER stress, supporting the suggestion that mammalian IRE1 is an apoptosis executioner. By contrast, *Arabidopsis ire1* double mutants display compromised ER stress tolerance, instead of a greater survival rate [39, 40]. Consistently, DNA fragmentation and ion leakage are enhanced in the *Arabidopsis ire1* double mutant on ER stress [53], suggesting that plant IRE1 may not function as an apoptosis executioner like its mammalian counterpart. Nevertheless, it cannot be excluded that the differences are related to dissimilar experimental settings; mammalian UPR research is mostly conducted in cell culture, whereas intact organisms are used in plant UPR studies. Moreover, except potential roles in protein-loading reduction under ER stress [53], biological significance of the plant RIDD in cell fate determination is unknown. Further experimental validation will reveal whether plant RIDD could process multiple substrates to control cell fate decisions, similar to that seen in mammals.

Shared components of the UPRosome and apoptosis

IRE1α activation is tightly controlled by its interacting protein complex, termed the UPRosome [37]. Most UPRosome components are involved in apoptosis, supporting the suggestion that intense crosstalk exists between IRE1α activity and apoptosis activation (Table 2.1). Specifically, although the UPRosome comprises multiple components, loss-of-function mutation of a single component, such as PARP16, Bi-1, Aip-1, PTP-1B, NMHCIIB, Jab1, Nck1, and Ask1, is sufficient to alter IRE1α splicing activity or apoptosis activation [78-85] (Table 2.1). Moreover, IRE1α-interactor mutants displaying either elevated or declined IRE1α splicing activity can show enhanced

apoptosis, indicating that a precise level of activation of IRE1α splicing is important for cell survival [78-85]. This further suggests IRE1α activation is controlled by a signaling network that maintains a delicate equilibrium of adaptive and apoptotic responses. A subtle imbalance of the equilibrium could disturb cellular homeostasis and thus alter cell fate determination [78-95]. Furthermore, the observation that a single mutation of the UPRosome leads to significant defects in IRE1α signaling hints that IRE1α is differentially regulated in a context-specific manner (Table 2.1). Because UPRosome analyses are conducted under various conditions, systematic and comparable analyses of UPRosome members will connect each hub and thus give a clearer view of IRE1α signaling network.

IRE1 sensing mechanisms

ER stress-sensing mechanisms are intensively studied in yeast and animals [16]. The ER stress sensors are relatively more inactive through physical association with BiP, the most abundant ER-resident chaperone. Dissociation with BiP or interaction with unfolded proteins is the major trigger of IRE1 activation. Yeast IRE1 is activated through association with unfolded proteins rather than disassociation with BiP [96]; however, the physical interaction of BiP is a fine-tuning mechanism to ensure that yeast IRE1 is appropriately activated [97]. Unlike yeast IRE1, the activation mechanisms of mammalian IRE1α rely on its dissociation with BiP as opposed to a direct interaction with unfolded proteins [98]. The differences in activation mechanisms between yeast and mammalian IRE1α can be partially explained by the dissimilarity in protein structure within the sensor domain [37]. Surprisingly, a recent study revealed that mammalian

IRE1β tends to interact with unfolded proteins like yeast IRE1 and it is unable to associate with BiP [99]. Accordingly, it is possible that, like yeast IRE1, binding of unfolded proteins is the primary trigger of mammalian IRE1β activation. Despite intense studies in mammals and yeast, the plant IRE1 sensing mechanisms are completely undefined. Further structural and functional analyses of plant IRE1 will be instrumental in revealing ER stress-sensing mechanisms in plants.

Cell-type specific sensing mechanisms: the role of mammalian IRE1β

How the cellular homeostasis is maintained in a cell-type specific manner is a fundamental question of cell biology. It has been recently shown that IRE1β is essential for the UPR specifically in goblet cells [30]. In goblet cells, IRE1β is dispensable for *Xbp-1* splicing and BiP induction. Instead, IRE1β mutation leads to enhance ER stress intensity evidenced by higher level of *Xbp-1* splicing and BiP induction. Moreover, IRE1β−/− mice display a distended ER phenotype, potentially due to overaccumulation of Mucin2 (MUC2), the most prominent protein secreted from goblet cells. This suggests that IRE1β controls MUC2 expression in goblet cells. Thus, IRE1β mutation leads to MUC2 overload in the ER and in turns trigger ER stress [30]. RIDD was proposed to be the mechanism underlying IRE1β regulation on MUC2 levels in goblet cells [30]. The cell type-specific target of IRE1β provides a molecular explanation of how the UPR maintains a dynamic and specific secretory ability in multicellular organisms. Consistent with the notion that unfolded proteins trigger IRE1β activation, IRE1β may interact physically with certain types of unfolded protein. In the case of goblet cells, IRE1β may specifically monitor the MUC2 level in the ER and adjusts its loading into the ER

through RIDD. Based on this scenario, the mammalian ER stress sensors may distinguish the type of unfolded proteins accumulated in the ER and trigger differential UPR signaling. More specifically, if the unfolded proteins are dispensable for cell survival, ER stress sensors could repress the expression of unfolded proteins through RNA decay or translational repression. Conversely, if unfolded proteins are essential for cellular function, the UPR may preferentially augment the expression of chaperones to recover the production of unfolded proteins. While ER stress duration and intensity are considered major factors in the apoptosis threshold, the type of misfolded protein may be also critical for determination of UPR signaling outputs.

Sensing mechanisms beyond protein-folding homeostasis

Emerging evidence shows that IRE1 monitors cellular homeostasis beyond sensing unfolded protein accumulation. For instance, CRY1/CRY2-mediated circadian rhythm regulates IRE1α activity in the liver [100], suggesting that IRE1α coordinates ER function to cope with circadian-related physiological processes. These observations provide a link between the IRE1α-dependent UPR, circadian regulation, and liver metabolic processes. More importantly, because circadian rhythm has a substantial influence on UPR activation, time-course studies of the UPR will require diligent experimental design and appropriate controls to avoid biases. Recently, lipid homeostasis is proven to impact UPR activation through an unconventional sensing mechanism, because the unfolded-protein-sensing domain of IRE1α and PERK is dispensable for lipid-dependent UPR activation [101]. Together, these observations support the suggestion that the UPR perceives physiological and cellular signaling

beyond ER protein folding homeostasis. Although it is unclear whether plant IRE1 senses signaling beyond protein-folding capacity, an *Arabidopsis ire1* double mutant displaying a root-specific phenotype under unstressed conditions hints that plant IRE1 also integrates physiological signals to maintain specific secretory activity [39]; however, this hypothesis awaits experimental validation.

Concluding remarks

Significant progress in defining IRE1 mechanisms has been achieved. We now know that IRE1 activities are coordinated at a systemic level to cope with dynamic secretion activity. Although *in vitro* experimental systems and conditional IRE1 induction approaches have made groundbreaking discoveries in basic UPR knowledge [69, 70, 102-105], we remain far from a comprehensive understanding of the UPR in intact organisms. The lethality of the mammalian IRE1α mutant represents a challenge to gaining insights into the IRE1 function *in vivo*. By contrast, the viability of plant IRE1 mutants enables *in vivo* analyses to reveal its roles in organ growth, pathogen defense, and abiotic stress responses [27, 39, 106, 107]. Moreover, with the ease of building high-order plant mutants, *in vivo* phenotypic analyses show that a conserved component of the G protein complex enhances *Arabidopsis ire1* phenotype in both plant UPR activation and growth regulation. The study underscores the building of UPR networks in intact organisms using plants as a model system [39]. With more systematic and quantitative studies of the UPR *in vivo*, there are significant findings ahead that will decipher the dynamic UPR maps close to a genuinely physiological scenario.

Aims of the thesis research

This thesis is aimed at understanding the plant UPR by characterizing plant ER stress regulators and identifying biological roles of the plant UPR. In Chapter 3, I established that *Arabidopsis* IREIA and IRE1B are functional ER stress sensors. I found that an *ire1a ire1b* (*ire1*) double mutant displays the ER stress-sensitive and the compromised UPR activation phenotype. To reveal regulatory relationship between IRE1 and other plant ER stress regulators, I showed that a mutant of G-protein complex component, AGB1, enhances both the ER stress sensitivity and the UPR activation phenotype in *ire1*. Moreover, I uncovered a role of the plant UPR in primary root growth by showing that the short-root phenotype of *ire1* under normal growth condition. In Chapter 4, I further explored the regulatory interaction between the plant UPR and the auxin response. I found that ER stress regulates the transcription of auxin receptors and transporters. Also, mutants of ER-localized transporters show the compromised UPR activation phenotype, indicating that ER-based auxin transport may play a role in the plant UPR. Moreover, I provided evidence that IRE1 is required for the auxin homeostasis and signaling. Together, the results reveal the inter-regulation of the plant UPR and auxin signaling. In appendices, I provided protocols of ER stress phenotypic assays and quantification of UPR activation.

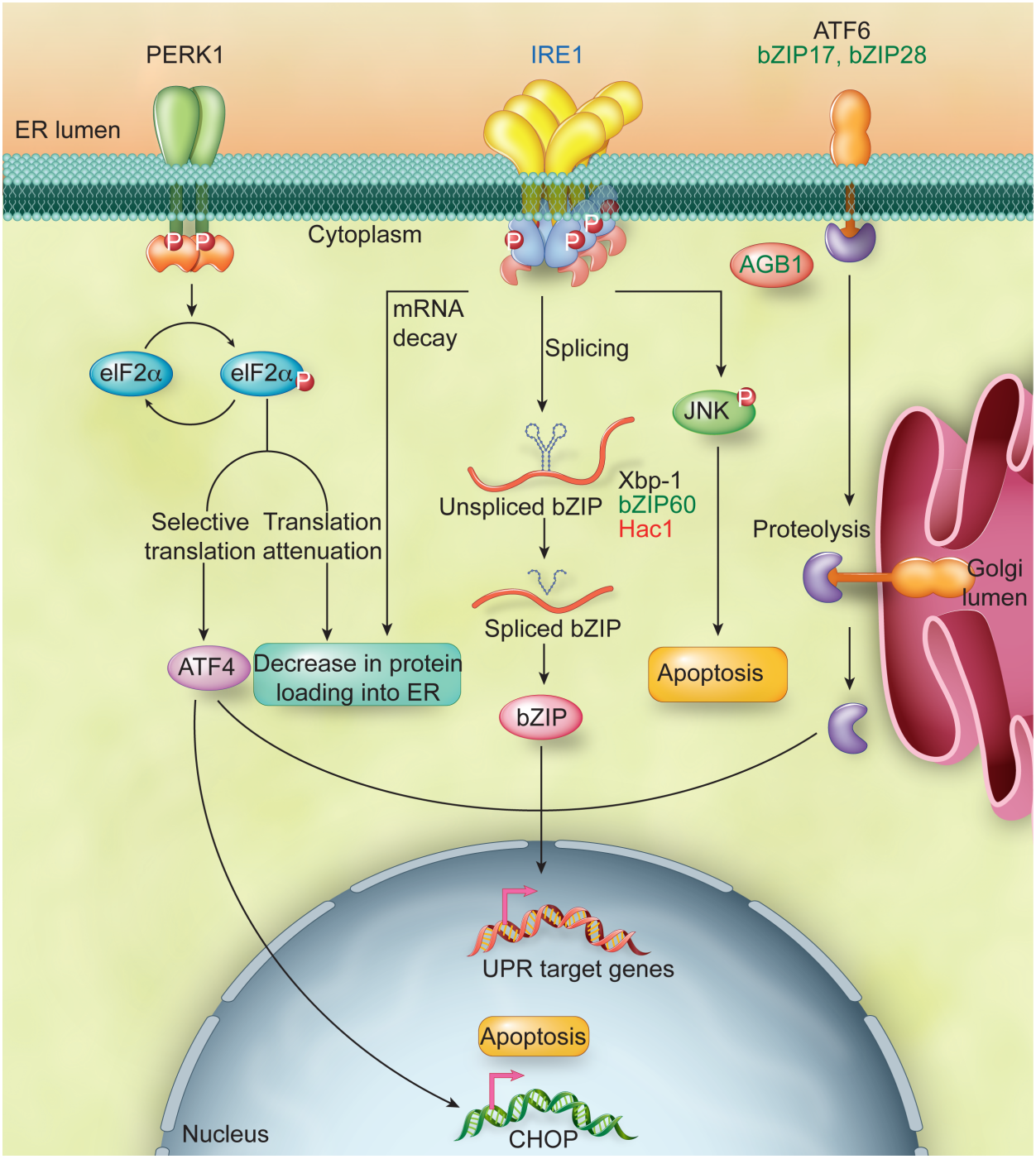

Figure 2.1. Overview of UPR arms in eukaryotes.

Figure 2.1 (cont'd)

The IRE1 arm is conserved in eukaryotes. IRE1 unconventionally splices the bZIP transcription factors *Xbp-1* and *bZIP60* and *Hac1* mRNA in mammals, plants, and yeast respectively. The spliced bZIP transcription factor enters the nucleus to regulate UPR target genes. In addition, two distinct arms mediated by PERK and ATF6 regulate the mammalian UPR. ATF6 is an ER transmembrane transcription factor. ER stress triggers the relocation of ATF6 from the ER to the Golgi apparatus, where it undergoes proteolytic cleavage. Subsequently, the transcription factor domain of ATF6 enters the nucleus to modulate transcription of UPR target genes. Two functional homologues of ATF6, bZIP17 and bZIP28, exist in plants. PERK, an ER transmembrane protein kinase is identified only in animals. On ER stress, PERK phosphorylates eukaryotic initiation factor 2 alpha (eIF2α), which leads to transient inhibition of general protein translation and selective translation of the transcription factor ATF4. Under irremediable ER stress, PERK-eIF2α-ATF4-CHOP and IRE1-JNK initiate apoptosis in mammals. Moreover, the beta subunit of the heterotrimeric G protein complex, AGB1, is essential for the plant UPR. Although the G protein complex is conserved in eukaryotes, its significance in the UPR is unclear in other eukaryotic organisms. Color code: blue, eukaryotes; black, mammals; green, plants; red, yeast. For interpretation of the references to color in this and all other figures, the reader is referred to the electronic version of this dissertation.

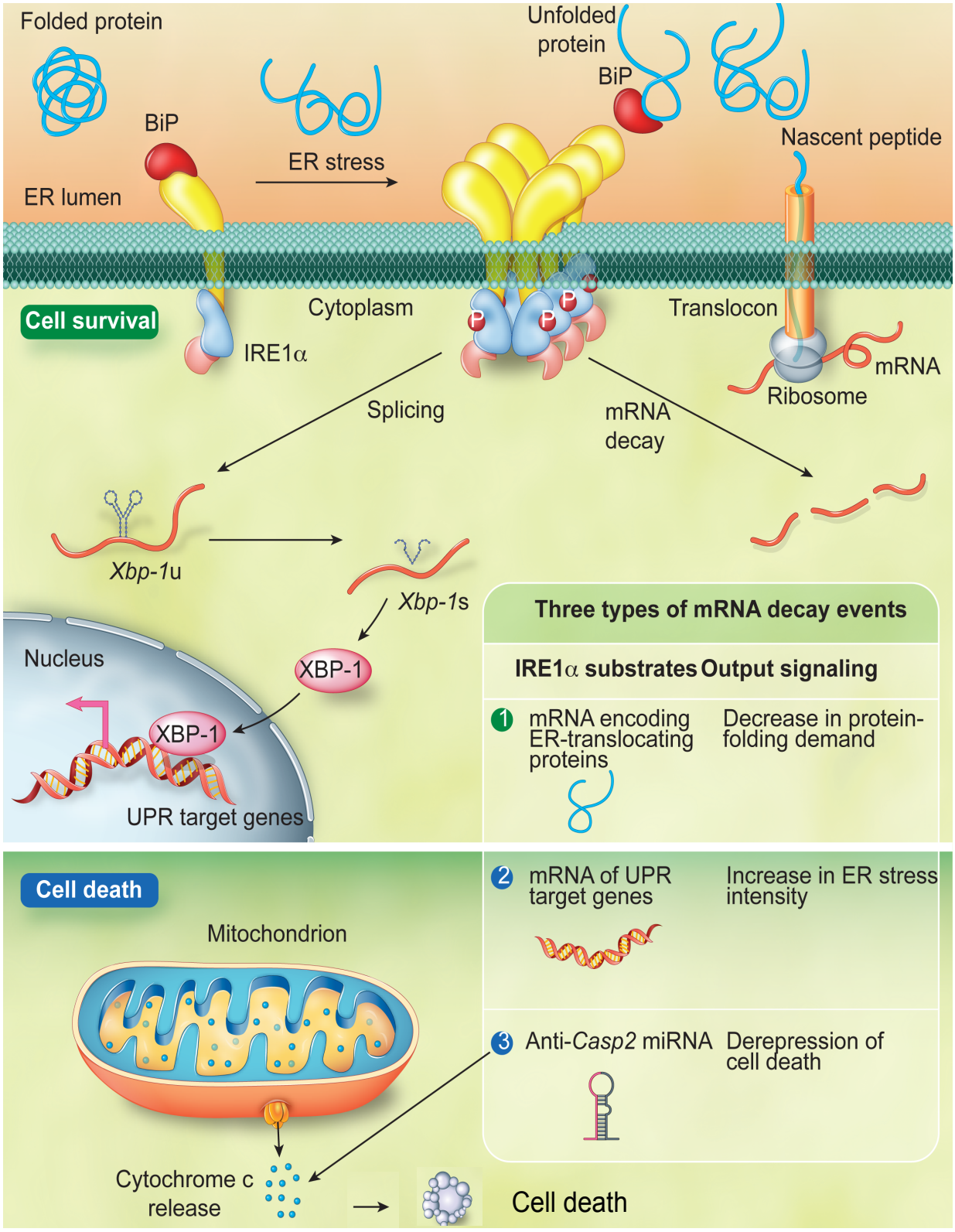

Figure 2.2. IRE1α regulatory mechanisms during ER stress.

Figure 2.2 (cont'd)

Mammalian IRE1α is repressed through a physical interaction with BiP when demand and capacity of protein folding is balanced in the ER. Dissociation of IRE1α from BiP due to an elevated level of unfolded protein in the ER leads to activation of IRE1α. The IRE1α-activating processes include its auto-phosphorylation, conformational change, and higher-order assembly. IRE1α directs cell fate decisions through unconventional splicing and Regulated IRE1-Dependent Decay (RIDD). To prevent increasing demand of ER protein folding, IRE1α conducts RIDD to degrade the transcripts of ER-translocating proteins. In parallel, IRE1α unconventionally splices the transcript of *Xbp-1* transcription factor. The spliced XBP-1 enters the nucleus to transcriptionally reprogram UPR target genes, including ER chaperones. Under irremediable ER stress, IRE1α ceases to splice *Xbp-1* mRNA. Instead, IRE1α operates RIDD on selective UPR target genes including BiP to enhance the intensity of the ER stress. Once the ER stress intensity reaches its threshold, IRE1α represses anti-*Casp2* microRNA (miR-17, miR-34a, miR-96, and miR-125b) through RIDD. IRE1α-mediated degradation of anti-*Casp2* miRNAs leads to activation of apoptotic initiator *Casp2* and subsequently triggers mitochondrion-dependent apoptosis.

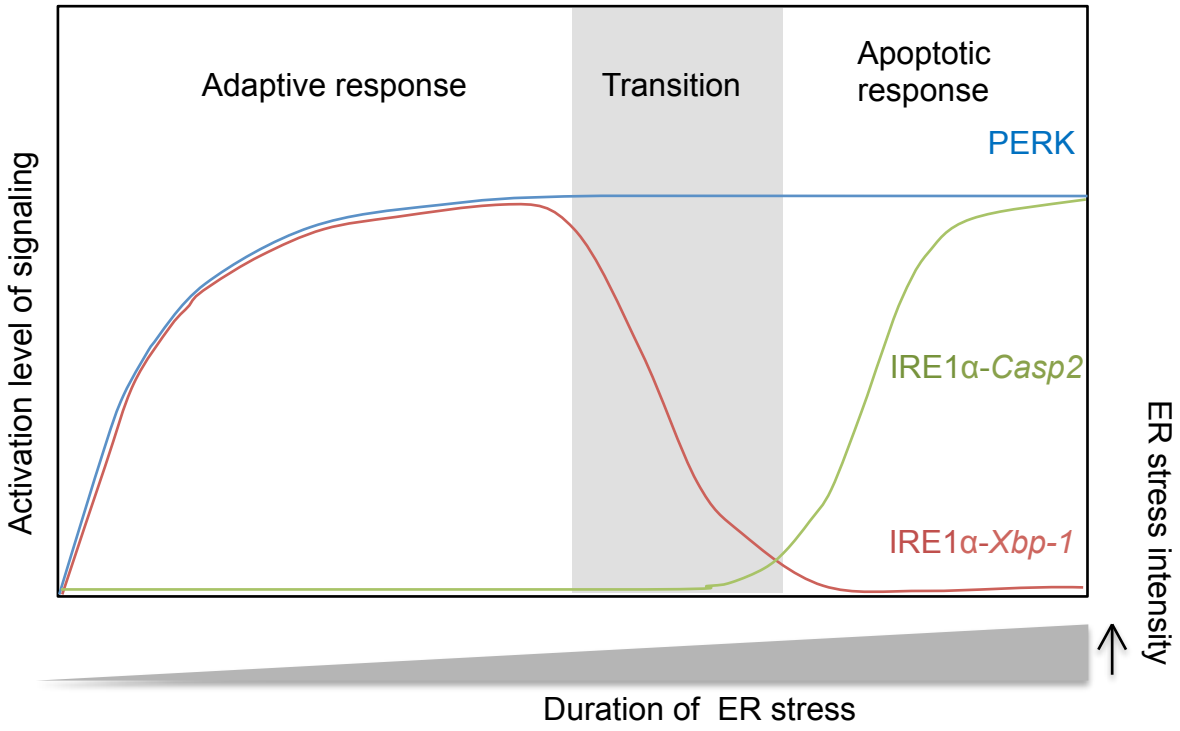

Figure 2.3. Updated model of IRE1α and PERK signaling in cell fate determination during ER stress.

Figure 2.3 (cont'd)

UPR signaling aimed for cell survival is considered an adaptive response during ER stress. Under irremediable ER stress, UPR represses the adaptive response and triggers an apoptotic response. IRE1α and PERK are two ER stress sensors that decrease ER protein-folding demand through mRNA decay and translational inhibition, respectively. Both PERK and IRE1α signaling appear to persist throughout ER stress. IRE1α differentially triggers diverse UPRs according to need. In the adaptive phase, to increase protein-folding capacity, IRE1α-mediated *Xbp-1* mRNA splicing is activated for transcriptional regulation of UPR target genes. In a transition phase between the adaptive and apoptotic responses, the signaling mediated by IRE1α-*Xbp-1* is attenuated. In parallel, IRE1α increases the intensity of the ER stress through mRNA decay of selective UPR target genes, including ER chaperones. During the apoptotic phase, IRE1α-*Casp2* signaling is activated to initiate cell death.

Table 2.1. Interacting proteins of IRE1α

IRE1α interators	Observed phenotype of loss-of-function mutations
PARP16	Decreased *Xbp-1* splicing / increased cell death
Bi-1	Increased *Xbp-1* splicing/ increased cell death
AiP-1	Decreased *Xbp-1* splicing / decreased cell death
Ptp-1b	Decreased *Xbp-1* splicing / decreased cell death
NMHCIIB	Decreased *Xbp-1* splicing/ compromised IRE1α foci formation
Bax/Bak	Decreased *Xbp-1* splicing/ impaired IRE1α oligomerization
Bim/Puma	Decreased *Xbp-1* splicing and UPR genes activation
Jab1	Decreased *Xbp-1* splicing and UPR genes activation
Nck1	Decreased cell death
Ask1	Decreased cell death/altered JNK activation

Table 2.1 (cont'd)

IRE1α interators	Observed phenotype of induction or overexpression
Traf2	Altered activation of JNK pathway
Jik	Altered activation of JNK pathway
Hsp90	Decreased IRE1α protein stability
Usp14	Altered activation of ERAD
SYVN1	Increased IRE1 ubiquitination and degradation
Hsp72	Increased *Xbp-1* splicing/ decreased cell death
Rack1	Decreased phosphorylation of PP2A

Acknowledgements

We thank Dr Danielle Loughlin for helpful comments and suggestions. They apologize to those authors whose work could not be cited owing to space constraints. This work was supported by grants from the National Institutes of Health (R01 GM101038-01), Chemical Sciences, Geosciences, and Biosciences Division, Office of Basic Energy Sciences, Office of Science, U.S. DOE (DE-FG02-91ER20021), NASA (NNX12AN71G) and the National Science Foundation (MCB0948584 and MCB1243792).

CHAPTER 3

IRE1 and AGB1 independently control two essential unfolded protein response pathways in *Arabidopsis*

This section has been previously published in *The Plant Journal*

YA-NI CHEN and FEDERICA BRANDIZZI (2012)

The plant journal **69**:266-277

Abstract

The endoplasmic reticulum (ER) has the ability to maintain the balance between demand for and synthesis of secretory proteins. To ensure protein-folding homeostasis in the ER, cells invoke signaling pathways known as the unfolded protein response (UPR). To initiate the UPR, yeasts largely rely on a conserved sensor, IRE1. In plants, some UPR transducers have been identified, but no functional relationship among them has yet been examined. The *Arabidopsis* genome encodes two *IRE1* sequence homologues*, IRE1A* and *IRE1B*. Here we provide evidence that IRE1A and IRE1B have overlapping functions that essential for the plant UPR. A double mutant of *IRE1A* and *IRE1B*, *ire1a ire1b* (*ire1*), showed reduced ER stress tolerance and a compromised UPR activation phenotype. By demonstrating that *ire1* has a root growth phenotype, we attribute a role to UPR transducers in organ growth regulation. We have also established that a mutant of *Arabidopsis AGB1*, a subunit of the ubiquitous heterotrimeric GTP-binding protein family, enhances both the ER stress and the short-root phenotype in *ire1*.

Introduction

Environmental or physiological factors that cause an accumulation of unfolded proteins in the ER lead to ER stress. To restore ER protein-folding homeostasis, eukaryotic cells invoke protective signaling pathways known as the unfolded protein response (UPR) [1, 2]. The regulatory mechanisms of the UPR have been extensively explored in yeast and metazoans. Inositol-requiring enzyme 1 (IRE1) is a highly conserved protein in eukaryotes and the major ER stress sensor in yeast [17, 18]. IRE1 is a type I membrane protein, which consists of an ER stress sensor domain at the N-terminus as well as a kinase and an endoribonuclease domains at the C-terminus. Upon sensing the accumulation of unfolded proteins in the ER, the endoribonuclease domain of IRE1 is activated through oligomerization and trans-autophosphorylation. Activated IRE1 splices the transcript of a specific transcription factor- *HAC1* in yeasts [19] and *XBP-1* in animals [20]. The spliced transcription factors control the expression of UPR target genes, which are involved in assisting protein folding, degrading misfolded protein, and regulating programmed cell death [19, 21]. To manage the UPR induced by various physiological or environmental conditions, animal cells use IRE1 pathway and two additional UPR regulatory pathways: the PKR-like ER Kinase (PERK) pathway and the Activating Transcription Factor 6 (ATF6) pathway [22]. Similar to IRE1, both PERK and ATF6 have a stress-sensing domain that protrudes into the ER lumen and a cytosolic region that initiates downstream responses. PERK mediates the UPR by repression of protein synthesis through phosphorylation of eukaryotic initiation factor 2α [23]. ATF6 is a membrane-tethered transcription factor that is activated by ER stress. The transcriptional activation domain of ATF6 is released from the ER membrane by

protease cleavage and translocated into the nucleus to regulate UPR target genes on ER stress [24].

A few conserved UPR transducers have been identified in plants. In *Arabidopsis*, bZIP28 is known to be a functional homolog of the mammalian ATF6. To activate the UPR, bZIP28 undergoes proteolytic release of its transcriptional activation domains to regulate expression of ER chaperones [108, 109]. The *Arabidopsis* genome also encodes two sequence homologues of *IRE1—IRE1A* (At2g17520) and *IRE1B* (At5g24360) [25]—that are ubiquitously expressed in plant tissues [110]. Analyses of three individual T-DNA insertion lines of *IRE1A* show that the induction of UPR target genes was similar between the *ire1a* mutants and wild-type Col-0 on ER stress [111]. Recently, it was demonstrated that the UPR target gene induction is reduced in a T-DNA insertion line of IRE1B (*ire1b-2*) [112]. In addition, the activation of *bZIP60* upon ER stress relies on its splicing by IRE1B, but not by IRE1A, suggesting that IRE1B is the only functional IRE1 homolog in plants [112]. However, it cannot be excluded that IRE1A also plays a role in the plant UPR, as the functional redundancy between IRE1A and IRE1B has not yet been test.

In addition to the conserved counterparts of mammalian UPR regulators, unexpected UPR mediators have also been identified in plants. It has been shown that GTP-binding protein beta 1 (AGB1), an ER-localized heterotrimeric GTP-binding protein (G protein), is involved in the UPR in *Arabidopsis* [113]. G proteins are ubiquitous signaling molecules in eukaryotes [114]. In plants, *AGB1* is known to be involved in vegetative and reproductive development as well as in light and oxidative stress responses [115-118].

Here, we have performed functional characterization of an *ire1* double mutant, providing genetic and molecular evidence showing that IRE1A and IRE1B are essential plant UPR regulators. We also show that an *agb1* loss-of-function mutant enhanced the *ire1* phenotype with respect to UPR activation. The functional relationship between *IRE1* and *AGB1* was also examined in term of the short-root phenotype of *ire1.* Hence, this study also sheds light on regulation of organ-specific growth by UPR transducers in plants.

Results

IRE1A and IRE1B are Essential for the Plant UPR

To determine whether IRE1A and IRE1B control the plant UPR, we performed functional analyses by isolating loss-of-function mutants of *IRE1A* and *IRE1B*. The *ire1a-4* (WISCDSLOX420D09) and *ire1b-2* (SAIL_238_F07) alleles were obtained from the *Arabidopsis* Biological Resource Center (ABRC). Homozygous lines of *ire1a-4* and *ire1b-3* were confirmed by genomic polymerase chain reaction (PCR) (Figure 3.1). To determine whether *ire1a-4* and *ire1b-2* represent RNA null alleles, 4 specific *IRE1A* and *IRE1B* primer sets—IRE1A-N, IRE1A-C, IRE1B-N, and IRE1B-C, annealing upstream or downstream of the T-DNA insertion sites, were used in RT-PCR analyses (Figure 3.2a, b). We detected no *IRE1A* transcript in *ire1a-4* using either primer sets, suggesting that *ire1a-4* is a knock-out mutant. By contrast, the *IRE1B* amplicon was found to be present in *ire1b-2* using the upstream primers set (IRE1B-N) while there was no *IRE1B* amplicon was detectable in *ire1b-2* using the downstream primer set

(IRE1B-C). The RT-PCR results indicate that *ire1b-2* is not an RNA null mutant, but it does not express the full-length *IRE1B* transcript.

To test ER stress tolerance, *ire1a-4*, *ire1b-2*, and wild-type Col-0 were germinated on medium containing DMSO (mock control) or 25 or 50 ng/ml tunicamycin (Tm), which is a typical UPR inducer that blocks protein *N*-glycosylation. Because *ire1a-4*, *ire1b-2*, and wild-type Col-0 displayed similar responses with respect to both ER stress tolerance and the UPR target gene induction (Figure 3.3a and 3.4), we hypothesized that the two IRE1 isoforms could compensate for each other in the single mutants. To test this possibility, we generated an *ire1a ire1b* (*ire1*) double mutant by crossing *ire1a-4* and *ire1b-2* (Figure 3.1 and 3.2). *ire1* was over-sensitive to Tm compared with wild-type Col-0 and the single mutants (Figure 3.3a). RT-PCR analyses showed that, after 6 h Tm treatment, induction of a known UPR activation indicator, *BiP3* [119], was drastically reduced in *ire1* compared with wild-type Col-0 (Figure 3.3b). Quantitative real time RT-PCR (qRT-PCR) confirmed that the expression level of *BiP3* in *ire1* was three to four times lower than that of wild-type Col-0 over 3-day time course of Tm treatment (Figure 3.3c). Consistently, the induction of two other UPR target genes, *AtERdj3A* and *AtERdj3B* [120], was lower in *ire1* than wild-type Col-0 on ER stress (Figure 3.3d). Thus, we concluded that the lower ER stress tolerance phenotype in *ire1* arose from defects in UPR target gene induction.

To prove that Tm-sensitive phenotype was due to loss-of-function of *IRE1A* and *IRE1B*, we complemented *ire1* using the *IRE1A* clone under control of the native promoter (*pIRE1A-IRE1A*) as well as a dexamethasone (Dex)-inducible clone of either *IRE1A* or *IRE1B*. We found that IRE1A or IRE1B alone at least partially rescued the ER

stress-sensitive phenotype of *ire1* (Figure 3.5). These data show that the Tm-sensitive phenotype of *ire1* is caused by the loss-of-function mutations in *IRE1A* and *IRE1B.* Therefore, the *IRE1* signaling is essential for the plant UPR, and *IRE1A* and *IRE1B* share partially overlapping functions in the plant UPR activation.

Loss-of-Function of *AGB1* Causes Sensitivity to ER Stress

Our data support that IRE1 is essential for the plant UPR. We next aimed to get insight into the plant UPR signaling networks by examination of functional relationship between IRE1 and other plant UPR regulators. Therefore, we first compared the ER stress tolerance between mutants of known UPR components, including *bZIP28*, *bZIP60*, *BiP2*, and *AGB1* [109, 113, 119, 121]. Among *bzip28-1*, *bzip60-1*, *bip2*, and *agb1-3*, only *agb1-3* showed a Tm-sensitive phenotype. We found that the *agb1-3* mutant was more sensitive to ER stress compared with wild-type Col-0 (Figure 3.6a). However, another T-DNA allele of *AGB1*, the *agb1-2* mutant, was previously shown to be more resistant to ER stress [113]. To clarify whether different *agb1* allelic mutants have similar ER stress sensitivity, we compared the ER stress tolerance between *agb1-3* and two other null allele of *AGB1*, *agb1-1* and *agb1-2* (Figure 3.6b) [113, 115]. Similar to the *agb1-3* mutant, the *agb1-1* and *agb1-2* mutants displayed over-sensitivity to ER stress compared with wild-type Col-0 (Figure 3.6b). Hence, we conclude that there is no substantial difference in ER stress tolerance among the *agb1-1*, *agb1-2*, and *agb1-3* mutants. To clarify that the opposite ER stress tolerance phenotype of the *agb1* mutants reported in here and Wang *et al*. (2007) was not due to use of different phenotypic assays, the higher ER stress sensitivity of *agb1-3* compared with wild-type Col-0 was

further confirmed using the same ER stress phenotypic assay as used by Wang *et al*. 2007. In detail, *agb 1-3* and wild-type seeds were germinated on high concentrations of Tm (300 ng/ml) for 6 days, and then transferred to normal growth medium without Tm for 10 days. Wild-type Col-0 seeds recovered from the ER stress as indicated by germination, but the *agb1-3* seeds failed to survive under the same treatment (Figure 3.6c). In addition, complementation of *agb1-3* by *AGB1* showed that the ER stress phenotype of *agb1-3* is due to the *AGB1* loss-of-function (Figure 3.6d). Therefore, these data provide evidence that an *AGB1* loss-of-function causes over-sensitivity to ER stress.

agb1* enhances ER stress phenotype of *ire1

To our knowledge, functional relationship between plant UPR transducers has not been reported yet. We have shown that both IRE1 and AGB1 are essential for the plant UPR. We further investigated regulatory relationship between IRE1 and AGB1 by generating an *ire1 agb1* triple mutant. Interestingly, compared with the *ire1* double mutant and the *agb1-3* single mutant, the triple mutant displayed an even more sensitive phenotype to ER stress using two phenotypic assays: Tm infiltration and germination on Tm-containing medium (Figure 3.7a, b). Leaf senescence and damage appeared more severe in the *ire1 agb1* triple mutant than in the *ire1* double mutant at 2-4 days after infiltration with 15 μg/ml Tm (Figure 3.7a). When germinated on Tm-containing medium, the *ire1 agb1* triple mutant was smaller than the *ire1* double mutant (Figure 3.7b). The enhanced growth defects of the *ire1 agb1* triple mutant compared

with t the *ire1* double mutant on ER stress were further visualized by induced hypocotyl elongation under dark growth conditions (Figure 3.7b).

We further investigated whether the lower ER stress tolerance in the *ire1 agb1* triple mutant compared with the *ire1* double mutant was the result of more extensive aberrant UPR target gene induction. We compared the expression of UPR target genes, *BiP3*, *AtERdj3A*, and *AtERdj3B* in the *agb1-3* single mutant, the *ire1* double mutant, and the *ire1 agb1* triple mutant over the time course Tm treatment. The qRT-PCR results showed that the three UPR target genes were induced to a lower level in the *ire1* double mutant compared with wild-type Col-0, but the induction was higher in the *agb1-3* single mutant compared with wild-type Col-0 (Figure 3.7c, d). These data suggest that IRE1 and AGB1 play an antagonistic role in UPR target gene induction. Furthermore, although the fold changes of UPR target gene induction were altered in the *ire1* double mutant and the *agb1-3* single mutant, the expression patterns of UPR target genes in the *ire1* double mutant and the *agb1-3* single mutant were similar to those of wild-type Col-0 over the time course of Tm treatment (Figure 3.7d). By contrast, both the expression levels and patterns of UPR target genes were severely affected in the *ire1 agb1* triple mutant (Figure 3.7d). Together with the evidence that the ER stress tolerance of the *ire1 agb1* triple mutant was lower than that of the *ire1* double mutant and the *agb1-3* single mutant (Figure 3.7a, b), these results enable us to conclude that *agb1* enhances ER stress phenotype in *ire1*. In metazoans, regulatory relationships have been established between components belonged to independent UPR pathways. For example, although ATF6 and IRE1 are known as two distinct UPR sensors in metazoans, ATF6 activates the transcription of *XBP-1*, whose product is the splicing

substrate of IRE1 and a key regulator of the IRE1-dependent signaling arm [122]. Because the transcription of *AGB1* is down-regulated upon UPR activation [113], we investigated whether the *AGB1* transcript is regulated by *IRE1*. Hence, we compared the *AGB1* expression level between wild-type Col-0 and the *ire1* double mutant over a time course of Tm treatment. Consistent with earlier findings [113], the *AGB1* RNA level decreased on ER stress in wild-type Col-0 (Figure 3.7e). In *ire1*, however, the *AGB1* transcript remained unchanged over the time course of Tm treatment (Figure 3.7e). These results imply that down-regulation of the *AGB1* transcript on ER stress relies on the *IRE1*.

IRE1A and IRE1B Have a Role in Root Growth

In multicellular organisms, the demand of secretory protein varies during cell differentiation and proliferation, and the UPR is required for maintenance of the ER protein-folding capability in specialized cell types or at specific developmental stages in metazoans. For example, deletion of mammalian *IRE1α* causes embryo lethality due to placental defects [29, 66]. To investigate whether *IRE1*-mediated UPR is involved in growth and development in plants, we compared plant morphology between wild-type Col-0 and *ire1* through developmental stages. We found that the primary root of the *ire1* double mutant was significantly shorter than wild-type Col-0 (T-test, p=3.92449E-18) (Figure 3.8a, c), but there was no visible morphological phenotype in the aerial parts (Figure 3.8b, d). These results indicate that *IRE1* is involved specifically in optimal root growth in plants. In addition, consistent with the previous findings [123, 124], the *agb1-3* single mutant had longer roots compared with wild-type Col-0 (T-test, p=0.0064)

(Figure 3.8a, c); however, the primary root of the *ire1 agb1* triple mutant was significantly shorter than that of the *ire1* double mutant (T-test, p=0.0024) (Figure 3.8a, c). The fact that the *agb1-3* mutation enhanced both the ER stress sensitivity and the root growth defects phenotype of *ire1* hints the possibility that *IRE1* and *AGB1* independently regulate two parallel UPR pathways, and that both these two plant UPR pathways contribute to root growth.

The root growth phenotype of *ire1* is associated with defects in cell elongation

To further explore the short-root phenotype, we visualized the root tissue anatomy by counterstaining cell walls with propidium iodide (Figure 3.9a). Four well-characterized growth zones are defined in the *Arabidopsis* root apex: meristematic zone, transition zone, elongation zone, and growth-terminating zone [125]. The length of each zone in *Arabidopsis thaliana* ecotype Col-0 has been determined based on their unique cellular activities: meristem, 200 μm from root cap junction (RCJ); transition zone, 200-520 μm from RCJ; elongation zone, 520-850 μm from RCJ; growth-terminating zone, 850-1500 μm from RCJ [125]. In addition, the onset of fast elongation in the elongation zone is indicated by root hair initiation (RHI) in epidermal cells. The results of propidium iodide staining show that the cell number and cell size within 400 μm from the RCJ were similar between wild-type Col-0, the *agb1-3* single mutant, the *ire1* double mutant, and *ire1 agb1* triple mutant (Figures 3.10), suggesting an absence of significant defects in distal root patterning. By contrast, in the region above 400 μm, the cell length was abnormal in the *ire1* double mutant and *ire1 agb1* triple mutant. In wild-type Col-0 and the *agb1-3* single mutant, the length of cells gradually increased

toward the growth-terminating zone (Figure 3.9); however, the pattern of cell elongation was different in the *ire1* double mutant and *ire1 agb1* triple mutant (Figure 3.9). Cells between 400–600 μm from the RCJ were significantly longer in the *ire1* double mutant and *ire1 agb1* triple mutant compared with that of wild-type Col-0 (Figure 3.9b). In addition, in the elongation zone, the mean cell length of cells showing root hair initiation was only 50% in the *ire1* double mutant and 40% in the *ire1 agb1* triple mutant compared with that of wild-type Col-0 (Figure 3.9c). These data indicate that the short-root phenotype of the *ire1* double mutant and the *ire1 agb1* triple mutant is due to a disorder in cell elongation in transition zone/elongation rather than to defects in the meristem. The data further imply that the maintenance of optimal root cell elongation relies on the IRE1- and -dependent signaling pathways.

The expression of UPR target genes is lower in the root of *ire1 agb1*

Our results from PI staining show that the *ire1* double mutant and the *ire1 agb1* triple mutant displayed defects in root cell elongation specifically (Figures 3.9); such elongation is characterized by rapid cell-wall synthesis [126]. The biosynthesis and assembly of plant cell wall relies on the secretory pathway. Hence, it is possible that the *IRE1*- and *AGB1*-dependent UPR pathways may be involved in the control of secretory pathway activities to achieve optimal root cell elongation. To test this hypothesis, we compared the transcription level of UPR target genes in the root tissue between wild-type Col-0, the *agb1-3* mutant, the *ire1* double mutant, and the *ire1 agb1* triple mutant using qRT-PCR. We found that, while only two out of ten tested UPR target genes showed lower expression in the root of *ire1* double mutant compared with wild-type Col-

0, the transcription of seven UPR target genes was significantly reduced in the *ire1 agb1* triple mutant compared with wild-type Col-0 (Figure 3.11). These data suggest that the enhanced short-root phenotype in the *ire1 agb1* triple mutant compared with the *ire1* double mutant is associated with a lower abundance of UPR target gene transcripts in the root of *ire1 agb1* triple mutant.

Discussion

We have established that *IRE1A* and *IRE1B* are critical for the plant UPR by showing that the loss of function of *IRE1A* and *IRE1B* leads to oversensitivity to ER stress and alteration of UPR target gene induction. By demonstrating that *agb1* enhances the ER stress phenotype in *Ire1*, we have also revealed a functional relationship between IRE1 and a G protein-signaling component in UPR. In addition, we have shown that *IRE1* and AGB1 contribute to root growth, which is considered an elegant model system for organogenesis studies. Hence, we have also associated the UPR transducers with a new biological role in a multicellular context.

IRE1A and *IRE1B* are Critical for the Plant UPR

IRE1 is essential for growth and development in mammals: inactivation of the *IRE1α* gene, encoding one of the two mammalian *IRE1* isoforms, leads to lethality in mouse due to severe placental dysfunction [29, 66]. In yeast, however, the knockout mutant of the single-copy *IRE1* gene is viable [17, 20]. Although *ire1b-2* is not lethal, it is still not clear whether *IRE1B* is dispensable for normal growth and development in plants. A homozygous line of a putative *IRE1B* T-DNA insertion mutant (SALK_018150,

ire1b-1) could not be isolated after selfing of a heterozygous line [111]. If the embryonic or reproductive lethality in *ire1b-1* is not caused by an *IRE1B* locus-linked mutation, then *IRE1B* is an essential gene. This possibility implies that the *ire1b-2* mutant is not a null allele. This hypothesis is supported by our data showing that the *ire1b-2* mutant is not an RNA null mutant (Figure 3.2b). In addition, mammalian *IRE1α* is an essential gene [29, 66] that mediates a diverse biological responses by physical interaction through its linker and kinase domains [37]. Since the T-DNA insertion site of the *ire1b-2* mutant is located at the end of the kinase domain, we propose that stress-sensor and kinase function may be preserved but RNase activity is probably abolished in *ire1b-2*. Hence, the truncated IRE1B protein in *ire1b-2* may still be able to sense ER stress and transduce the signals through protein-protein interaction or other unknown mechanisms. In particular, the partial loss of function of IRE1B in the *ire1b-2* may be sufficient to maintain the signaling responses required for growth and development. Thus, the leaky *ire1b-2* mutant is viable. By contrast, the T-DNA insertion site in the *ire1b-1* mutant is located close to the transmembrane domain, implying that either the membrane insertion of IRE1B or the kinase and RNase activity are affected severely enough to result in complete loss of function in the *ire1b-1* mutant. As *IRE1B* may be essential for embryonic or reproductive development, the null allele, *ire1b-1*, is lethal.

Although it is undetermined whether *IRE1B* is an essential gene, our data clearly show that UPR activation is compromised in *ire1* (Figure 3.3), and both *IRE1A* and *IRE1B* are critical UPR transducers in plants.

While this paper was under review, Nagashima et al. reported a similar ER stress tolerance phenotype of *ire1* using another viable T-DNA insertion line of *IRE1B* (*ire1b-3*)

[34]. The T-DNA insertion in *ire1b-3* is at the N-terminus of transmembrane, suggesting that the transmembrane and kinase domain are probably disrupted in *ire1b-3*. The fact that *ire1b-3* is viable implies that *IRE1B* may not be an essential gene; however, whether *ire1b-3* is an RNA null mutant is still uncertain because the transcript analysis of IRE1B in *ire1b-3* has only been examined by the primer set cross the T-DNA insertion. A complementation test of *ire1b-1* with *IRE1B* will clarify that whether *IRE1B* is an essential gene in plants.

Is bZIP60 the only AtIRE1 substrate in UPR Signaling?

It has been recently demonstrated that the activation of *bZIP60* on ER stress relies on mRNA splicing by IRE1B, but not by IRE1A [112]. Unlike the *ire1* double mutant, neither the *ire1b-2* nor *bzip60-1* mutant showed reduced ER stress tolerance phenotype compared with wild-type Col-0 (Figure 3.3a and 3.6a). This indicates that IRE1A is sufficient to compensate the absence of IRE1B-bZIP60 regulation on the plant UPR. Hence, the splicing of *bZIP60* mRNA may not be the only regulatory mechanism in IRE1-dependent UPR pathway. Furthermore, because there were no detectable phenotypic changes in ER stress tolerance in the *bzip60-1* mutant (Figure 3.6a), we propose that the ER stress-sensitive phenotype of *ire1* is not simply caused by the defects in *bZIP6*0 mRNA splicing. Instead, other target(s) may exist that may be recognized and activated by either IRE1A alone or by both IRE1A and IRE1B. In animals and yeast, only one splicing substrate of IRE1 has been identified and confirmed as a UPR regulator; however, the existence of multiple splicing targets of IRE1 in plants may allow them to respond to a variety of stimuli that they encounter as

sessile organisms. Also, we cannot exclude the possibility that IRE1 may regulate the plant UPR through protein-protein interaction or some unidentified regulatory mechanisms.

Again, while this paper was under review, Nagashima *et al*. reported that the defect of *bZIP60* mRNA splicing was only detected in the *ire1* double mutant, but not the *ire1a* or *ire1b* single mutants. Although there is discrepancy in the results regarding bZIP60 mRNA splicing in single mutants of *IRE1B* [16, 34], the fact that *bzip60-1* did not show an ER stress-sensitive phenotype comparable to *ire1* supports the hypothesis that IRE1 control the plant UPR not only through the splicing of *bZIP60* mRNA.

AGB1 has a Positive Role in Cell Survival upon ER Stress

Unlike *IRE1*, a well-characterized ER stress sensor in yeasts and metazoans, the molecular mechanisms of *AGB1* regulation on the UPR are yet unclear. In particular, it is unknown that whether *AGB1* controls the UPR through a classical G-protein signaling function, such as maintaining ion homeostasis [127]. Sustained ER stress may lead to the apoptotic pathway. Because induction of UPR target genes is higher in the *agb1-3* mutant compared with that of wild-type Col-0 (Figure 3.7c, d), we propose that *AGB1* monitors the induction level of UPR target genes to ensure the UPR is not over-activated, which may lead to cell apoptotic pathway. G-protein components are involved in certain fundamental cellular function, including ion homeostasis and cell proliferation, in both plants and animals [36]; however, to our knowledge, G-protein signaling pathways have not been reported to regulate the UPR in metazoans. It is possible that in *AGB1* has evolved unique functions in the UPR in plants, but we cannot exclude the

possibility that the G-protein signaling pathways are also involved in the metazoan UPR. Uncovering roles of-G protein signaling in the metazoan UPR may be challenging due to the functional redundancy resulted from the presence of multiple copies of G-protein components in metazoans.

Antagonistic Regulation of *IRE1* and *AGB1* on the Plant UPR

Studies of genetic interactions between UPR regulators in *Caenorhabditis elegans* have uncovered complex functional relationships of UPR regulators [128]. Our results suggest that there are two parallel signaling pathways mediated by *IRE1* or *AGB1*, supporting the hypothesis that multiplicity of UPR arms is advantageous for cells in response to diverse stimuli in multicellular organisms. ER protein-folding homeostasis is known to be exquisitely dynamic and to require timely and fine-tuned regulation [129]. The evidence that induction of UPR target genes is lower in the *ire1* double mutant but higher in the *agb1-3* single mutant compared with that of wild-type Col-0 suggests that *IRE1* and *AGB1* act antagonistically to maintain a proper UPR (Figure 3.7c, d). The hypothesis is further supported by the fact that the down-regulation of *AGB1* transcript on ER stress seen in wild-type Col-0 is disrupted in *ire1*.

The Regulation of *IRE1* and *AGB1* on Root Growth

The UPR is essential for growth and development in mammals. Although we cannot exclude the possibility that *IRE1A* and *IRE1B* regulate root growth via a mechanism unrelated to the UPR, the most likely scenario is that the *IRE1*- and *AGB1*-dependent UPR pathways coordinately contribute to primary root growth. The fact that

the *ire1 agb1* triple mutant displayed enhanced phenotypes compared with the *ire1* double mutant in terms of both ER stress sensitivity and root growth defects. Also, the lower transcription level of UPR target genes in the root of the *ire1 agb1* triple mutant suggests that the shorter root length is partially due to compromised secretory capacity (Figure 3.11). Identification and characterization of differentially expressed genes in root tissue between wild-type Col-0 and the *ire1 agb1* triple mutant will further help to determine whether the UPR contribute to root growth, and possibly define novel regulatory pathways in root growth and development.

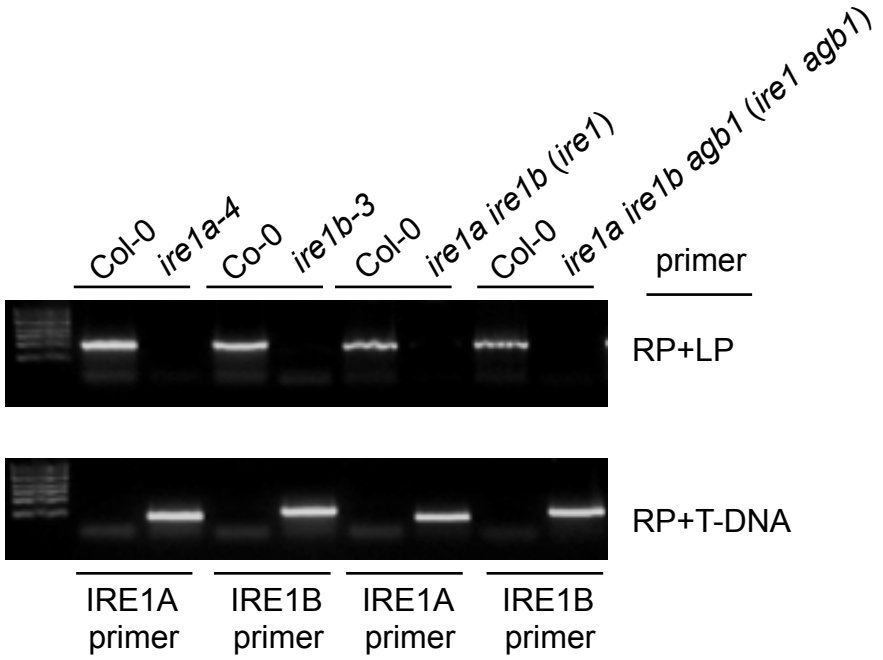

Figure 3.1. Genotyping of mutants of *IRE1A*, *IRE1B*, and *AGB1*.

PCR of genomic DNA from wild-type Col-0, *ire1a-4*, *ire1b-2*, and *ire1* showing the presence of azygous (wild-type Col-0) and homozygous insertion alleles of *IRE1A* and *IRE1B*. Gene-specific primers (LP and RP) for *IRE1A and IRE1B* were used to amplify the upper band. The lower band indicates the presence of a T-DNA insertion; it was amplified with a RP annealing in *IRE1* and a T-DNA primer. Both upper and lower bands were sequenced.

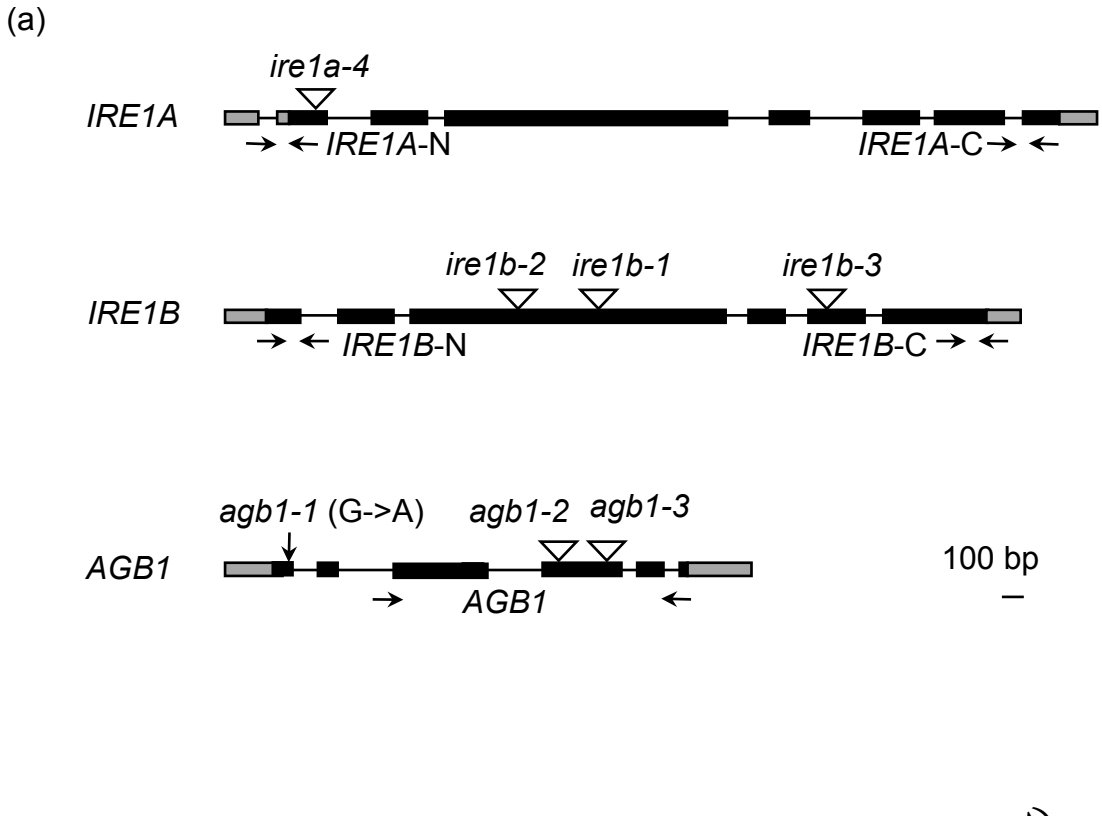

Figure 3.2. Isolation of mutants of *IRE1A*, *IRE1B*, and *AGB1.*

Figure 3.2. (cont'd)

(a) Genomic structure of *IRE1A*, *IRE1B*, and *AGB1*. The coding regions and the UTRs are shown in black and gray rectangles, respectively. The T-DNA insertions in *ire1a-4*, *ire1b-1, ire1b-2*, *ire1b-3, agb1-2* and *agb1-3* are shown as open triangles; the point mutation in *agb1-1* is shown with an arrow.

(b) RT-PCR analyses of *IRE1A*, *IRE1B*, *AGB1*, and UBQ10 transcript in wild-type Col-0, *ire1a-4*, *ire1b-2, ire1a ire1b* (*ire1*), *agb1-3*, and *ire1a ire1b agb1* (*ire1 agb1*). The primer location is shown in (a) and primer sequences are indicated in Table 3.1.

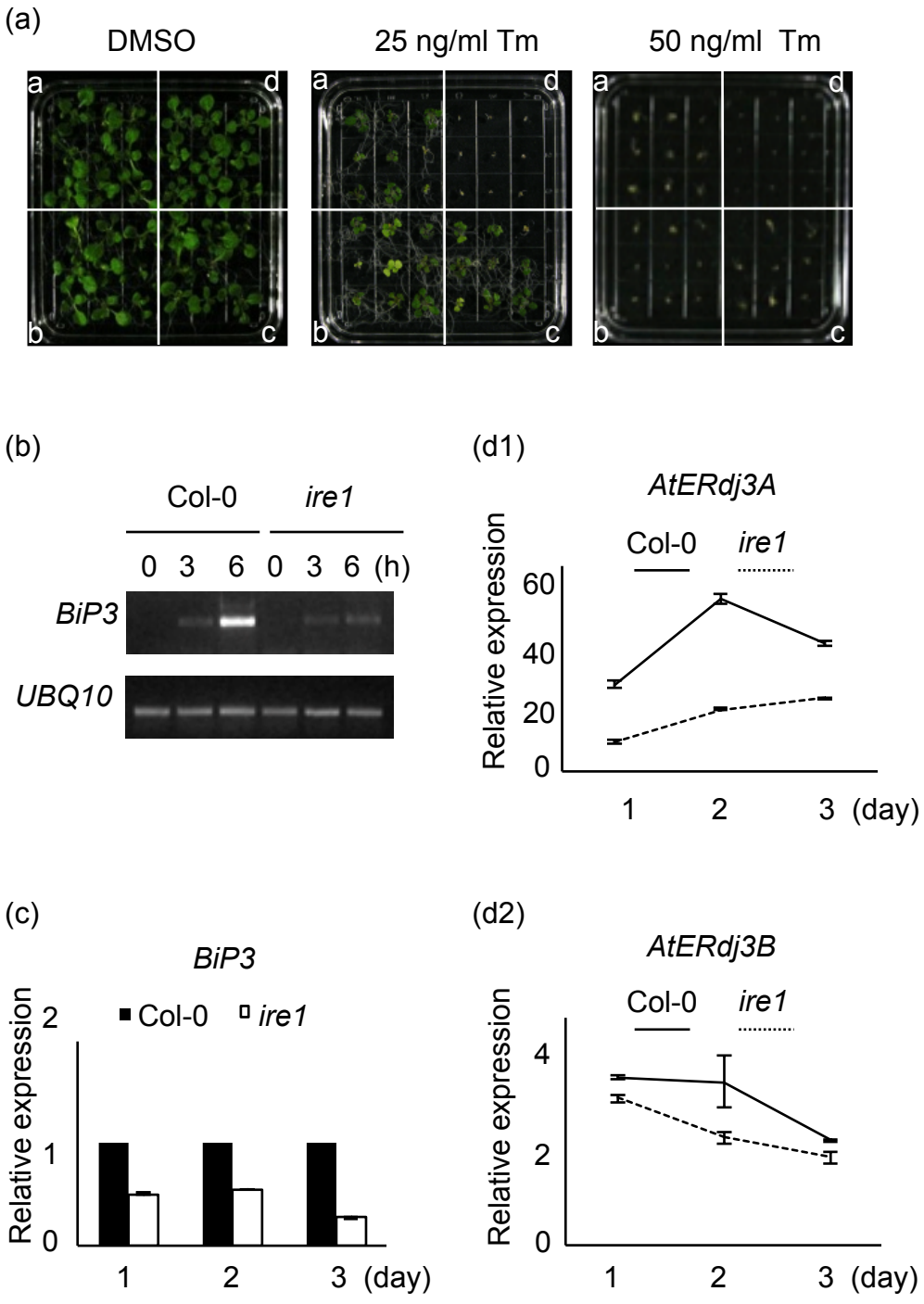

Figure 3.3. IRE1A and IRE1B are required for the plant UPR.

Figure 3.3 (cont'd)

(a) a, Wild-type Col-0; b, *ire1a-4*; c, *ire1b*-2; d, *ire1* were germinated on LS medium containing DMSO, 25 ng/ml or 50 ng/ml Tm for 2 weeks.

(b) RT-PCR of *BiP3* transcript in 4-week-old wild-type Col-0 and *ire1* seedlings after treatment with 10 μg/ml Tm for 0, 3, or 6 h in a hydroponic system.

(c) qRT-PCR of *BiP3* transcript in 2-week-old wild-type Col-0 and *ire1* seedlings after treatment with 50 μg/ml Tm for 1, 2, or 3 days in a plate system.

(d) qRT-PCR of *AtERdj3A* and *AtERdj3B* transcripts under the same condition as (c).

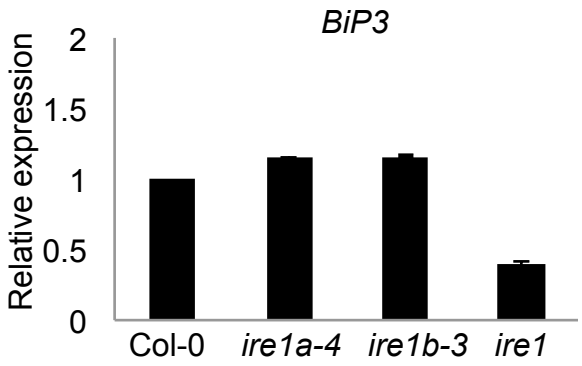

Figure 3.4. No significant differences in *BiP3* induction in *ire1a-4* and *ire1b-2*.

qRT-PCR of *BiP3* transcript in 2-week-old wild-type Col-0, *ire1a-4*, *ire1b-2*, and *ire1* after treatment with 50 μg/ml Tm for 4 h in a plate system.

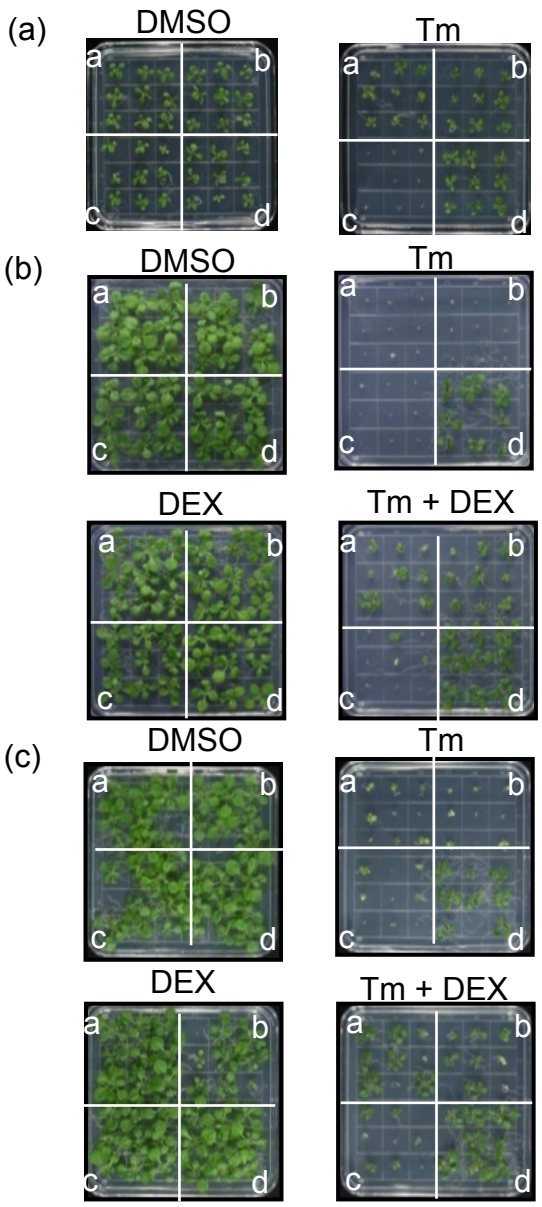

Figure 3.5. Complementation of Tm sensitivity phenotype of *ire1* by *IRE1*A or *IRE1B*.

Figure 3.5 (cont'd)

(a) Complementation of *ire1* by *IRE1A*; b, *ire1* expressing *pIRE1A-IRE1A*#1-7; d, *ire1* expressing *pIRE1A-IRE1A*#2-11; c, *ire1*; a, wild-type seeds germinated on ½ LS containing DMSO or 50 ng/ml Tm. (*ire1 pIRE1A-IRE1A*#1-7 and *ire1 pIRE1A-IRE1A*#2-11 refer to two independent homozygous lines).

(b) Complementation of *ire1* by Dex-inducible-*IRE1A.* a, *ire1* expressing *pDex-IRE1A*#3; b, *ire1* expressing *pDex-IRE1A*#6; c, *ire1*; d, wild-type seeds germinated on ½ LS containing DMSO, 30 µM Dex, 50ng/ml Tm, or 30 µM Dex+50ng g/ml Tm(*ire1 pDex-IRE1A*#3 and *ire1 pDex-IRE1A*#6 refer to two independent T2-segregating lines).

(c) Complementation of *ire1* by Dex-inducible-*IRE1B.* a, *ire1* expressing *pDex-IRE1B*#3; b, *ire1* expressing *pDex-IRE1B*#6; c, *ire1*; d, wild-type seeds germinated on ½ LS containing DMSO, 30 µM Dex, 50ng/ml Tm, or 30 µM Dex+50ng /ml Tm (*ire1 pDex-IRE1B*#3 and *ire1 pDex-IRE1B*#6 refer to two independent T2 segregating lines).

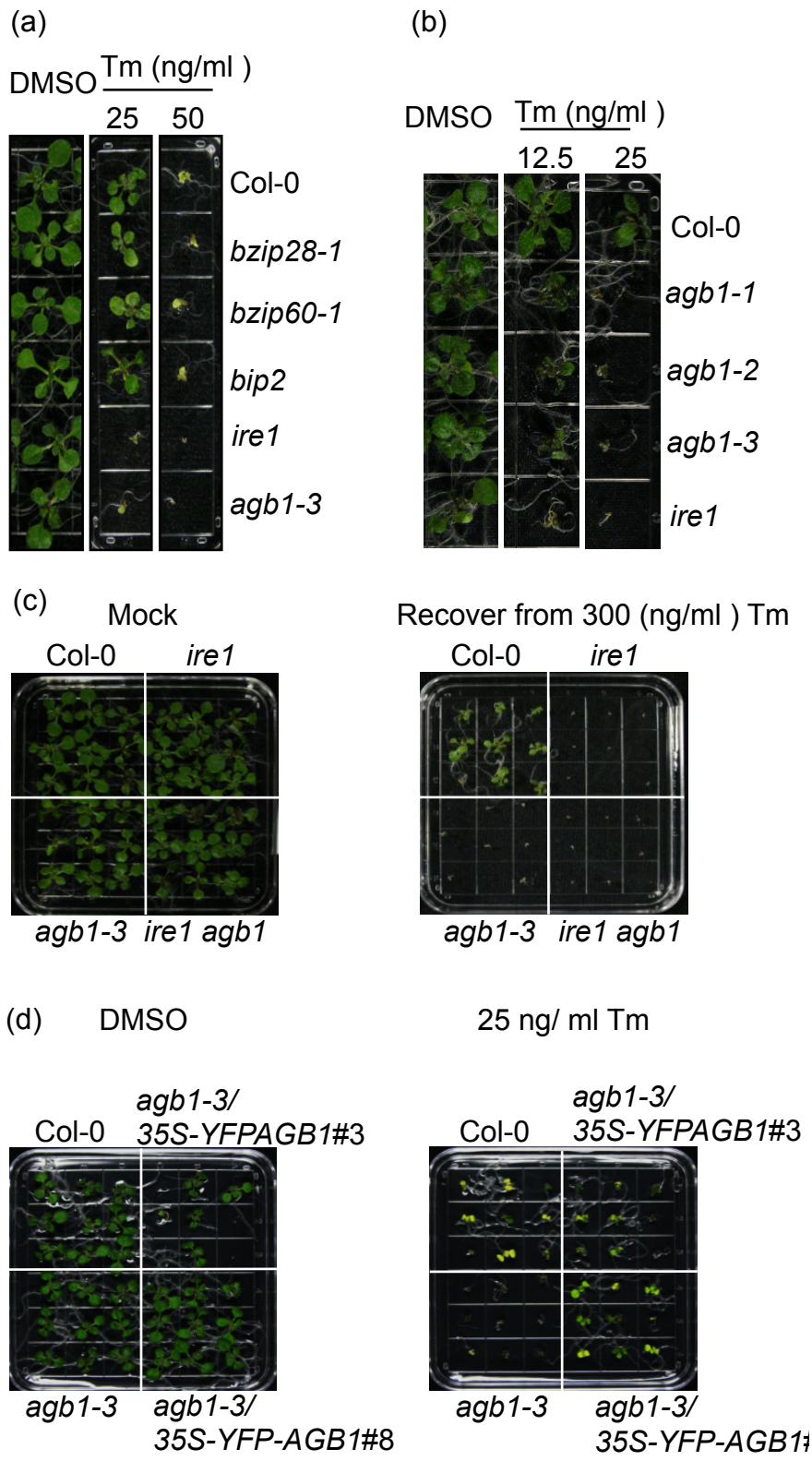

Figure 3.6. Loss-of-function of *AGB1* leads to oversensitivity of ER stress.

Figure 3.6 (cont'd)

(a) Wild-type Col-0, *bzip28-1*, *bzip60-1*, *bip2*, *agb1-3*, and *ire1* were germinated on LS medium containing DMSO, 25 ng/ml or 50 ng/ml Tm for 2 weeks.

(b) Wild-type Col-0, *agb1-1*, *agb1-2*, *agb1-3*, and *ire1* were germinated on LS medium containing DMSO, 12.5 ng/ml or 25 ng/ml Tm for 2 weeks.

(c) Wild-type Col-0, *agb1-3*, *ire1*, and *ire1 agb1* were germinated on ½ LS containing 300 ng/ml Tm for 6 days, and then transferred to ½ LS without Tm. The plants were photographed after 10-day recovery recovered on ½ LS without Tm. Mock control: The plants were germinated on ½ LS with DMSO for 6 days, and then transferred to ½ LS without DMSO or Tm.

(d) Complementation of *agb1-3* by 35S-YFP-AGB1. Wild-type Col-0, *agb1-3*, *agb1-3* expressing 35S-YFP-AGB1 #3, and *agb1-3* expressing 35S-YFP-AGB1 #8 seeds were germinated on ½ LS containing DMSO, or 50ng/ml Tm for 2 weeks (*agb1-3* expressing 35S-YFP-AGB1 #3 and *agb1-3* expressing 35S-YFP-AGB1 #8 refer to two independent T2-segregating lines).

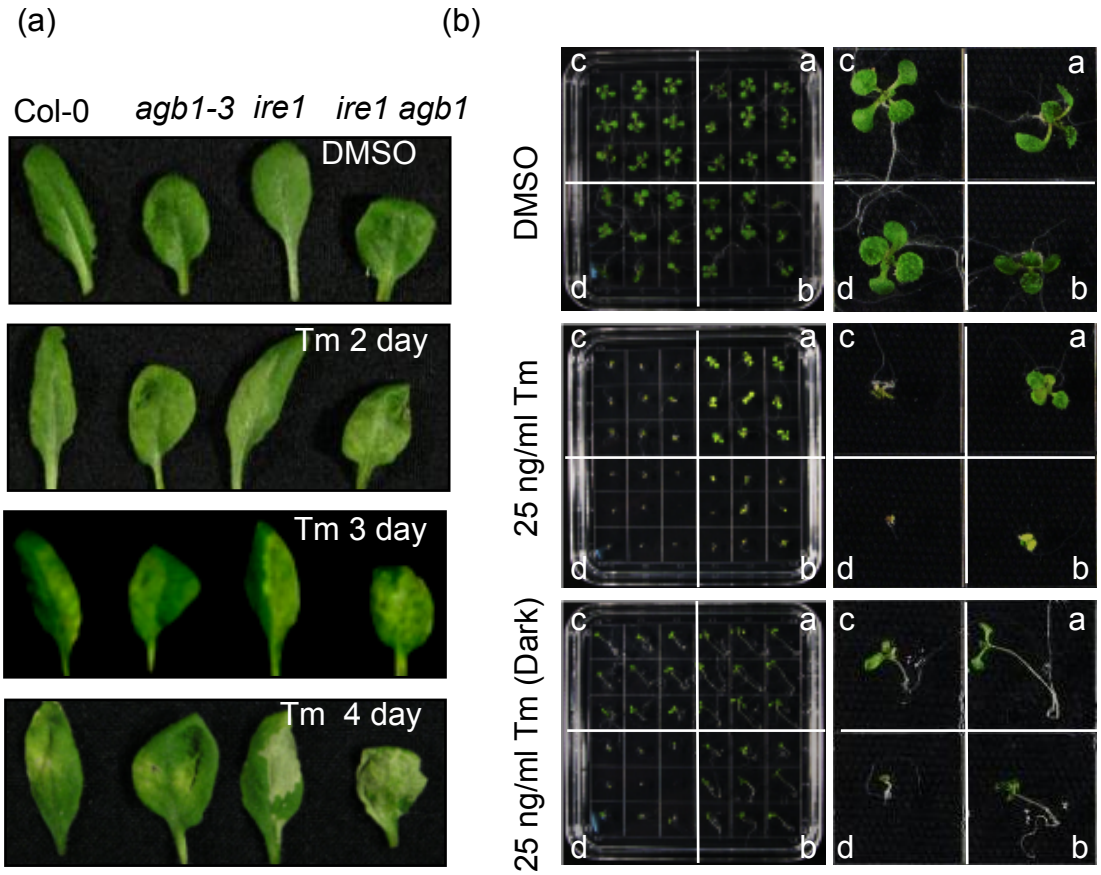

Figure 3.7. *agb1-3* enhances the Tm-sensitive phenotype in *ire1*.

Figure 3.7 (cont'd)

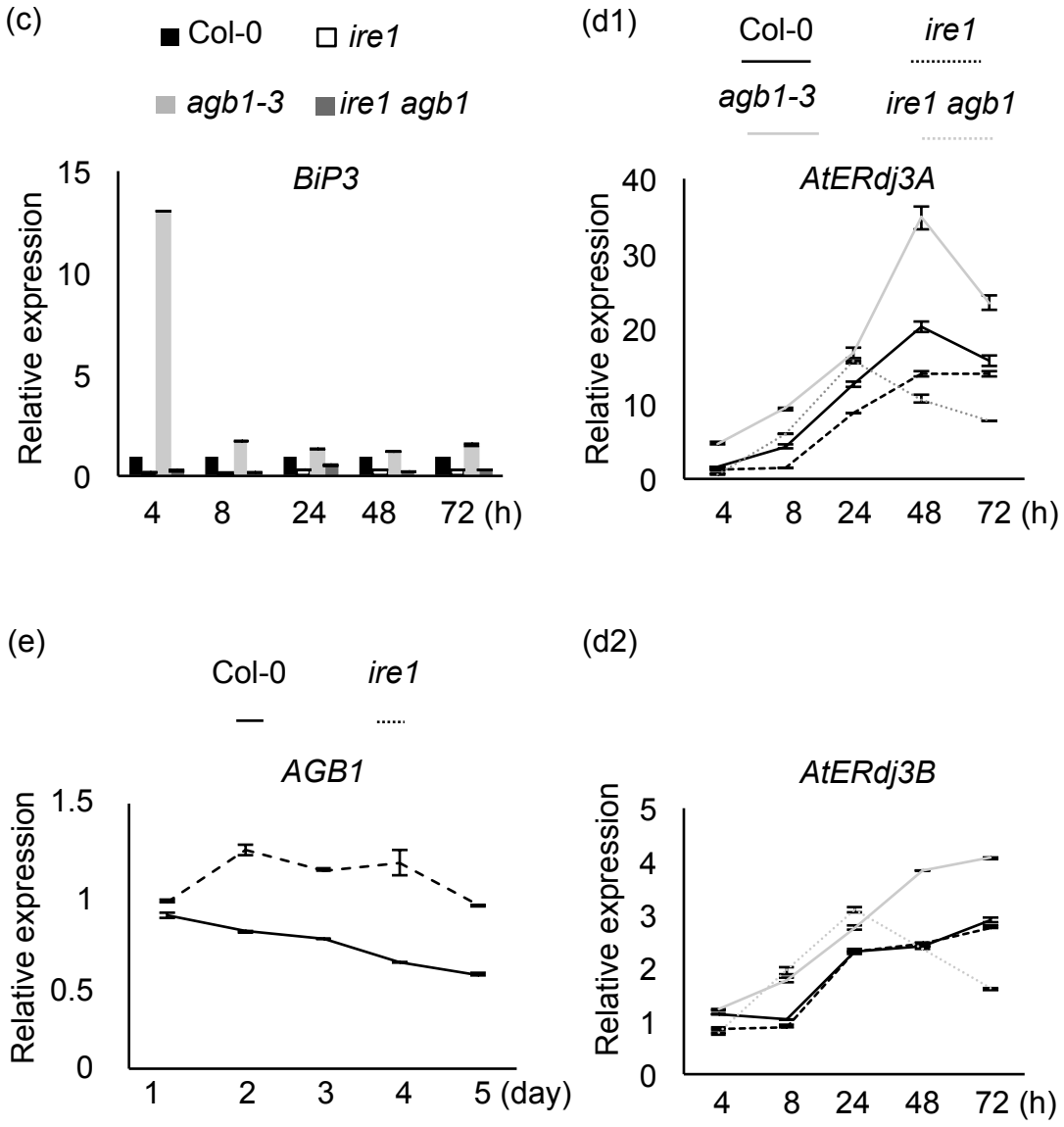

Figure 3.7 (cont'd)

(a) Leaves of 5-week-old wild-type Col-0, *agb1-3*, *ire1,* and *ire1 agb1* were infiltrated with DMSO or 15 μg/ml Tm.

(b) a, wild-type Col-0; b, *agb1-3*; c, *ire1;* and d, *ire1 agb1* were germinated on LS medium containing DMSO or 25 ng/ml Tm under either normal growth or dark conditions for 10 days.

(c) qRT-PCR of *BiP3* transcript in 2-week-old wild-type Col-0, *agb1-3*, *ire1* and *ire1 agb1* after treatment with 50 μg/ml Tm for 4, 8, 24, 48, 72 h Tm in a plate system.

(d) qRT-PCR of *AtERdj3A* (d1) and *AtERdj3B* (d2) transcripts in 2-week-old wild-type Col-0, *agb1-3*, *ire1*, and *ire1 agb1* after treatment with 50 μg/ml Tm for 4, 8, 24, 48, 72 h Tm treatment in a plate system.

(e) qRT-PCR of *AGB1* transcript in 2-week-old wild-type Col-0 and *ire1* after treatment with 50 μg/ml Tm for 1, 2, 3, 4, 5 day treatment in a plate system.

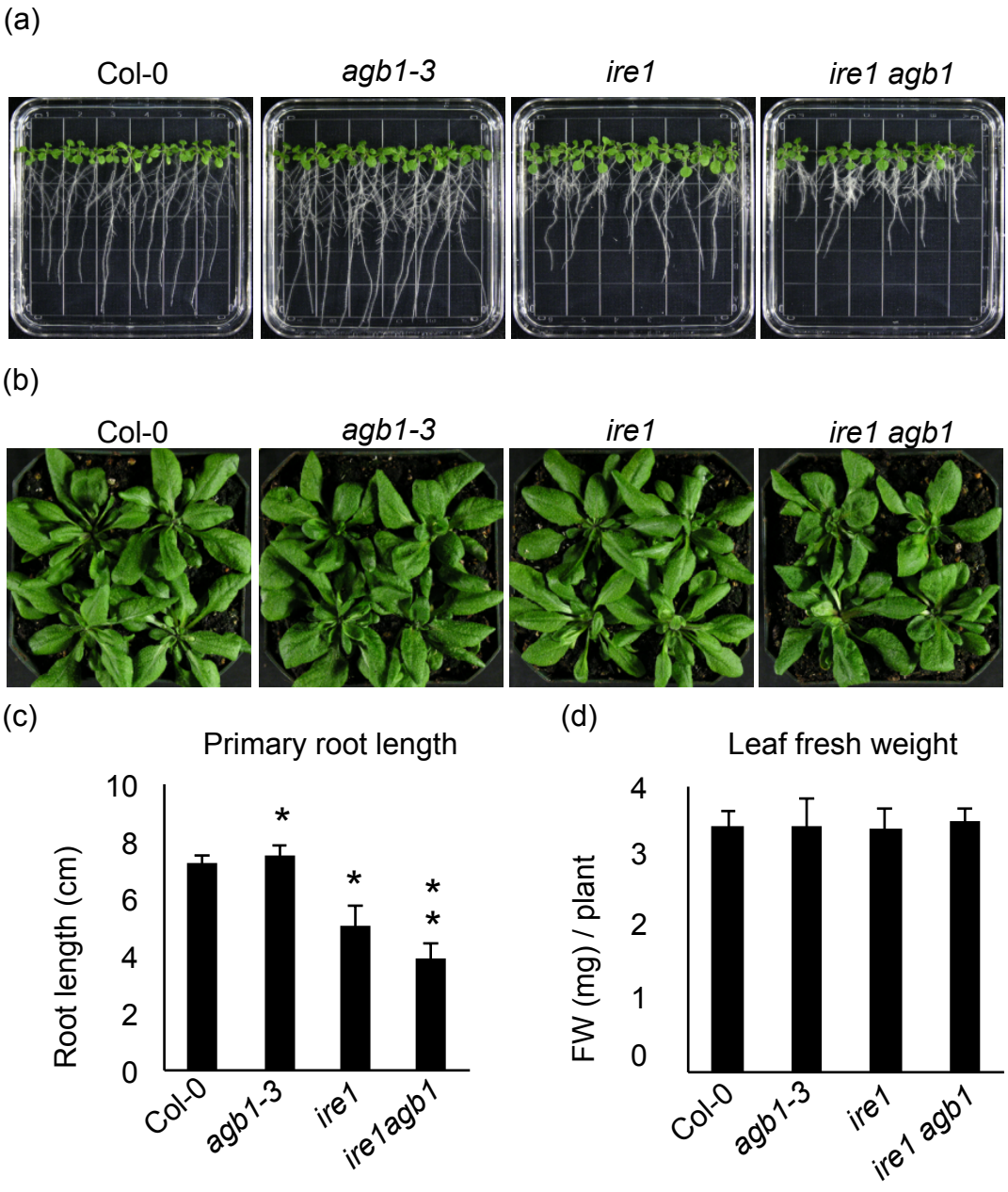

Figure 3.8. *agb1-3* enhances the short-root phenotype in *ire1*.

Figure 3.8 (cont'd)

(a) Wild-type Col-0, *agb1-3*, *ire1*, and *ire1 agb1* were grown on LS medium for 2 weeks.

(b) Macromorphology of wild-type Col-0, *agb1-3*, *ire1,* and *ire1 agb1*.

(c) Measurement of primary root length (cm) of wild-type Col-0, *agb1-3*, *ire1,* and *ire1 agb1*. An asterisk indicates significant differences between *agb1-3* and wild-type Col-0 or between *ire1* and wild-type Col-0. The double asterisk indicates a significant difference between *ire1* and *ire1 agb1*.

(d) Fresh weight (mg) of leaves from rosettes of 2-week-old plants.

(a)

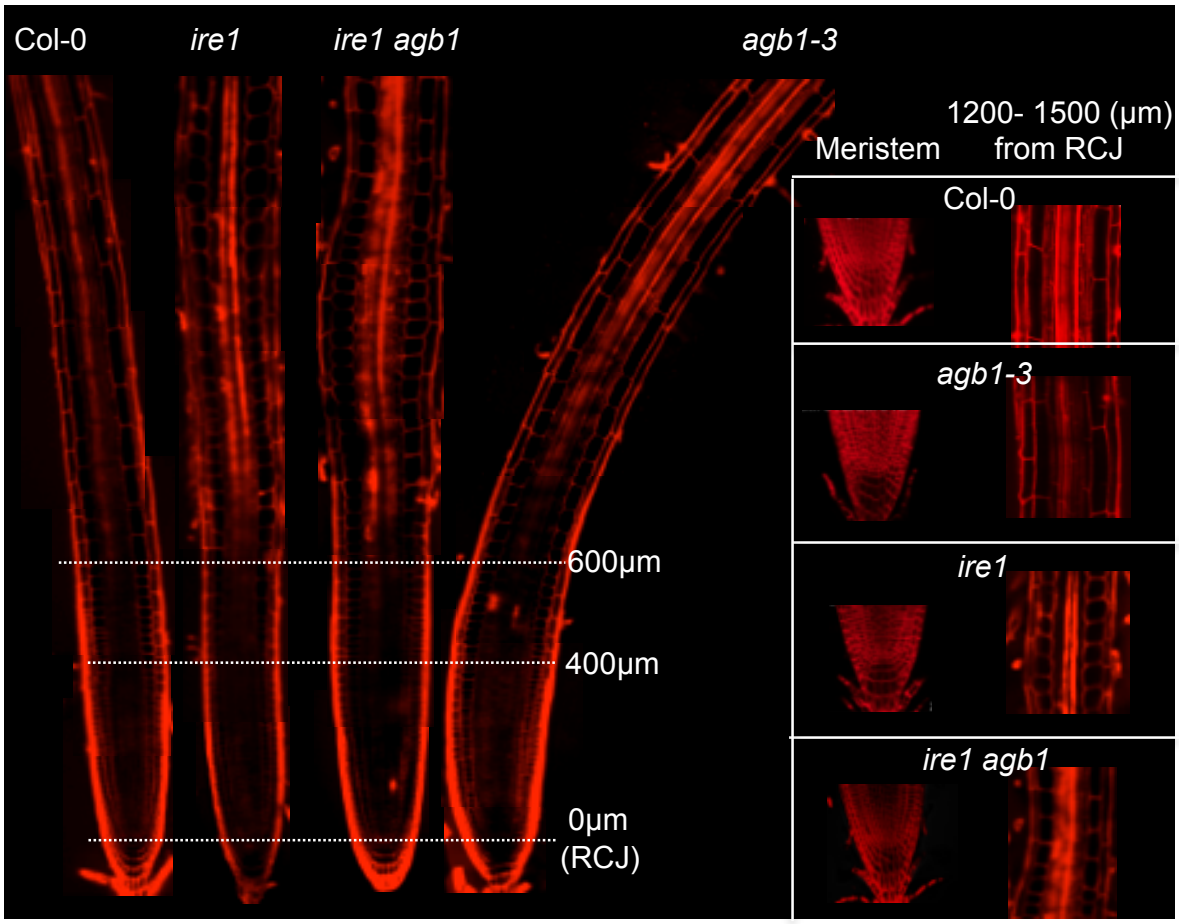

(b)

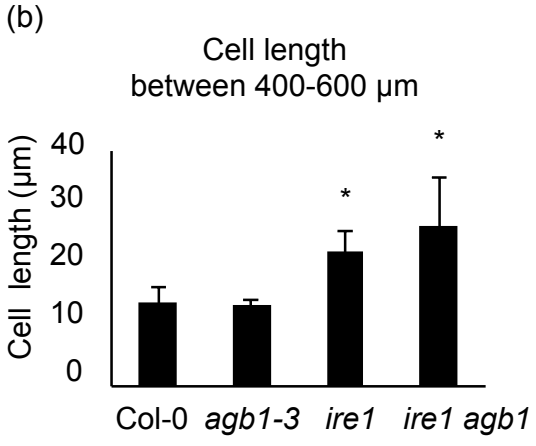

(c)

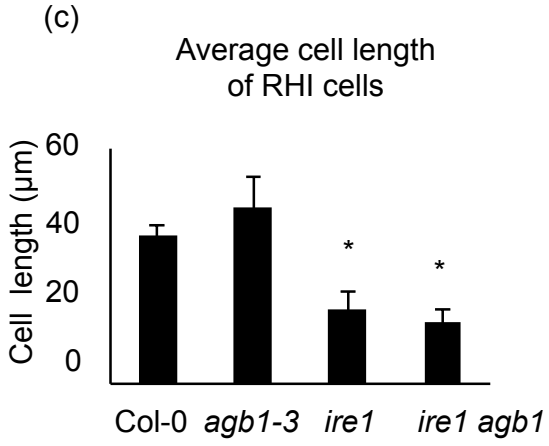

Figure 3.9. The elongation zone of *ire1* and *ire1 agb1* root is defective.

Figure 3.9 (cont'd)

(a) Confocal microscopy images of roots (longitudinal axis) of wild-type Col-0, *ire1, ire1 agb1*, and *agb1-3* labeled with PI. '0 μm' is the position of the root cap junction (RCJ).

(b) Mean cell length for wild-type Col-0 and mutants in the regions between the 400-600 μm from the RCJ.

(c) Mean cell length for wild-type Col-0 and mutants in the regions showing root hair initiation (RHI).

Asterisks indicate significant differences between the mutants and wild-type Col-0.

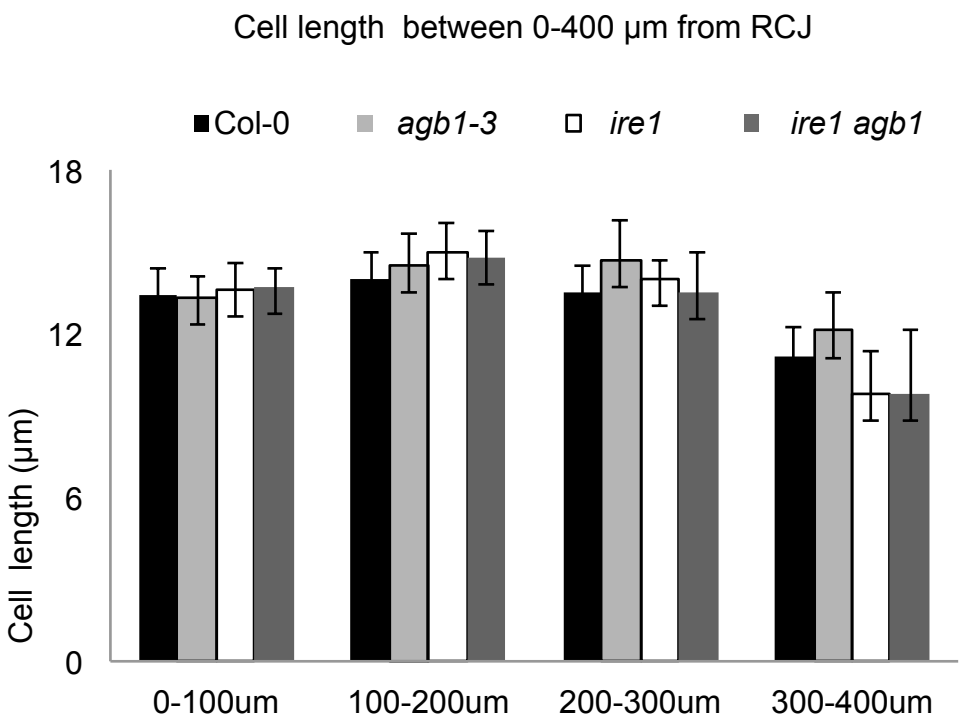

Figure 3.10. No significant differences in cell length in the root meristems of *agb1-3*, *ire1*, and *ire1 agb1*.

Mean cell number for wild-type Col-0 and mutants in the regions within 400 µm from the root cap junction.

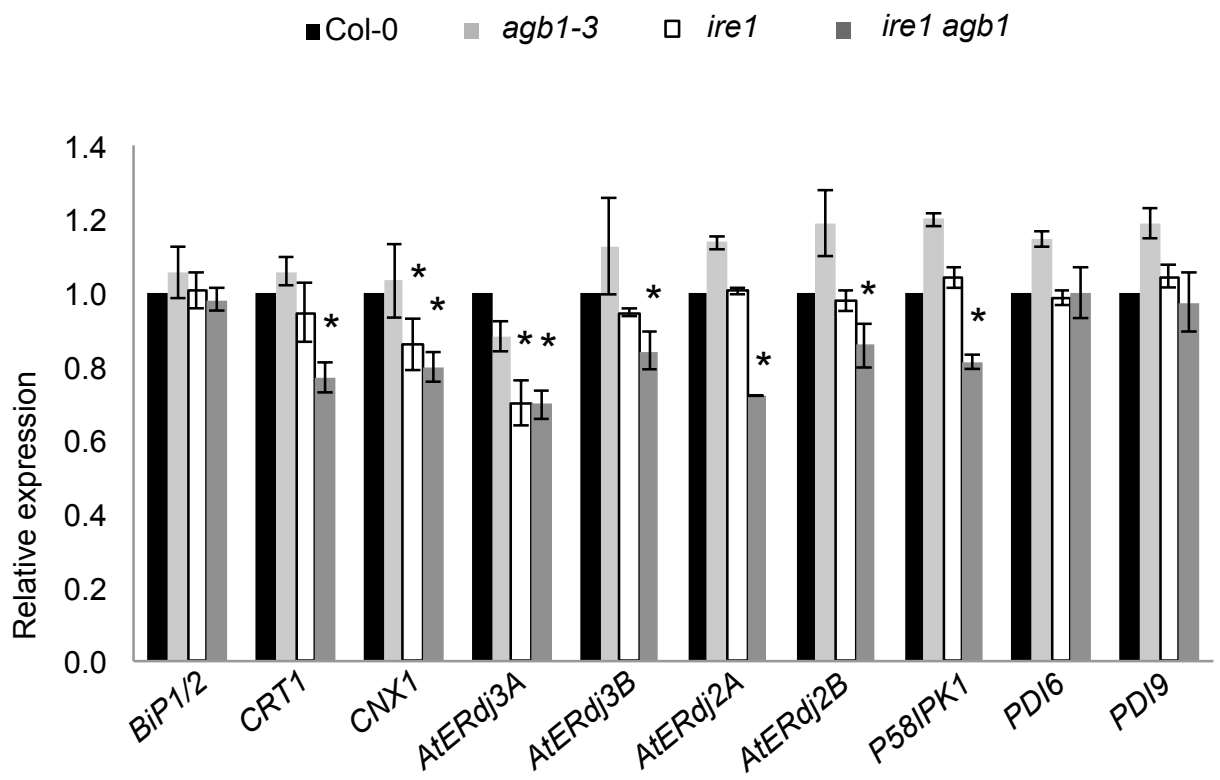

Figure 3.11. Expression of UPR target genes is lower in the root of *ire1 agb1*.

qRT-PCR of *BiP1/2*, *CRT1*, *CNX1, P58IPK1, PDI6, PDI9, AtERdj3A, AtERdj3B*, *AtERdj2A*, and *AtERdj2B* transcripts in the root tissue of 2-week-old wild-type Col-0, *agb1-3*, *ire1*, and *ire1 agb1*. Asterisk indicate significant differences between *ire1* and wild-type Col-0 or between *ire1 agb1* and wild-type Col-0.

Table 3.1. DNA primers used in this study

primers	Sequence (5'–3')
WiscDsLox420D09 RP	tatctccgatccatcgttgac
WiscDsLox420D09 LP	caaaatcttcagtgctagcgg
WiscDsLox LP	aacgtccgcaat gtgttattaagttg
SAIL_238_F07RP	gaaggaaaacggacatccttc
SAIL_238_F07LP	cctctcgaacccttcaggtac
SAIL-LB2	gcttcctattatatcttcccaaattaccaataca
SALK_061896RP	tgtgaatcctgctgtaatccc
SALK_061896LP	tcattagattggacaccggag
LBa1	tggttcacgtagtgggccatcg
AtIRE1A-N For	agaccctgatttacgtcctagc
AtIRE1A-N Rev	ccgacaagttcctgaatttccg
AtIRE1B-N For	caaatttgagaccgagagcac
AtIRE1B-N Rev	ctagaatacagtggtcttag
AtIRE1A-C For	agaccctgatttacgtcctagc
AtIRE1A-C Rev	ccgacaagttcctgaatttccg
AtIRE1B-C For	caaatttgagaccgagagcac
AtIRE1B-C Rev	ctagaatacagtggtcttag

Table 3.1 (cont'd)

AGB1 For	gacacaccggaaaggtttattcattag
AGB1 Rev	caaacgcccatatctttagatttgaatc
BiP3 For	gtttggtttttctgactgtgcttgatttttttaatg
BiP3 Rev	catcattgaaatacgctggaaccgtgatc
UBQ10 For	tcaattctctctaccgtgatcaagatgca
UBQ10 Rev	ggtgtcagaactctccacctcaagagta
BiP3-qP For	aaccgcgagcttggaaaat
BiP3-qP Rev	tcccctgggtgcaggaa
AtERdj3A-qP For	tcaagtggtggtggtttcaact
AtEdj3A-qP Rev	cccaccgcccatattttg
AtERdj3B-qP For	gaggaggcggcatgaatatg
AtERdj3B-qP Rev	ccatcgaacctccaccaaaa
AGB1-qP For	gcggcgcaaggacgta
AGB1-qP Rev	acaacaaaccagatccgttgct
BiP1/2-qP For	ccaccggccccaagag
BiP1/2-qP Rev	ggcgtccacttcgaatgtg
PDI6-qP For	cgaagtggctttgtcattcca
PDI6-qP Rev	gcggttgcgtccaatttt
PDI9-qP For	ggccctgttgaagtgactgaa
PDI9-qP Rev	cagcagaaccacacttcttttcc

Table 3.1 (cont'd)

CNX1-qP For	gtgtcctcgtcgccattgt
CNX1-qP Rev	ttgccaccaaagataagcttga
CRT1-qP For	gatcaagaaggaggtcccatgt
CRT1-qP Rev	gacggaggacgaaggtgtaca
AtERdj2A-qP For	tgggcttgtaggcgctctt
AtERdj2A-qP Rev	aacccaatagttttcctccttgtg
AtERdj2B-qP For	tgaaacgtcccaatggactca
AtERdj2B-qP Rev	cctctttgtggaaaggaaagtaagg
AtP58IPK-qP For	gcgttatagtgatgccctcgat
AtP58IPK-qP Rev	gaaagcgcagggtctgctt
IPP2-qP For	atttgcccatcgtcctctgt
IPP2-qP Rev	gagaaagcacgaaaattcggtaa
attB1-AGB1+1	ggggacaagtttgtacaaaaaagcaggcttcatgtctgtctccgagctc
attB2-AGB1+1132	ggggaccactttgtacaagaaagctgggtccaaatcactctcctgtgtc
attB1-IRE1A-1503	ggggacaagtttgtacaaaaaagcaggcttctgactactaaaattttcaattc
attB2-IRE1A+2526	ggggaccactttgtacaagaaagctgggtcttagatgatgtcgcatttgaag
XhoI-IRE1B+1	ctgggtctcgagatgtggttattggccatctc
SpeI-IRE1B+2646	ctgggtactagtctagaatacagtggtcttagag
XhoI-IRE1A+1/F	ctgggtctcgagatgccgccgagatgtcctttc
XhoI-IRE1A+2526/	ctgggtctcgagttagatgatgtcgcatttgaag

Methods

Plant Materials and Growth Conditions

Arabidopsis thaliana ecotype Columbia (Col-0) was used as the wild-type control. *Arabidopsis* transfer-DNA insertion (T-DNA) mutants, *ire1a-4* (WISCDSLOX420D09*)*, *ire1b-2* (SAIL_238_F07), *agb1-3* (SALK_061896), *agb1-2* (CS6535), *bzip28-1* (SALK_132285), *bzip60-1* (SALK_050203), *bip2* (SALK_047956) and the mutant with point mutation *agb1-1* (CS3976) were obtained from the *Arabidopsis* Biological Resource Center (Ohio State University, Columbus OH [109, 113, 119, 121]. The primers used for genotyping are listed in the Table S1. Surface-sterilized seeds were plated directly onto square Petri dishes containing ½ Linsmaier and Skoog's (LS) medium, 1.5% (w/v) sucrose, and 0.4% Phytagel. For the normal growth condition, plants were grown at 21°C under 16-h-light/8-h-dark conditions.

Tm Treatment

In a plate system, the Tm (Sigma, T7765; dissolved in DMSO) was directly added in the half-strength LS medium containing 1.5% (w/v) sucrose and 0.4% Phytagel, at the concentrations indicated in the text. Seeds were directly germinated in Tm-containing medium for observation of ER stress tolerance. To harvest tissue for UPR gene expression analysis, the seeds were germinated in half-strength LS medium without Tm for 2 weeks, and then transferred to Tm-containing medium. In a hydroponic system (Araponics), seedlings were grown in liquid medium (FloraSeries by GHE) without Tm for 4 weeks; then 10 mg/ml Tm dissolved in DMSO was added in the liquid medium. For the infiltration method, needleless syringe was used to infiltrate 15 μg/ml Tm into the

abaxial side of leaves. As mock control of the Tm treatment, a volume of DMSO equivalent to that of used to dissolve Tm in each method was used in the same experimental procedure.

Genotyping and Isolation of Multiple T-DNA Insertion Mutants

Genotyping of the T-DNA insertion mutants was accomplished by genomic DNA extraction followed by DNA amplification with T-DNA and gene-specific primers. The primers used for genotyping and phenotyping are listed in the Table S1. PCR experiments were performed in standard conditions and were carried out using 0.2 mM dNTPs, 0.2 μM primer, and 1 unit of *Taq* polymerase (Promega). Homozygous lines for T-DNA insertion of transgenic plants were isolated through segregation analyses on media containing the selective marker encoded in the T-DNA. Isolation of multi-allelic lines was performed through reciprocal crosses followed by genotyping of the F2 generation.

RNA Extraction and Quantitative RT–PCR (qRT–PCR) Analysis

Total RNA was extracted from whole seedlings using the RNeasy Plant Mini Kit (Qiagen) and treated with DNaseI (Qiagen). All samples within an experiment were reverse transcribed at the same time using High Capacity RNA-to-cDNA Master Mix Kit (ABI 4390777). A ‘‘No-RT’’ reaction, in which RNA was subjected to the same conditions of cDNA synthesis except without reverse transcriptase, was included as a negative control in all qRT–PCR assays to ensure the purity of RNA samples. Real-time qRT-PCR with SYBR green detection was performed in triplicate using the Applied

Biosystems 7500 Fast Real-Time PCR System. Data were analyzed by the DDCT method. Transcript level was normalized to *ISOPENTENYL PYROPHOSPHATE* (*IPP2*) for each sample. For *AtERdj3A*, *AtERdj3B*, and *AGB1*, the relative transcript level is expressed as the fold change (mean ± SEM) in each genotype under Tm treatment relative to the mock control (set to a value of 1). For *BiP3*, as the transcript level is extremely low in the mock control, the relative transcript level is expressed as the fold change (mean ± SEM) in *ire1* under each time point of Tm treatment relative to the wild-type Col-0 under the same treatment condition (set to a value of 1). For all the UPR-response genes examined in the root or shoot tissue, the relative transcript level is expressed as the fold change (mean ± SEM) in each genotype relative to the wild-type Col-0 under the normal growth condition (set to a value of 1). We performed three independent experiments in triplicates. Values are presented in the figures are averages of three samples from one representative experiment. A similar pattern was observed from three independent biological replicates.

Phenotypical Analyses

Root length measurements were averaged from 30 plants for each genotype; aerial tissue from 10 plants was pooled to estimate the fresh weight. Values were averaged from 3 individual samples for each genotype. Cell length calculations were performed on 10 roots for each genotype. Statistical analyses included the Student's two-tailed t-test, assuming equal variance; data with $p<0.05$ were considered significant.

Arabidopsis Stable Transformation and Complementation

For cloning in the Dex-inducible vector (pTA7002), standard molecular cloning techniques were used. Complementation of *agb1-3* was achieved by a 35S-AGB1-YFP fusion. pAtIRE1A-AtIRE1A and 35S-YFP-AGB1 were generated using binary vectors pGWB1 and pEarleygate104, respectively [130, 131]. The genomic or coding regions of genes were amplified with the Gateway-compatible primers from the cDNA synthesized from total RNA of wild-type (Col-0) seedlings using Phusion High-Fidelity DNA polymerase (New England Biolabs). The PCR fragments were cloned to the donor vector (pDonorTM207) and destination vectors pGWB1 and pEarleygate104. Primer sequences used in this work are listed in Table 3.1. *Arabidopsis* plants were transformed by the floral dip method [132] and transformants were selected on half-strength LS media supplemented with hygromycin (final concentration, 20 μg/ml) and 0.8% (w/v) agar. Induction of Dex-inducible clone was achieved with DEX (30 μM; Sigma).

Confocal Laser Scanning Microscopy

An inverted laser scanning confocal microscope (LSM510 META, Carl Zeiss) was used for imaging analyses. Imaging of propidium iodide-labeled roots (10 μg/ml) was carried out using a 543-nm excitation of a He/Ne laser and a LP 560 emission filter. Post-acquisition analyses were performed with Zeiss AIM software. Adobe Illustrator was used for further image handling.

Acknowledgements

We acknowledge support by the Chemical Sciences, Geosciences and Biosciences Division, Office of Basic Energy Sciences, Office of Science, U.S. Department of Energy (award number DE-FG02-91ER20021) and National Aeronautics and Space Agency (NNH08ZTT003N NRA – 08-FSB_Prop-0052)

CHAPTER 4

Inter-regulation of the unfolded protein response and auxin signaling

This section has been accepted in the Plant Journal

DOI: 10.1111/tpj.12373

Abstract

The unfolded protein response (UPR) is a signaling network triggered by overload of protein-folding demand in the endoplasmic reticulum (ER), a condition termed ER stress. The UPR is critical for growth and development; nonetheless, connections between the UPR and other cellular regulatory processes remain largely unknown. Here, we identify a novel link between the UPR and the phytohormone auxin, a master regulator of plant physiology. We show that ER stress triggers down-regulation of auxin receptors and transporters in *Arabidopsis thaliana*. We also demonstrate that an *Arabidopsis* mutant of a conserved ER stress sensor IRE1 exhibits defects in the auxin response and levels. These data not only support that the plant IRE1 is required for auxin homeostasis, they also reveal a species-specific feature of IRE1 in multicellular eukaryotes. Furthermore, by establishing that UPR activation is reduced in mutants of ER-localized auxin transporters, including PIN5, we define a long-neglected biological significance of ER-based auxin regulation. We further reveal the functional relationship of IRE1 and PIN5 by showing that an *ire1 pin5* triple mutant enhances defects of UPR activation and auxin homeostasis in *ire1* or *pin5*. Our results imply that the plant UPR has evolved a hormone-dependent strategy for coordinating ER function with physiological processes.

Introduction

The UPR adjusts the ER protein folding capacity to cope with the dynamic secretory protein demands in cells [1, 2]. When the ER protein folding machinery is competent, stress sensors are restrained in the ER by ER-resident chaperones [133, 134]. Accumulation of unfolded proteins in the ER activates ER stress sensors either by causing them to dissociate from protein chaperones or to associate with unfolded proteins [96, 133-135]. Activated ER stress sensors transmit signals to the nucleus for transcriptional regulation of UPR target genes [1, 2]. If ER stress is not resolved, the UPR triggers the activation of cell death [67]. IRE1, the only identified ER stress sensor in yeast, is conserved in multicellular eukaryotes [17, 136]. Two IRE1 homologues, IRE1A and IRE1B, have been proven to be functional ER stress sensors in *Arabidopsis* [39, 40]. The activation of IRE1 relies on auto-phosphorylation, conformational modification, and oligomerization. Activated IRE1 splices an intron from the mRNA of a UPR-specific bZIP transcription factor [19]. The spliced transcription factor enters the nucleus to control UPR target genes [19].

The UPR is critical for numerous fundamental cellular processes [28]. IRE1 alpha knockout mice exhibit embryonic lethality [66]. Dysregulation of the UPR contributes to the pathology of several significant diseases, including diabetes, neurodegeneration, and cancer [137]. In *Arabidopsis*, mutations of IRE1 lead to a short primary root phenotype [39]. Despite the high significance of the UPR in growth and development in multicellular eukaryotes, the regulatory connections between the UPR and other cellular responses remain unclear.

Because the hormone auxin has profound roles in most plant developmental processes, nucleus-based auxin signaling and plasma membrane (PM)-based intercellular auxin transport have been intensively studied. Three major classes of auxin signaling regulators exist in the nucleus: TIR1/AFB auxin co-receptors [138-140], AUX/IAA transcriptional repressors [141], and ARF transcription factors [142]. To initiate the auxin response in the nucleus, TIR1/AFBs and auxin coordinately promote degradation of AUX/IAA transcriptional repressors. Consequently, ARFs are released from repression and activate the transcription of auxin responsive genes [138-140].

Directional (polar) transport between cells is another crucial regulatory aspect of the auxin response. The auxin efflux carriers of the PIN family are the principal components of the polar auxin transport machinery [143, 144]. Based on protein topology and subcellular localization, PINs can be classified into PM- or ER-localized types [145-147]. While PM-based intercellular auxin transport has been considered the most critical point of regulation in the auxin response, it has recently been revealed that ER-based auxin regulation is also important. A putative auxin receptor, ABP1, and several auxin transporters (PIN5, PIN6, PIN8, and PILSs) have been shown to localize to the ER. The requirement of the ER-localized regulators in the auxin response underscores the existence of ER-based auxin biology [145-148]. Despite accumulating evidence that the ER is crucial for auxin regulation [149], the physiological impact of ER-based auxin signaling is largely unknown.

As the UPR is critical for growth and development, we sought to identify the regulatory connection between the UPR and other cellular regulatory processes. Given the central roles of auxin in numerous aspects of plant physiology, we hypothesized that

the UPR regulates auxin signaling for coordinating secretory activities and physiological responses. Through biochemical, molecular biology, and genetic analyses, we demonstrate a connection between the UPR and auxin biology. Specifically, we show that ER stress negatively influences auxin signaling and that the ER-based auxin homoeostasis is important for UPR activation, supporting that the plant UPR alters auxin signaling to cope with ER stress. On the contrary, by establishing that IRE1 is required for the auxin responses, our work reveals that IRE1 has a specific role in hormonal signaling. The regulatory connections between the UPR and auxin biology revealed here hint that plants have evolved an organism-specific strategy to maintain balance between stress adaption and growth regulation.

Results

ER Stress Alters the Expression of Auxin Regulators

To examine whether ER stress modulates the transcription of auxin regulators, we monitored the expression of four auxin co-receptors: *TIR1*, *AFB1*, *AFB2,* and *AFB3* (*TIR1*/*AFBs*), under ER stress. The UPR was activated by inhibiting protein *N*-glycosylation using a classical ER stress inducer termed tunicamycin (Tm). *Arabidopsis* seedlings were subjected to Tm for various periods of time, as adopted in established protocols [26, 53, 75]. The transcriptional induction of UPR target genes is a molecular indication of UPR activation. To quantify the UPR activation levels, we monitored the transcription of classical UPR activation indicators, *BiP1/2* and *PDI6* over a 4-hr time course of Tm treatment using quantitative reverse transcription–polymerase chain

reaction (qRT-PCR) analyses [150]. *BiP1/2* is an ER chaperone essential for the UPR and a primary UPR target gene. *PDI6* encodes protein disulfide isomerase. Similar to BiP proteins, upregulation of PDI6 under ER stress contributes to increasing protein folding capacity in the ER. qRT-PCR showed that both *BiP1/2* and *PDI6* were induced more than 2-fold at 0.5 h of Tm treatment and their levels increased over the time course of treatment (Figure 4.1). Interestingly, we found that there was a 20 to 55% percent reduction in the level of *TIR1*/*AFB* transcripts 4 h after Tm treatment in seedlings (Figure 4.2a). These results imply that ER stress negatively influences auxin signaling by repressing *TIR1*/*AFB* transcripts. As *TIR1*/*AFBs* activate the auxin response by promoting degradation of the AUX/IAA transcriptional repressors, we sought to determine whether the ER stress-induced repression of *TIR1*/*AFB* transcripts resulted in the stabilization of AUX/IAA proteins. To do so, we conducted western blot analyses using transgenic *Arabidopsis* plants expressing DII-VENUS, a fluorescently tagged auxin-interaction domain (DII) of AUX/IAAs that contains the canonical degron responsible for auxin- and TIR1/AFB-mediated protein degradation [151]. As the stabilization of AUX/IAAs is a downstream response of TIR1/AFB reduction, we examined DII-VENUS protein levels 6 h after Tm treatment. Indeed, immunoblot analyses showed that the protein levels of DII-VENUS increased in wild-type Col-0 roots under ER stress treatment (Figure 4.2b). Consistent with the western blot analysis results, a confocal microscopy approach revealed that DII-VENUS fluorescence levels, and therefore AUX/IAA protein levels, were consistently greater in roots challenged by the ER stress inducer than in mock-treated ones (Figure 4.2c). Together these observations support that ER stress leads to an increase in AUX/IAA levels, which is

most likely a consequence of protein stabilization resulting from the down-regulation of *TIR1*/*AFBs* (Figure 4.2a).

Next, we investigated whether ER stress could control the transcription of auxin transporters. Using qRT-PCR analyses, we detected a 30-80% decrease in the mRNA levels of *PIN1*, *PIN2*, *PIN3*, *PIN4*, *PIN5*, *PIN6*, and *PIN7* in wild-type Col-0 seedlings during ER stress treatment (Figure 4.2d). In contrast, the transcriptional levels of an ER-associated ethylene receptor (ETR1), two ER-localized cytokinin receptors (AHK2 and AHK3), three nuclear protein (RAN2, ABH1, and FIB1), and two secretory proteins (VSR1 and SCAMP3) [152-158] remained unchanged in ER stress conditions (Figure 4.3). Thus, we conclude that the Tm-induced decrease in the abundance of *TIR1*/*AFB* and *PIN* transcripts is a specific cellular response. When ER stress was triggered by reduction of disulfide bond formation using dithiotreitol (DTT) treatment, similar down-regulation of *TIR1/AFB* and *PIN* transcripts was observed (Figure 4.4). Overall, these results show that ER stress specifically modulates the auxin response by repressing the transcription of auxin co-receptors and transporters.

Next, we examined whether either IRE1 or TIR1/AFBs is essential for ER stress-induced down-regulation of auxin regulators. To do so, we performed the same ER stress treatment coupled with qRT-PCR analyses in an *ire1a ire1b* (*ire1*) double mutant and a *tir1 afb1 afb2 afb3* (*tir1 afbs*) mutant [39, 138]. In *ire1*, both *TIR1*/*AFB* and *PIN* transcripts were still reduced under ER stress conditions (Figure 4.5a-c), similar to the decreased *TIR1*/*AFB* and *PIN* transcripts pattern seen in wild-type Col-0 (Figure 4.2a). The *PIN* transcripts also decreased under ER stress conditions in *tir1 afbs* mutant backgrounds (Figure 4.5c). However, with the exception of *PIN7*, in *ire1*, the *PIN* and

TIR1/*AFB* transcription levels were further slightly reduced compared with wild-type Col-0 (Figure 4.5b, d). In contrast, the reduction of *PIN1*, *PIN2*, and *PIN4* transcript levels was larger in the *tir1 afbs* mutant compared with wild-type Col-0 (Figure 4.5d). These data indicate that down-regulation of *PIN* transcripts upon ER stress is partially and slightly affected by mutations of either IRE1 or TIR1/AFBs. These results further suggest that the *IRE1* and *TIR1*/*AFBs* play unessential but fine-tuning roles in ER stress-mediated repression of auxin regulators.

IRE1 is Required for the Auxin Responses and Homeostasis

While the UPR is necessary for growth and development, the manner by which the UPR influences other cellular regulatory processes is largely unknown. Mammalian IRE1 controls multiple physiological responses under normal growth conditions. Our findings that auxin signaling is altered under ER stress hint that the UPR participates in the auxin response in plants. Although IRE1 is not essential for ER stress-triggered down-regulation of auxin regulators, we aimed to determine whether IRE1-dependent UPR is required for the auxin response without chemical induction of ER stress. Thus, we performed root-inhibition assays to test the sensitivity of exogenous auxin application in *ire1*. To do so, *ire1* and wild-type Col-0 were germinated on medium that contain a synthetic auxin analog, 1-naphthaleneacetic-acid (NAA), a naturally occurring auxin, indole-3-acetic acid (IAA), or an auxin transport inhibitor, 1-*N*-naphthylphthalamic-acid (NPA). Interestingly, we found that *ire1*was significantly less sensitive to exogenously applied NAA, IAA, or NPA than wild-type Col-0 (Figure 4.6a-c). The findings that *ire1* and wild-type Col-0 displayed comparable root-inhibition

responses to three other plant hormone, jasmonic acid (JA), abscisic acid (ABA) and ethylene, indicate that the plant *IRE1* has a role specifically in the auxin response, as opposed to general hormones responses or growth regulation (Figure 4.7). To further confirm that IRE1 is involved in the auxin response, we investigated the transcriptional activation of auxin-responsive genes in *ire1* upon external application of auxin. qRT-PCR analyses showed that the transcriptional induction of five auxin-responsive genes, *IAA3*, *IAA5*, *IAA19*, *IAA20*, and *GH3.6*, was compromised after 2 and 4 h of NAA treatment in *ire1* relative to wild-type Col-0 (Figure 4.6d). The lower induction of auxin-responsive genes was repeatedly observed after both 1 and 2 h of IAA treatment (Figure 4.6e). These data further indicate that *ire1* exhibits an impaired response to exogenously applied auxin. The transcription of *BiP1/2* or *PDI6* was not significantly altered under IAA or NPA treatment in wild-type Col-0, suggesting that IAA or NPA treatment does not trigger ER stress like Tm treatment (Figure 4.8). Furthermore, we found that there was a 30% reduction in the free auxin level in roots of 10-day-old *ire1*plants compared with wild-type Col-0 (Figure 4.6f). While IRE1 is required to maintain the free auxin level without ER stress treatment, the free auxin level remained unaffected within 4 h after Tm treatment (Figure 4.9). All together, these data support that plant *IRE1* is required for the auxin response and homeostasis.

ER-localized Auxin Regulators are Involved in UPR Activation

Our observations that auxin signaling is regulated by ER stress led us to test whether auxin homeostasis influences UPR activation. To this end, we examined whether mutations in auxin signaling, polar transport, or biosynthesis affected the

induction of UPR target genes. Intriguingly, we found that a mutation in *PIN5* or *PIN6,* two ER-localized auxin transporters, compromised UPR activation under ER stress. Compared with wild type, *pin5-5* [145] and *pin6-4* [146] exhibited a 30-40% reduction in the level of *BiP1/2* and *PDI6* transcripts during ER stress treatment (Figure 4.10a). These data imply that ER-based auxin homeostasis contributes to UPR regulation in plants. This hypothesis was supported by the observation that mutants of other types of ER-localized auxin transporters, *pils2-2*, *pils5-2*, and *pils2-2 pils5-2* [148] exhibited similar defects in UPR activation (Figure 4.10a). We found that the expression levels of *BiP1/2* and *PDI6* were comparable among wild-type Col-0 and the auxin mutants without ER stress treatment (Figure 4.10b), supporting that the ER-localized auxin transporters are involved in ER stress-triggered UPR activation. In contrast, we found no significant differences in the induction of UPR target genes in mutants defective in either PM-localized auxin exporters, *pin1-1* (*pin1*), *eir1-1* (*pin2*), *pin3-4* (*pin3*), *pin4-3* (*pin4*)*, pin7-2* (*pin7*)*, pin3-5 pin4-3 pin7-1* (*pin3 pin4 pin7*)*,* an overexpressor of *PIN1* (*OxPIN1*), or the auxin importer *aux1-22* (*aux1*) compared with wild-type Col-0 under the same ER stress treatment conditions (Figure 4.10c). These results show that ER-based intracellular auxin transport, but not intercellular auxin transport, is required for the optimal UPR activation in plants.

We next investigated whether the ER-localized putative auxin receptor ABP1 and the auxin biosynthesis enzyme YUC were also involved in the UPR activation. Similar to the auxin mutants defective in ER-based transport, the *abp1-5* [160] and *YUC* [161] mutants also exhibited reduced levels in the activation of UPR target genes under ER stress (Figure 4.10a). Conversely, the transcription levels of UPR target genes were

higher in the *tir1 afbs* auxin co-receptor mutant than in wild-type Col-0 (Figure 4. 10a), suggesting that TIR1/AFBs play a negative role in UPR target gene induction. Altogether, these data highlight that the ER-based regulation of auxin homeostasis may operate as a molecular link between the UPR and other cellular processes.

pin5 Enhances the *ire1* Phenotype in Auxin Responses and UPR Activation

To investigate a functional relationship of IRE1 and PIN5 in the UPR and auxin response, we generated an *ire1 pin5* triple mutant and performed phenotypic analyses. Consistent with previous reports, *ire1* and *pin5-5* displayed a short primary root phenotype [39, 145]. We found that the roots of the *ire1 pin5* triple mutant were significantly shorter than those of *ire1* or *pin5-5* (Figure 4.11a). However, *ire1*, *pin5-5*, and *ire1 pin5* showed comparable lateral root density and hypocotyl length to wild-type Col-0 (Figure 4.12), suggesting that the IRE1 and PIN5 have a role specifically in regulation of primary root elongation. In addition, *ire1 pin5* also displayed lower free auxin levels compared with *ire1* or *pin5-5* (Fig 4.11b). Specifically, compared with wild-type Col-0, the roots of *pin5-5* and *ire1* exhibited a 15 and 30% reduction in free auxin levels, respectively. Nonetheless, the roots of *ire1 pin5* displayed a 45% reduction in free auxin level (Figure 4.11b). Finally, in agreement with previous findings [145], root-inhibition assays showed that *pin5-5* was less sensitive than wild-type Col-0 to low concentrations of IAA but displayed a normal response to NAA, NPA, or high concentrations of IAA [145]. Intriguingly, the *ire1 pin5* mutant was significantly less sensitive than *ire1* to all three treatments (Figure 4.11c-e). A comparable root-inhibition

response to JA, ABA, and ethylene in *ire1 pin5* indicated that the genetic interaction between IRE1 and PIN5 is specific to the auxin response (Figure 4.7).

We next tested the functional relationship of IRE1 and PIN5 under ER stress. qRT-PCR revealed that the induction of *BiP1/2* and *PDI6* was also reduced in *ire1 pin5* compared with *ire1* or *pin5-5* (Figure 4.11f), supporting that PIN5 participates in the UPR activation in a manner not entirely dependent on *IRE1*. Altogether, our results imply that regulation of ER-based auxin homeostasis is part of ER stress adaptive mechanisms that plants have evolved to parallel the classical UPR signaling pathways.

Discussion

Our findings uncover an unpredicted but critical regulatory relationship between two fundamental signaling pathways in plants, the UPR and auxin response. Studies of the mammalian UPR indicate that distinct UPR signaling pathways mediate specific physiological processes [28]. While the *IRE1*-dependent mRNA splicing event is the most evolutionarily conserved UPR pathway in eukaryotes, *IRE1* has also evolved specific functions in multicellular organisms to associate the UPR with more complex physiological processes [86, 87]. Nevertheless, our understanding of the connection between the UPR and other cellular processes is still in its infancy. Here, we have defined a plant-specific regulatory role for *IRE1* in the auxin response. The auxin polar transport is one of the most crucial regulatory mechanisms in the auxin biology. As most regulatory components of the auxin polar transport system are secretory proteins, we speculate that the *IRE1*-dependent UPR maintains a robust and efficient membrane trafficking system for the supply of functional auxin regulators. The identification of auxin

regulators directly controlled by IRE1 will elucidate how the UPR modulates specific aspects of auxin biology to coordinate the secretory pathway with physiological responses. Together with the involvement of UPR-specific membrane tethered transcription factors in brassinosteroid signaling [162], our results support the significance of the plant UPR in hormone signaling.

IRE1 regulates the UPR through various mechanisms including unconventional splicing, RNA decay, and protein-protein interaction. It has recently been reported that similar to its mammalian counterpart, plant IRE1 controls gene expression through RNA decay in addition of splicing bZIP60 transcription factor [53]. Mammalian IRE1 operates RNA decay to trigger diverse UPR signaling pathways. It would be interesting to test whether plant IRE1 also relies on its RNA decay function for the auxin response. If IRE1-dependent RNA decay contributed at least partially to the regulation of auxin signaling under ER stress, it would represent a specific regulatory event of the UPR as opposed to random RNA decay under stress. Notably, we have established that IRE1 is required for the optimal auxin response under exogenously applied auxin (Figure 4.6), but plays only partial role in ER stress-induced down-regulation of auxin regulators (Figure 4.5). These findings support that distinct mechanisms regulate auxin signaling under various conditions to achieve context-specific auxin responses.

We have established that only ER-localized auxin transporters, but not PM-localized auxin exporters or importers, are required for the optimal UPR activation (Figure 4.10). Studies of ER-localized auxin regulators suggest that a distinct auxin signaling pathway exists in the ER [149]. Accordingly, we propose that ER-based auxin signaling actively transports free auxin through the ER membranes to modulate the

signaling response in the nucleus. More specifically, plant cells can transmit signals between sub-cellular compartments by adjusting the free auxin level in the ER, cytosol, and nucleus. We thus propose a novel cellular function for auxin as a signaling molecule that connects subcellular compartments and maintains cellular homeostasis in plants. It has long been believed that intercellular polar auxin transport is the key regulatory component of the auxin response; however, the biological significance of intracellular auxin transport has been overlooked. Our findings support a specific cellular function of ER-based intracellular auxin distribution in the UPR activation, and thus emphasize the importance of ER auxin biology in plant physiology.

We have shown that ER-localized auxin transporters have a role in the UPR activation. A plausible hypothesis to explain this is that the auxin levels in the ER lumen contribute to UPR activation under ER stress. Namely, ER-localized auxin transporters or their associated proteins may sense ER stress and rapidly adjust auxin levels in the ER lumen. The consequent fluctuation of auxin levels in the ER could in turn affect the magnitude of UPR activation. Nevertheless, because a mutation of PIN5 enhances the *ire1* mutant phenotype in the UPR activation (Figure 4.11f), PIN5-dependent regulation of auxin levels under ER stress does not completely rely on IRE1. Whether ER-localized auxin transporters can directly monitor ER stress or indirectly sense ER stress-related cellular homeostasis is yet to be established; however, the findings presented here support that ER-localized transporters play a role in the UPR activation. Once a reliable system to monitor auxin levels in the ER lumen is developed, it will be interesting to experimentally confirm that ER-localized transporters mediate auxin transport between ER lumen and cytosol during ER stress.

PIN5 has been proposed to play a unique role in the auxin response since its transcriptional regulation and regulatory mechanisms appear to be different from PM-localized PINs. It was reported that the transcription of PIN5 is decreased under exogenous application of auxin although PIN5 is required for the auxin response [145]. Likewise, our study also showed that ER stress induces a decrease in the transcription of PIN5 while PIN5 is required for the optimal induction of UPR activation. As the PIN5 protein levels have not been monitored under auxin or ER stress treatment, one possibility is that the down-regulation of PIN5 transcript represents a feedback regulatory mechanism. Namely, the cellular availability or the activity of PIN5 may be increased in response to ER stress (e.g. by protein stabilization or post-translational modifications). This in turn may cause reduction of PIN5 transcriptional levels to safeguard cellular auxin homeostasis. Another possibility is that ER stress represses general auxin responses including inter- and intra-cellular auxin transport to optimize cellular responses to cope with stress. Thus, both PM- and ER-localized transporter are down-regulated under ER stress; however, a basal level of ER-localized transporters may be still required for optimal induction of UPR target gene as they may be involved in stress signal transmission through transport the auxin between subcellular compartments. Thus, mutants of ER-localized auxin regulators would display a compromised UPR activation. Further experimental evidence are needed to verify the possibilities. Nonetheless, our data support that regulation of PIN5 transcripts is a mechanism to maintain PIN5-related cellular homeostasis.

In contrast with animals, plants, as sessile organisms, have an extraordinary plasticity in post-embryonic development, responding to both internal and external cues.

Nonetheless, our understanding of how plants integrate developmental and environmental signals to balance growth and adaptive regulation is limited. The inter-regulation between the UPR and auxin response demonstrated in this study provides a new paradigm in plant physiology. Given the essential roles of the UPR in multiple stresses adaptation, the integrated action of the UPR and auxin response highlights a plant-specific strategy that evolved to maintain the crucial balance between stress response and growth regulation for ultimate fitness.

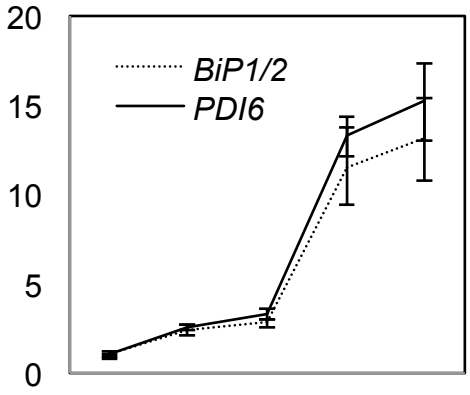

Figure 4.1. Tunicamycin induces activation of UPR target genes.

qRT-PCR analyses of *BiP1/2* and *PDI6* transcripts in 10-day-old Col-0 *Arabidopsis* seedlings after treatment with 5 μg/ml Tm for 0.5, 1, 4, or 6 h. Error bars represent standard error of the mean (SEM) from three independent biological replicates.

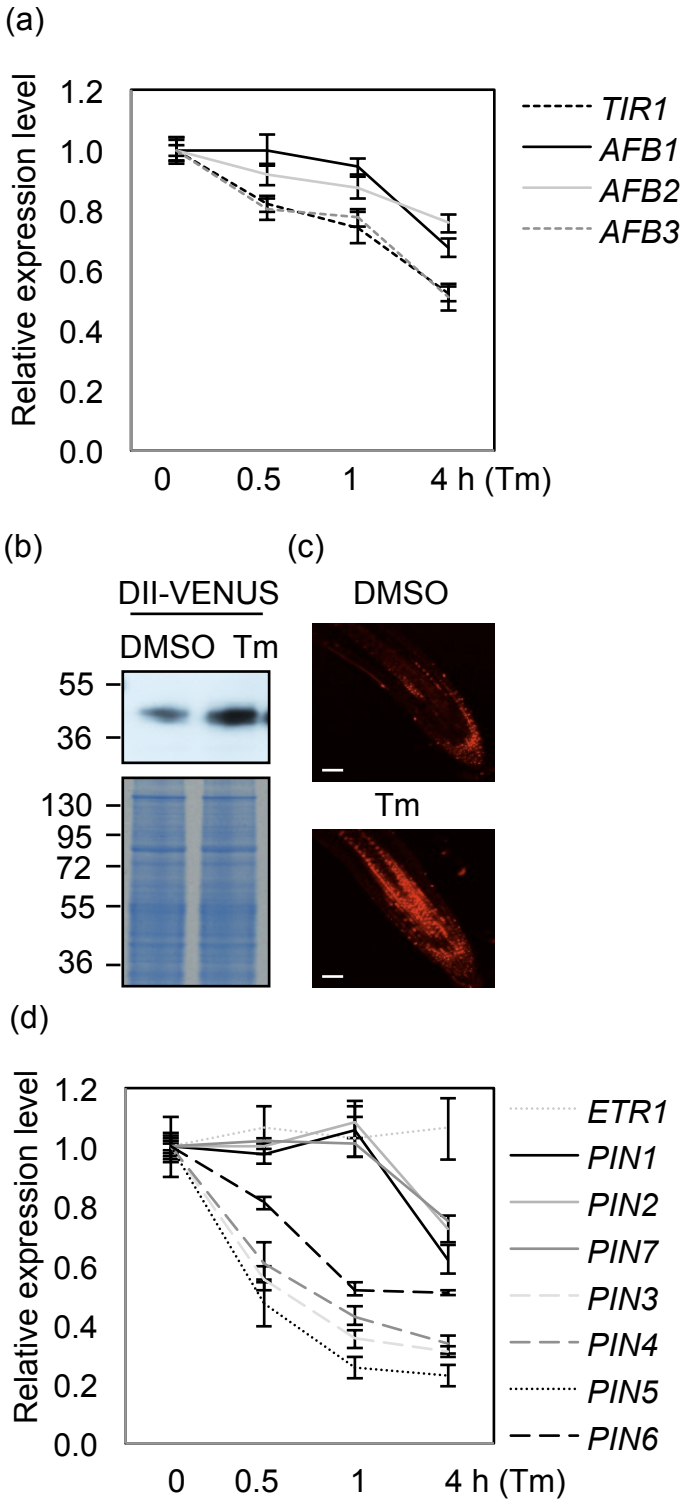

Figure 4.2. ER stress alters the expression of auxin regulators.

Figure 4.2 (cont'd)

(a) qRT-PCR analyses of *TIR1*, *AFB1*, *AFB2*, and *AFB3* expression in 10-day-old Col-0 *Arabidopsis* seedlings after treatment with 5 μg/ml Tm for 0.5, 1, or 4 h. Error bars represent standard error of the mean (SEM) from three independent biological replicates. *P*-values were calculated by Student's two-tailed t test against expression levels at 4 h relative to 0 h: *TIR1* (*P* = 0.00036), *AFB1* (*P* = 0.00041), *AFB2* (*P* = 0.00048), *AFB3* (*P* = 0.00032).

(b) The levels of DII-VENUS fusion proteins increase upon ER stress. 10-day-old DII-VENUS transgenic plants were treated with 5 μg/ml Tm or dimethyl sulfoxide (DMSO) for 6 h. Proteins were extracted from root tissues and the fusion proteins were detected by immunoblot analysis using anti-GFP serum (upper panel). Comassie blue staining gel used as loading control (lower panel).

(c) 10-day-old transgenic plants expressing DII-VENUS were treated with 5 μg/ml Tm or DMSO for 6 h. Primary root tips were subjected to confocal microscopy analyses. Scale bars = 50 μm.

(d) *PIN* mRNA levels decrease upon exposure to ER stress. qRT-PCR analyses of *PIN* family transcripts in 10-day-old wild-type Col-0 seedlings during treatment with 5 μg/ml Tm for 0.5, 1, or 4 h. Error bars represent standard error of the mean (SEM) from three independent biological replicates. *P*-values were calculated against expression levels at 4 h relative to 0 h: *PIN1* (*P* = 0.00221), *PIN2* (*P* = 0.00316), *PIN3* (*P* = 5.4E-05), *PIN4* (*P* = 4.9E-05), *PIN5* (*P* = 6.4E-05), *PIN6* (*P* = 0.00012), *PIN7* (*P* = 0.00353). The transcriptional level of ETR1, an ER-associated ethylene receptor, was unchanged after treatment with Tm for 0.5, 1, or 4 h.

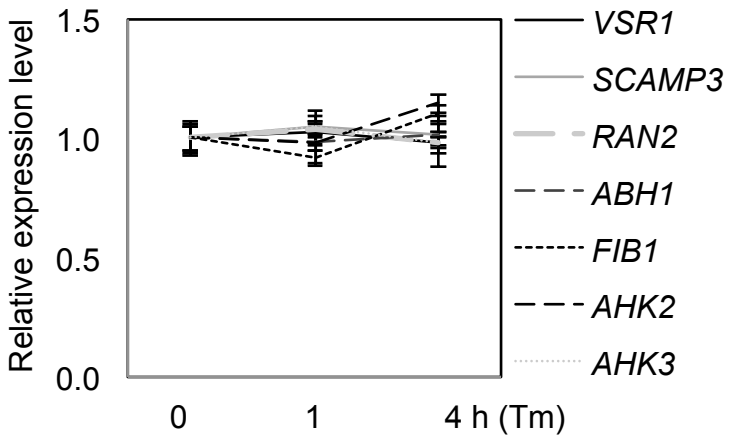

Figure 4.3. The transcripts of genes encoding ER-localized and nuclear proteins remain unchanged under Tm treatment.

qRT-PCR analyses of *VSR1*, *SCAMP3*, *RAN2*, *ABH1*, *FIB1*, *AHK2*, and *AHK3* transcripts in 10-day-old Col-0 *Arabidopsis* seedlings after treatment with 5 μg/ml Tm for 0, 1, or 4 h. Error bars represent standard error of the mean (SEM) from three independent biological replicates. No statistical differences were observed between the expression levels of individual genes in the time course.

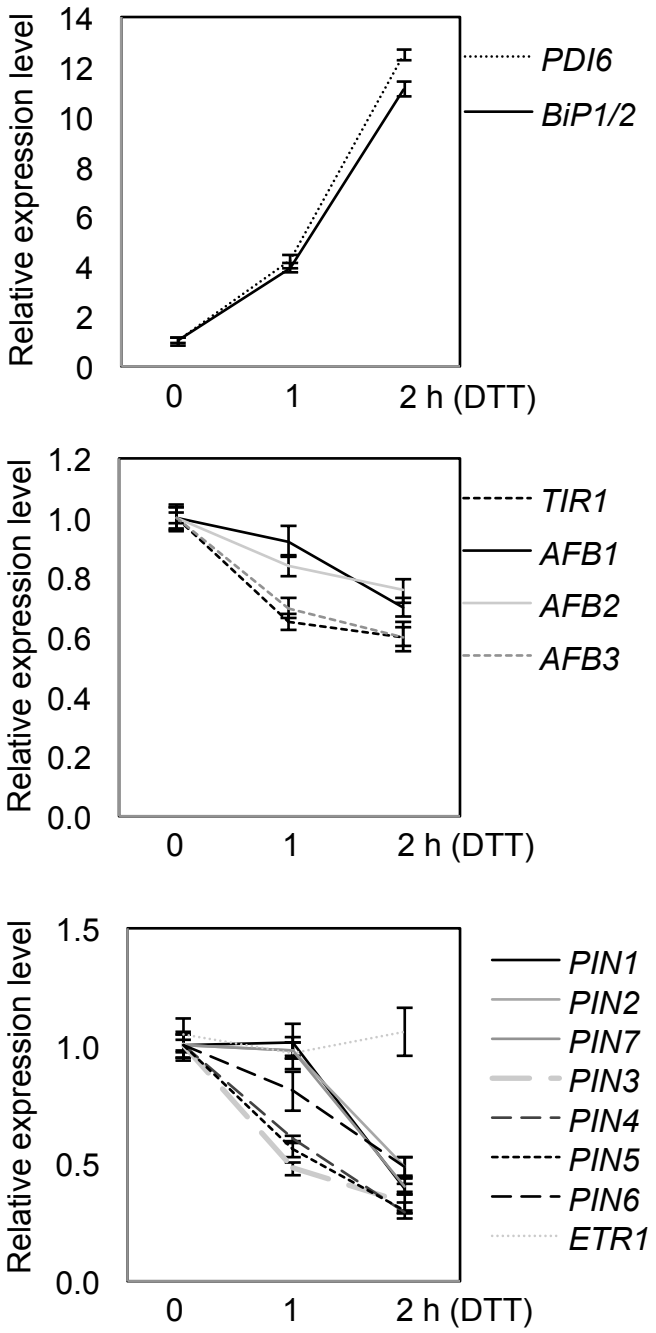

Figure 4.4. DTT transcriptionally activates UPR target genes and down-regulates auxin regulators.

Figure 4.4 (cont'd)

qRT-PCR analyses of *BiP1/2*, *PDI6*, *TIR1*, *AFB1*, *AFB2*, *AFB3,* and *PIN* family transcripts in 10-day-old Col-0 *Arabidopsis* seedlings after treatment with 2mM DTT for 0, 1, or 2 h. Error bars represent standard error of the mean (SEM) from three independent biological replicates.

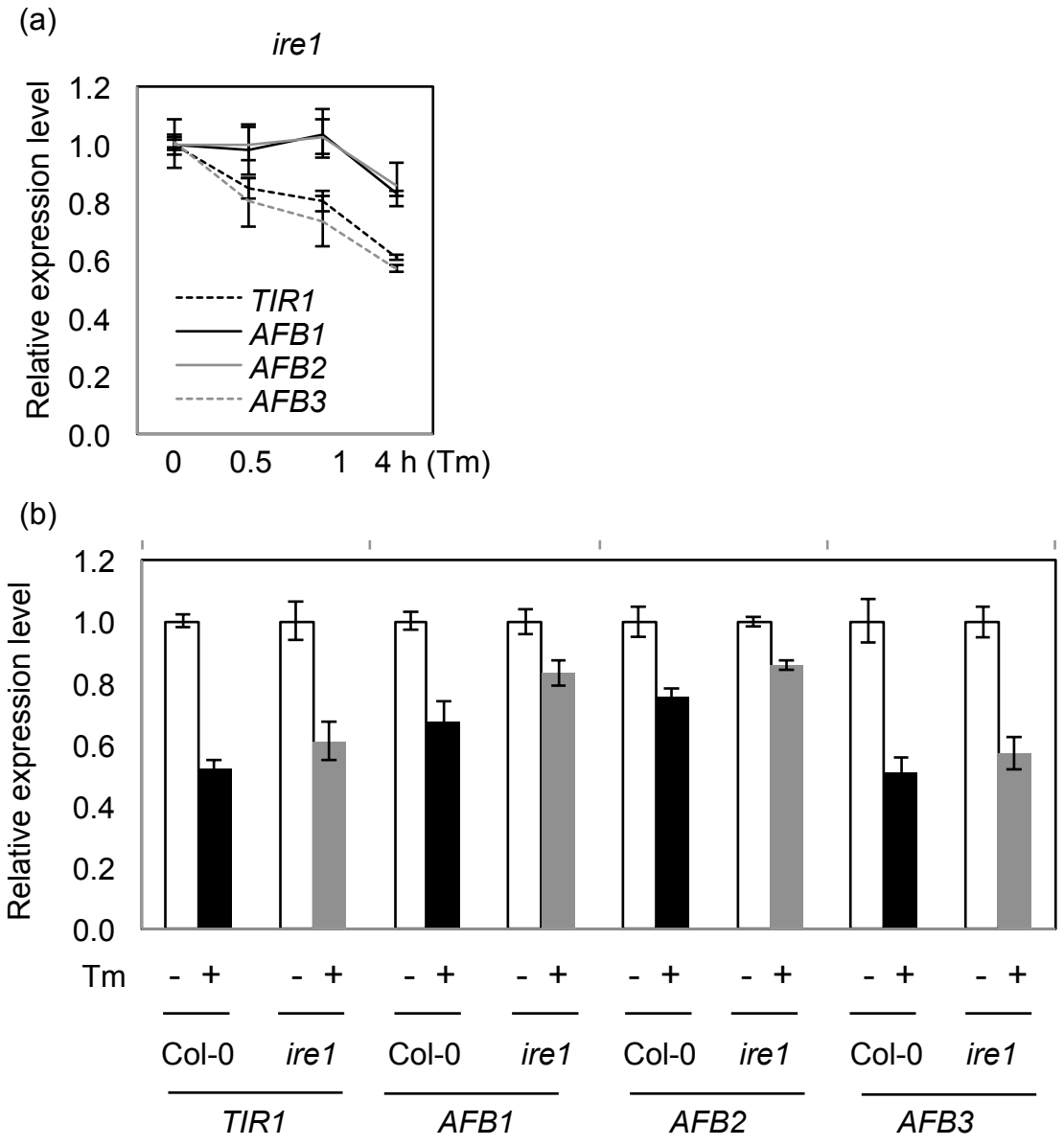

Figure 4.5. IRE1 and TIR1/AFBs play fine-tuning roles in ER stress-induced down-regulation of auxin regulators.

Figure 4.5 (cont'd)

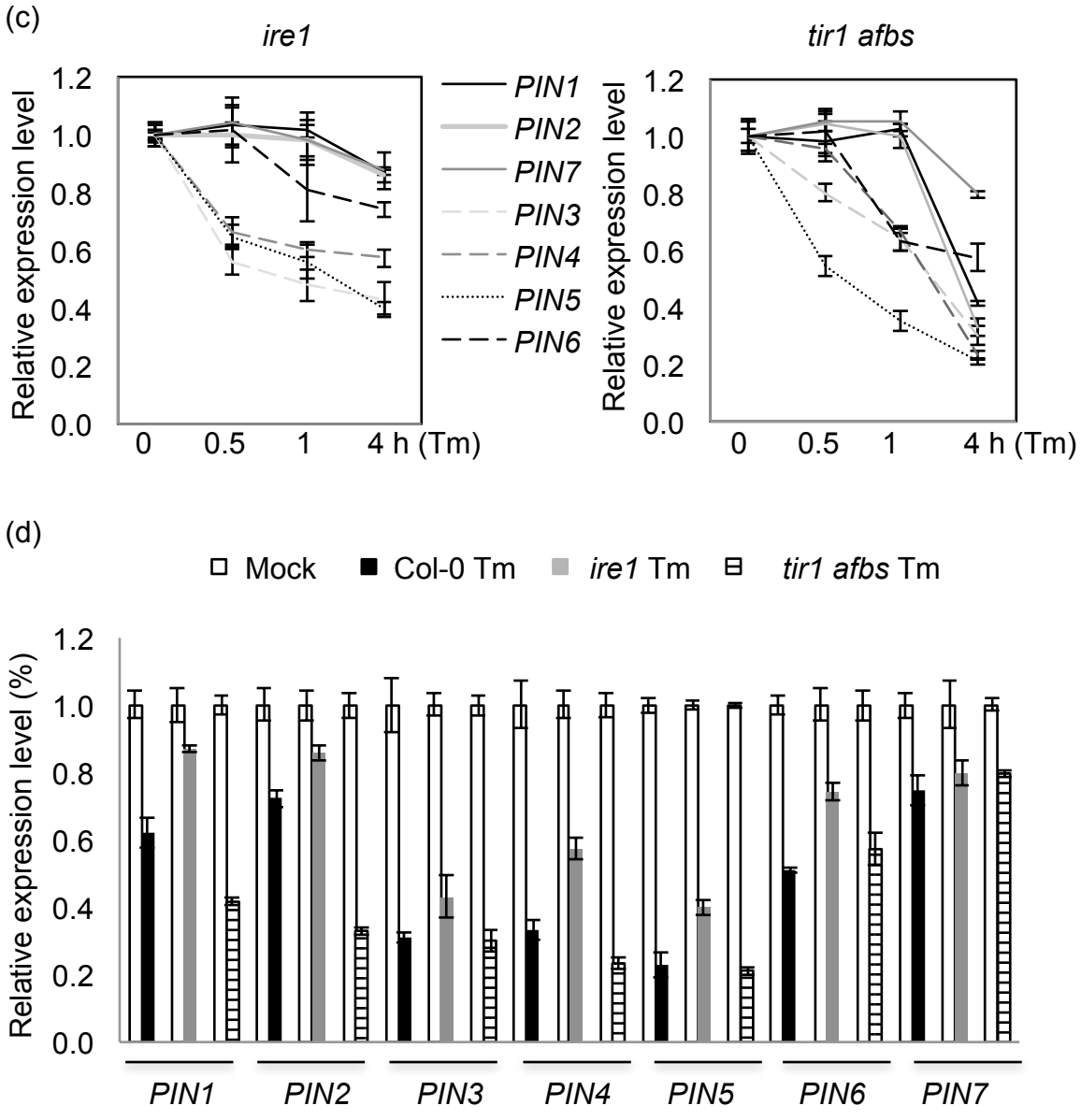

Figure 4.5 (cont'd)

(a) qRT-PCR analyses of *TIR1*, *AFB1*, *AFB2*, and *AFB3* expression in 10-day-old *ire1 Arabidopsis* seedlings after treatment with 5 μg/ml Tm for 0.5, 1, or 4 h.

(b) qRT-PCR analyses of *TIR1*, *AFB1*, *AFB2*, and *AFB3* expression in 10-day-old wild type Col-0 and *ire1 Arabidopsis* seedlings after treatment with 5 μg/ml Tm for 4 h.

(c) *PIN* mRNA levels decrease upon exposure to ER stress in 10-day-old *ire1* or *tir1 afb*. qRT-PCR analyses of *PIN* family transcripts in 10-day-old *ire1* or *tir1 afb* seedlings after treatment with 5 μg/ml Tm for 0.5, 1, or 4 h.

(d) Transcriptional repression of *PIN*s after treatment with 5 μg/ml Tm for 4 h in 10-day-old Col-0, *ire1*, or *tir1 afb Arabidopsis* seedlings.

Error bars represent standard error of the mean (SEM) from three independent biological replicates.

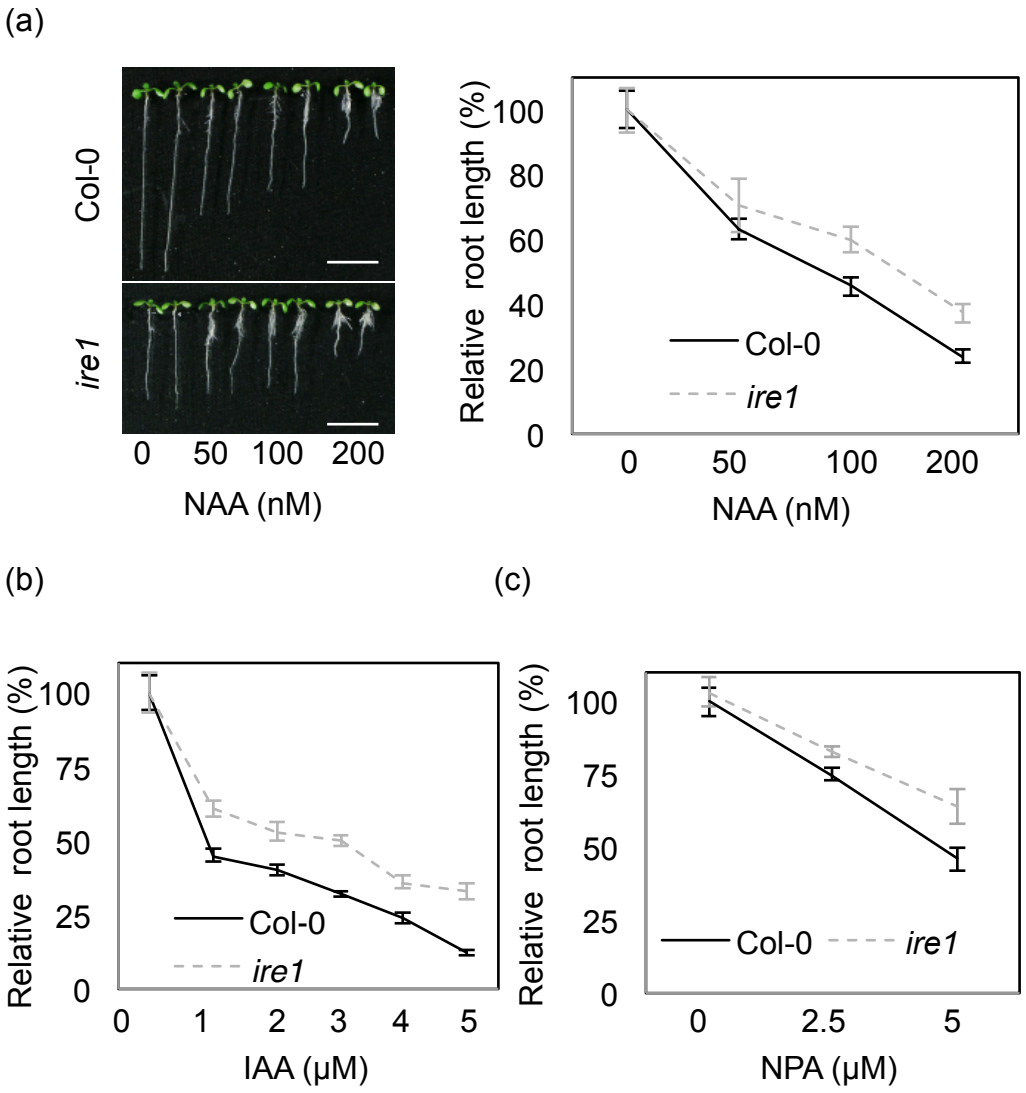

Figure 4.6. *ire1* exhibits the compromised auxin responses.

Figure 4.6 (cont'd)

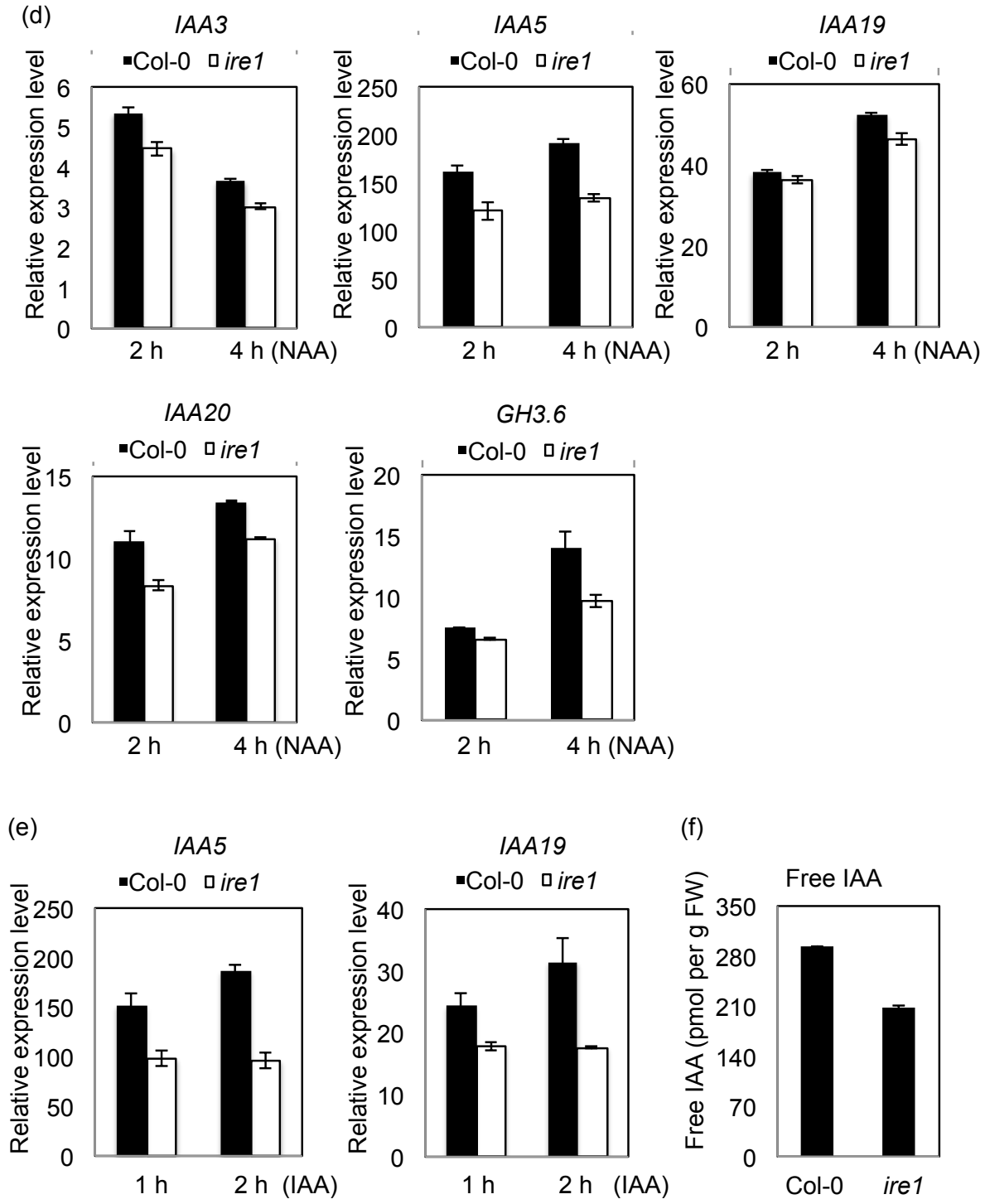

Figure 4.6 (cont'd)

(a-c) In *ire1*, root growth is largely resistant to treatments with auxin (NAA and IAA) or an auxin transport inhibitor (NPA). Relative primary root length of 10-day-old Col-0 and *ire1 Arabidopsis* seedlings grown in the presence 50, 100, 200 nM NAA (a), or 1, 2, 3, 4, 5 μM IAA (b), or 2.5, 5 μM NPA (c) compared with those grown in the absence of the chemicals. Error bars represent standard error of the mean (SEM), n > 30. Scale bars = 1 cm. *P*-values are relative to Col-0: 100, 200 nM NAA ($P < 0.00078$), 1, 2, 3, 4, 5 μM IAA ($P < 0.00050$), 2.5, 5 μM NPA ($P < 0.00344$).

(d) qRT-PCR analyses of *IAA3*, *IAA5*, *IAA19*, *IAA20*, and *GH3.6* expression in 10-day-old Col-0 and *ire1 Arabidopsis* seedlings after a 2- or 4-h treatment with 10 μM NAA. Error bars represent SEM from three independent biological replicates. *P*-values are relative to Col-0: *IAA3* ($P < 0.00098$), *IAA5* ($P < 0.00016$), *IAA19* ($P < 0.00479$), *IAA20* ($P < 0.00036$), and *GH3.6* ($P < 0.00391$).

(e) qRT-PCR analyses of *IAA5* and *IAA19* in 10-day-old Col-0 and *ire1 Arabidopsis* seedlings after a 1- or 2-h treatment with 10 μM IAA. *P*-values are relative to Col-0: *IAA5* ($P < 0.00086$) and *IAA19* ($P < 0.00112$).

(f) Free IAA concentration in 10-day-old Col-0 and *ire1 Arabidopsis* roots. Error bars represent standard error of the mean (SEM) from three independent biological replicates. *P*-value is relative to Col-0: $P = 4.9E-05$.

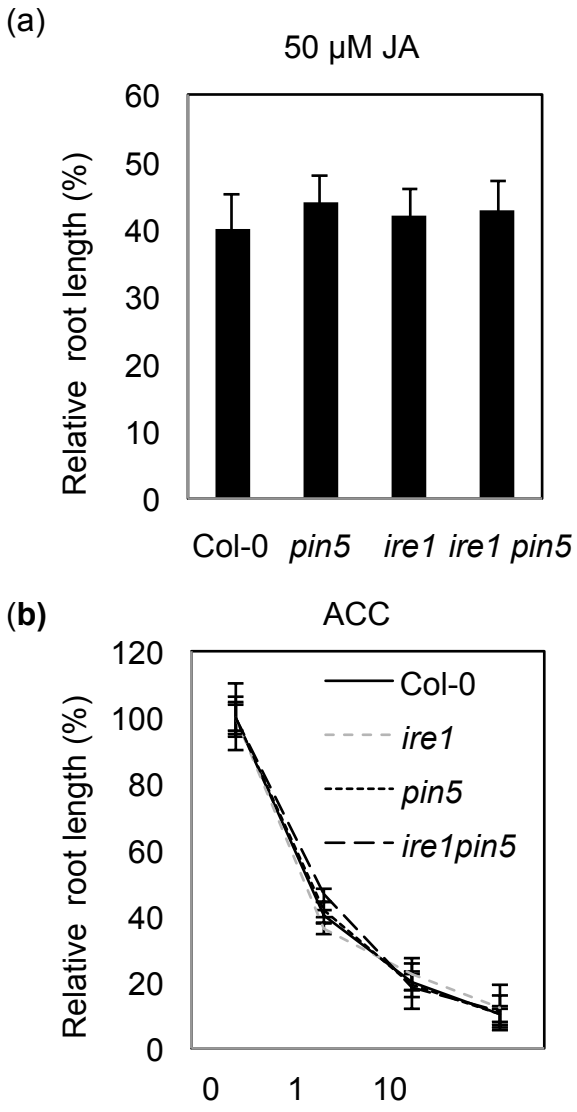

Figure 4.7. *ire1* and *ire1 pin5* display comparable sensitivity to JA, ACC, and ABA.

Figure 4.7 (cont'd)

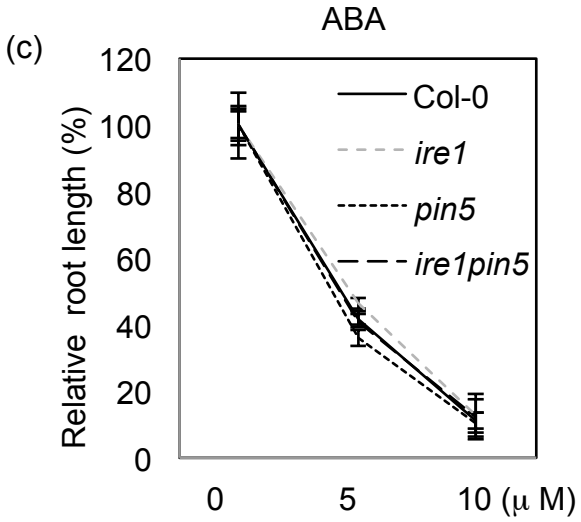

(a-c) Relative primary root length of 10-day-old Col-0, *pin5*, *ire1*, and *ire1 pin5* *Arabidopsis* seedlings grown in the presence of 50 μM JA (a) or 1, 10, 100 μM ACC (b), or 5, 10 μM ABA (c) compared with those grown in the absence of the chemicals. Error bars represent standard error of the mean (SEM), n > 30.

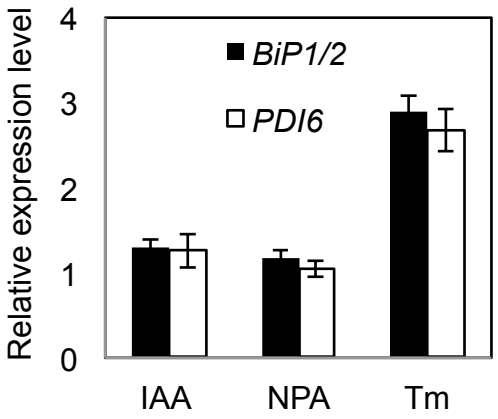

Figure 4.8. The UPR target genes were not altered under IAA or NPA treatment. qRT-PCR analyses of *BiP1/2* and *PDI6* in 10-day-old Col-0 *Arabidopsis* seedlings relative to DMSO or EtOH mock control after a 1-h treatment with 10 μM IAA, 50 μM NPA, or 5 μg/ml Tm. Error bars represent standard error of the mean (SEM) from three independent biological replicates.

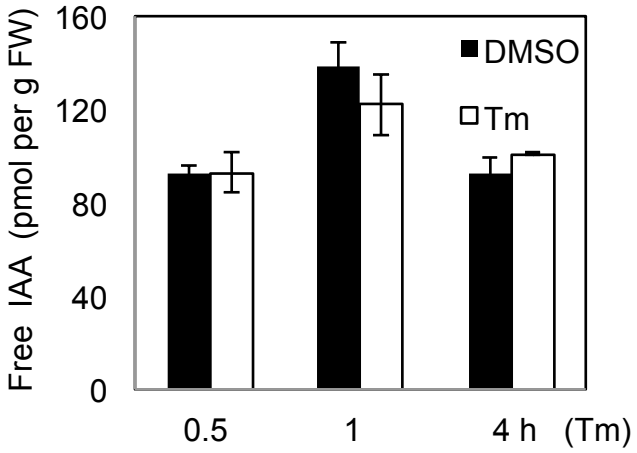

Figure 4.9. The free auxin level is unchanged on ER stress.

Free IAA measurement in the roots of 10-day-old Col-0 after treatment with 5 μg/ml Tm or DMSO for 0.5, 1, or 4 h. Error bars represent standard error of the mean (SEM) from three independent biological replicates.

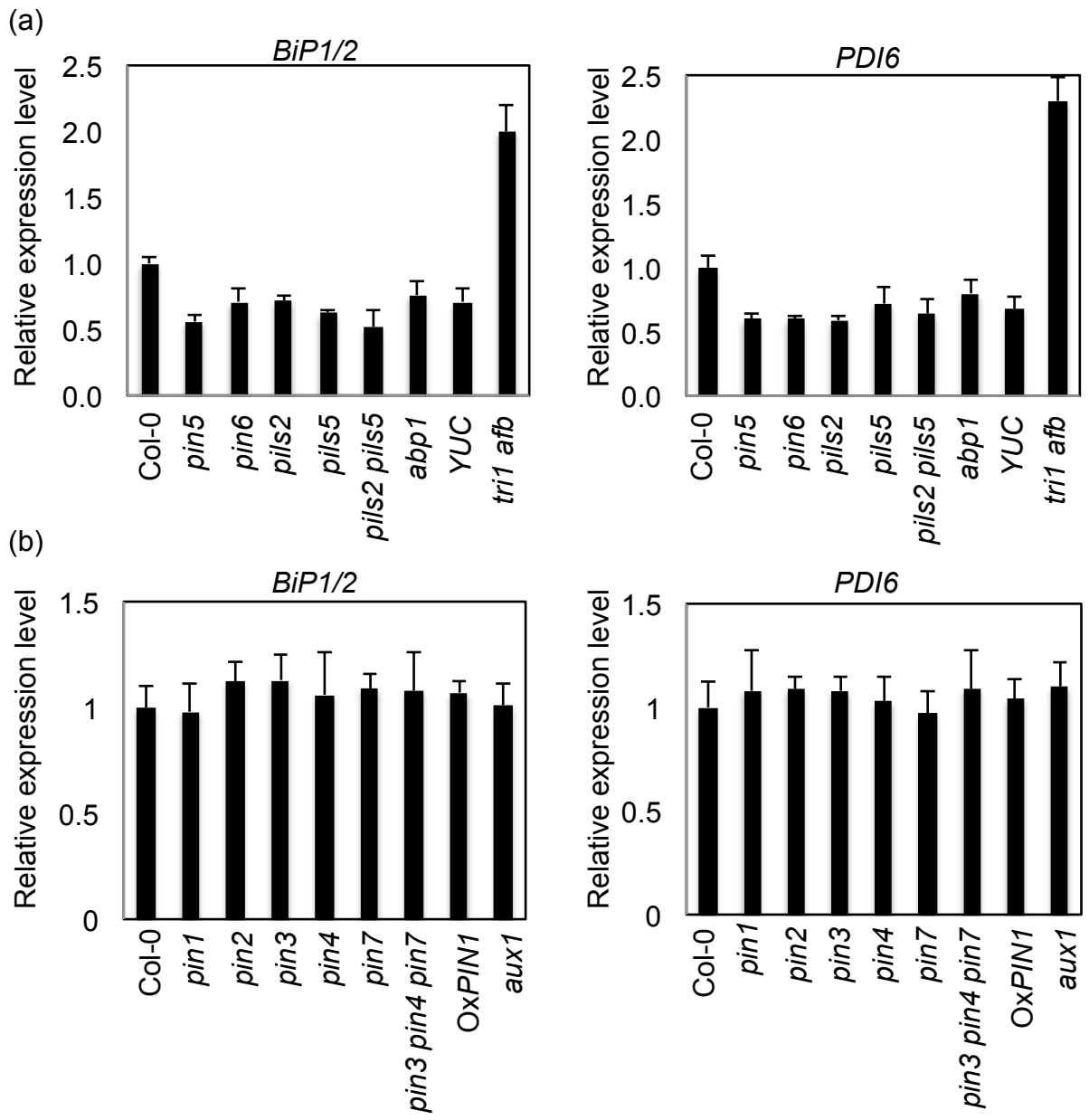

Figure 4.10. Mutants impaired in intracellular auxin transport display a defective UPR phenotype.

Figure 4.10 (cont'd)

(c)

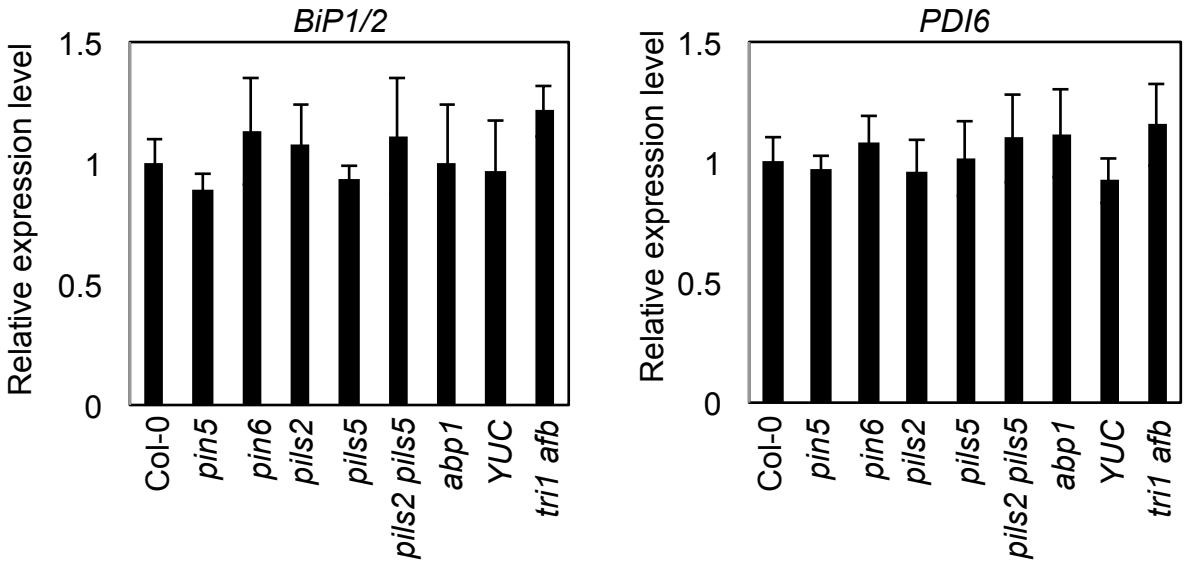

Figure 4.10 (cont'd)

(a) qRT-PCR analyses of *BiP1/2* and *PDI6* in 10-day-old *pin5-5* (*pin5*), *pin6-4* (*pin6*), *pils2-2* (*pils2*), *pils5-2* (*pils5*), *pils2-2 pils5-2* (*pils2 pils5*), *abp1-5* (*abp1)*, *YUC*, and *tir1 afbs*(*tir1 afb*) relative to wild-type Col-0 *Arabidopsis* seedlings after a 1-h treatment with 5 μg/ml Tm. Error bars represent standard error of the mean (SEM) from three independent biological replicates. *P*-values are relative to Col-0: *pin5* (*P* = 0.00029), *pin6* (*P* = 0.00095), *pils2* (*P* = 0.00093), *pils5* (*P* = 0.00067), *pils2 pils5* (*P* = 0.00089), *abp1* (*P* = 0.00215), *YUC* (*P* = 0.00014), *tir1 afb* (*P* = 0.00026).

(b) qRT-PCR analyses of *BiP1/2* and *PDI6* in 10-day-old *pin1-1* (*pin1*), *eir1-1* (*pin2*), *pin3-4* (*pin3*), *pin4-3* (*pin4*), *pin7-2* (*pin7*), *pin3-4 pin4-3 pin7-2* (*pin3 pin4 pin7*), *OxPIN1*, and *aux1-22* (*aux1*) relative to wild-type Col-0 *Arabidopsis* seedlings after a 1-h treatment with 5 μg/ml Tm. Error bars represent SEM from three independent biological replicates.

(c) qRT-PCR analyses of *BiP1/2* and *PDI6* in 10-day-old Col-0, *pin5-5* (*pin5*), *pin6-4* (*pin6*), *pils2-2* (*pils2*), *pils5-2* (*pils5*), *pils2-2 pils5-2* (*pils2 pils5*), *abp1-5* (*abp1)*, *YUC*, and *tir1 afbs* (*tir1 afb*) *Arabidopsis* seedlings without Tm treatment. Error bars represent standard error of the mean (SEM) from three independent biological replicates.

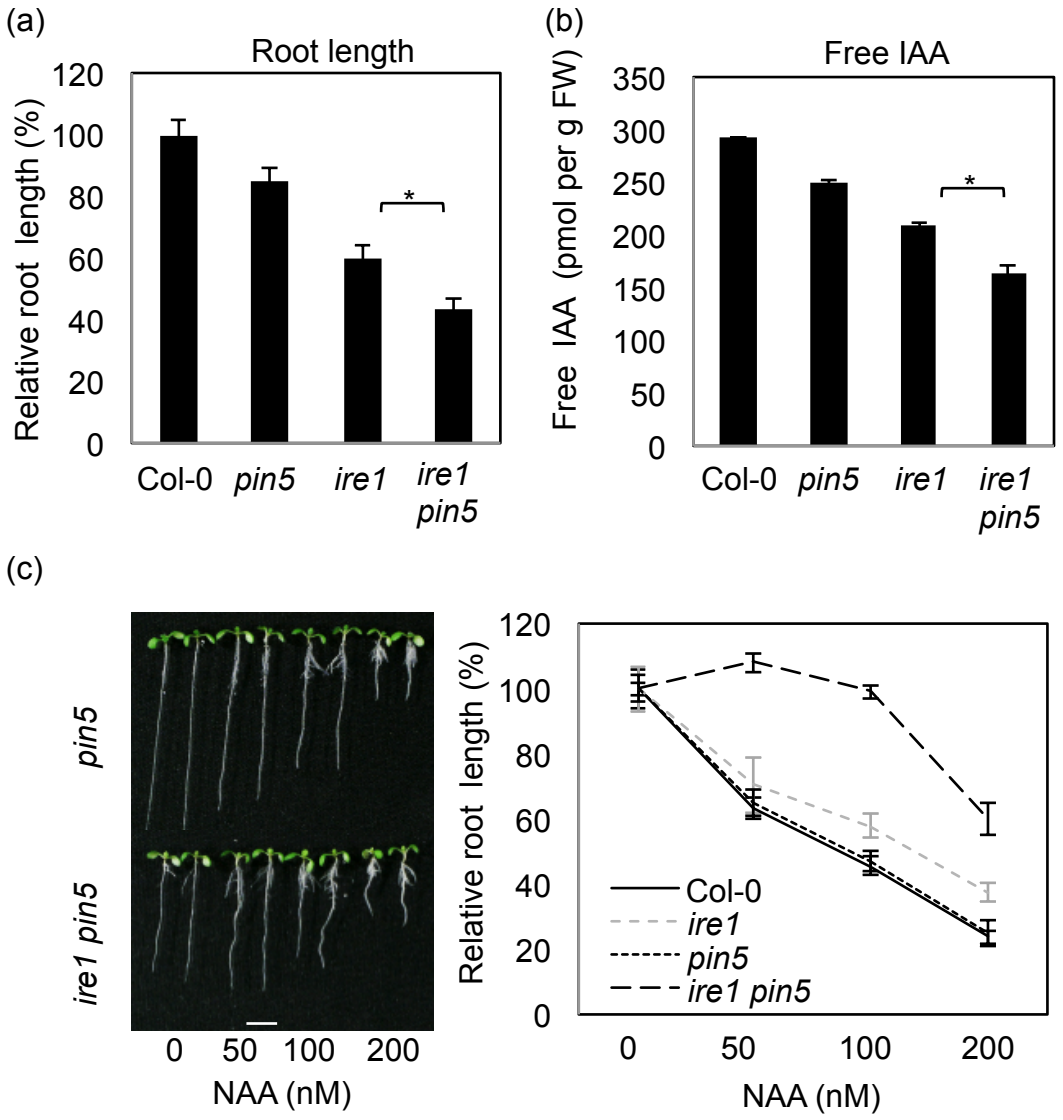

Figure 4.11. *pin5* enhances the auxin and ER stress response phenotype in *ire1*.

Figure 4.11 (cont'd)

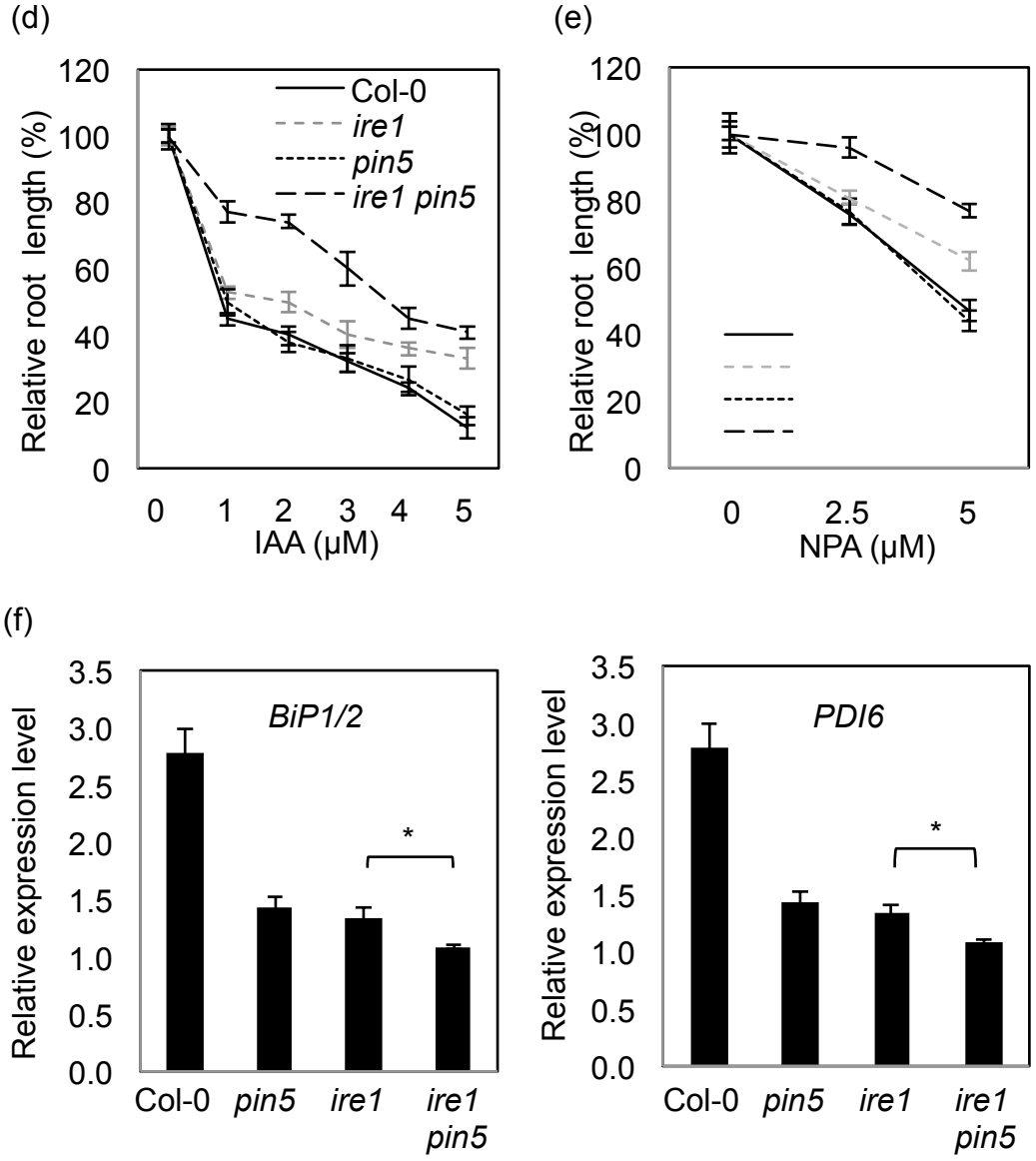

Figure 4.11 (cont'd)

(a) *pin5-5* (*pin5*) enhances the short-root phenotype of *ire1*. Relative primary root length of *pin5*, *ire1*, and *ire1 pin5* compared with Col-0 under unstressed conditions. Error bars represent standard error of the mean (SEM), n > 30. *P*-value is *ire1 pin5* relative to *ire1*: **P* = 0.00226.

(b) Free IAA measurement in the roots of 10-day-old Col-0*, pin5*, *ire1*, and *ire1 pin5 Arabidopsis* seedlings. Error bars represent SEM from three independent biological replicates. *P*-value is *ire1 pin5* relative to *ire1*: **P* = 0.00182.

(c-e) Relative primary root length of 10-day-old Col-0*, pin5*, *ire1*, and *ire1 pin5 Arabidopsis* seedlings grown in the presence 50, 100, 200 nM NAA (c), or 1, 2, 3, 4, 5 μM IAA (d), or 2.5, 5 μM NPA (e) compared with those grown in the absence of the chemicals. Error bars represent SEM, n > 30. *P*-values are *ire1 pin5* relative to *ire1*: 50, 100 or 200 nM NAA (*P* < 0.00032), 1, 2, 3, 4, or 5 μM IAA (*P* < 0.00075), 2.5, 5 μM NPA (*P* < 0.00149). Scale bars = 1 cm.

(f) *pin5* enhances the UPR defects in *ire1* under ER stress. qRT-PCR analyses of *BiP1/2* and *PDI6* in 10-day-old Col-0*, pin5*, *ire1*, and *ire1 pin5 Arabidopsis* seedlings relative to DMSO mock control after a 1-h treatment with 5 μg/ml Tm. Error bars represent standard error of the mean (SEM) from three independent biological replicates.

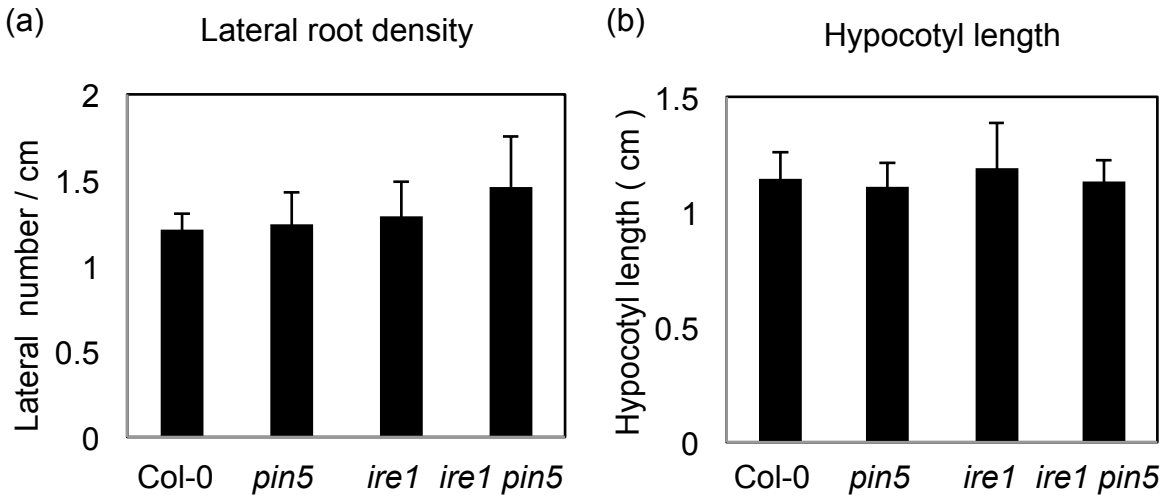

Figure 4.12. *ire1* and *ire1 pin5* display normal root density and hypocotyl elongation.

(a) Lateral root density of 10-day-old Col-0, *pin5*, *ire1*, and *ire1 pin5 Arabidopsis* seedlings Lateral root density is calculated as the number of lateral roots per cm of primary root Error bars represent standard error of the mean (SEM), n > 30.

(b) Quantification of the hypocotyl length of five-day-old Col-0, *pin5*, *ire1*, and *ire1 pin5 Arabidopsis* seedlings grown under dark condition. Error bars represent standard error of the mean (SEM), n > 30.

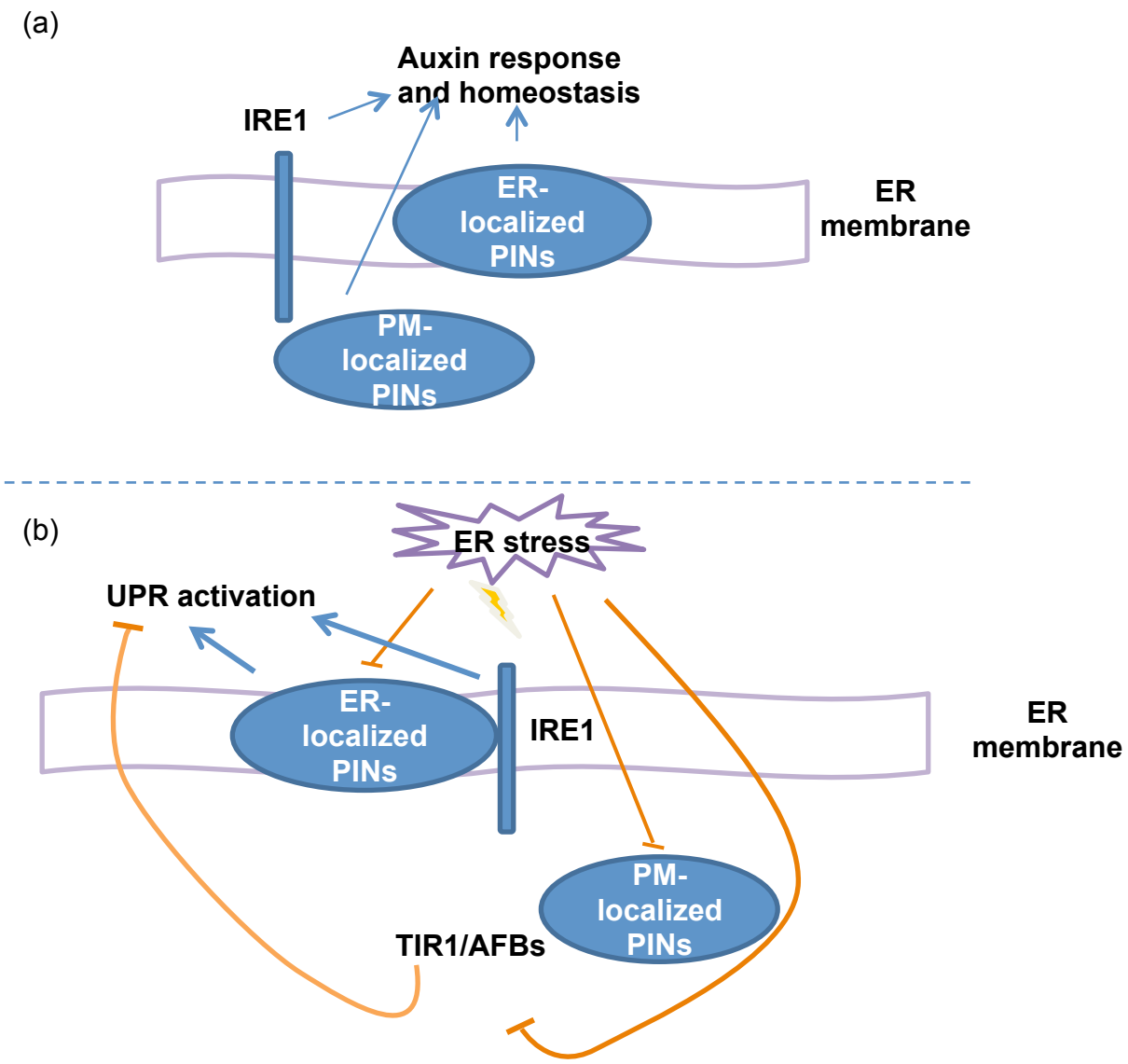

Figure 4.13. Working model.

Figure 4.13 (cont'd)

(a) IRE1 is required for the auxin responses upon external auxin application. IRE1, ER- and PM-localized PINs are involved in the maintenance of auxin homeostasis without chemical induction of ER stress.

(b) ER stress triggers down-regulation of auxin receptors TIR1/AFBs, ER- and PM-localized PINs. IRE1 and ER-localized PINs are required for the optimal induction of UPR target genes.

Table 4.1. DNA primers used in this study

Primers	Sequence (5'–3')
WiscDsLox420D09 RP	TATCTCCGATCCATCGTTGAC
WiscDsLox420D09 LP	CAAAATCTTCAGTGCTAGCGG
WiscDsLox LP	AACGTCCGCAAT GTGTTATTAAGTTG
SAIL_238_F07 RP	GAAGGAAAACGGACATCCTTC
SAIL_238_F07 LP	CCTCTCGAACCCTTCAGGTAC
SAIL_LB2	GCTTCCTATTATATCTTCCCAAATTACCAATACA
SM_3_28638 RP	CTCCTGAGTCCCTGATCACAC
SM_3_28638 LP	TAGAATCATATGCCACGGCAC
Spm32	TACGAATAAGAGCGTCCATTTTAGAGTGA
TIR1 qP For	TTCCGTCCGAGCCTTTTG
TIR1 qP Rev	AAGCCCCTGTTCCGTCAAT
AFB1 qP For	GGTCAGTCCTGCTGCGGTTA
AFB1 qP Rev	CCCCTTCAAAGTCAAAGATCTCA
AFB2 qP For	GAGTCTGAAGCTAAATCGTGCAGTA
AFB2 qP Rev	GCGCACACGCCATTAACC
AFB3 qP For	GGGCTTTGGTGCAATCGTA
AFB3 qP Rev	CGGAGACAGAGAGCCGTCTT

Table 4.1 (cont'd)

PIN1 qP For	CGGTGGGAACAACATAAGCA
PIN1 qP Rev	CACACTTGTTGGTGGCATCAC
PIN2 qP For	AACGCAAGCAAAGCTCCAA
PIN2 qP Rev	GCGCCGCCGTAGCTATTA
PIN3 qP For	CGGAGCACCTGACAACGAT
PIN3 qP Rev	CGGATCTCTTTAGCACCTTGGT
PIN4 qP For	GTTGCTGGGATTGCCATTG
PIN4 qP Rev	GCAGCCTGAACGATGGCTAT
PIN5 qP For	CCATGGCCATCGGCTCTAT
PIN5 qP Rev	TGGCTACGCGGAGGACAT
PIN6 qP For	CGCCGGCGCAATGT
PIN6 qP Rev	GGACTGGGACGGCGAAA
PIN7 qP For	CATAAACCGCTTCGTCGCTAT
PIN7 qP Rev	TTGAGGAGATGAAGTGGAAAGAGA
BiP1/2 qP For	CCACCGGCCCCAAGAG
BiP1/2 qP Rev	GGCGTCCACTTCGAATGTG
PDI6 qP For	CGAAGTGGCTTTGTCATTCCA
PDI6 qP Rev	GCGGTTGCGTCCAATTTT

Table 4.1 (cont'd)

IAA3 qP For	TCTTTTTATCTTCTCCTGCAATTCTTG
IAA3 qP Rev	CCAGCCTCAGCTCTGTTTCC
IAA5 qP For	GTCCATCTCCGGGAAGAAGAG
IAA5 qP Rev	CGCCGGTTCACATTTCAAAT
IAA19 qP For	TGGCCACCGGTTTGTTCTT
IAA19 qP Rev	TTCGTGGTCGAAGCTTCCTT
IAA20 qP For	AATGGCTACCGCGACTTGAT
IAA20 qP Rev	CCAGAGAATGGATGCGTTGA
GH3.6 qP For	GCTCGTGACATTAGAACCGGTACT
GH3.6 qP Rev	GCCTCACGAACCGAAGAATC

Table 4.1 (cont'd)

ETR1 qP For	AACCGTGGCGCTTGTGAT
ETR1 qP Rev	CACACGAGACAACAGCGGTTA
VSR1 qP For	CTCCCAACTCTTGTCGTGAACA
VSR1 qP Rev	AGCACTGCCCCCTTTTCC
SCAMP3 qP For	AGGCGGGAGCAGGAAATC
SCAMP3 qP Rev	ACAATTCCGGCCTGTGCTAT
RAN2 qP For	TCAGCCTCTCCCCGATGAT
RAN2 qP Rev	CACAGCAGACATTTTTGGAAGATT
ABH1 qP For	GGCGCTGTTCGTGCACTA
ABH1 qP Rev	GACGCGTCCTGGATTCCAT
FIB1 qP For	CAGCCACCACCGCACAT
FIB1 qP Rev	CGAAAGACGAGAACCGAAAAA
AHK2 qP For	GGTTCCGGCAGATCATTACAA
AHK2 qP Rev	CCCCTTTCCTGTGTGAATTTG
AHK3 qP For	TCCAATGCAACGCCAAAA
AHK3 qP Rev	CAAACACTCCCCCGAGATACC
IPP2 For	ATTTGCCCATCGTCCTCTGT
IPP2 Rev	GAGAAAGCACGAAAATTCGGTAA

Methods

Plant material and growth conditions

Arabidopsis thaliana ecotype Columbia (Col-0) plants were used. Surface-sterilized seeds were plated directly onto petri dishes containing half-strength Linsmaier and Skoog (LS) medium, 1.5% w/v sucrose, and 0.4% Phytagel (Sigma). For normal growth conditions, plants were grown at 21°C under a 16-h light/8-h dark cycle.

Tm treatment

Seeds were germinated and grown on half-strength LS medium for 10 days, and then transferred to half-strength LS medium containing 5 μg/ml Tm (Sigma) for the indicated periods of time.

RNA extraction and quantitative RT-PCR analysis

Total RNA was extracted from whole seedlings using an RNeasy Plant Mini Kit (Qiagen) and treated with DNase I (Qiagen). All samples within an experiment were reverse-transcribed simultaneously using SuperScript® VILO™ Master Mix, (Invitrogen). A no-RT reaction, in which RNA was subjected to the same conditions of cDNA synthesis but without reverse transcriptase, was included as a negative control in all real-time quantitative PCR (qRT-PCR) assays. qRT-PCR with SYBR Green detection was performed in triplicate using the Applied Biosystems 7500 Fast Real-Time 7500 PCR system. Data were analyzed by the summary of efficiency (DDCT) method. The values presented are the mean of three independent biological replicates. Primers used are listed in Supplementary Table S1.

Phenotypic analysis

Root length and hypocotyl elongation measurements were averaged from 30 plants for each genotype. Data were analyzed by Student's two-tailed *t*-test, assuming equal variance; differences with a *P*-value < 0.05 were considered significant.

Immunoblotting and confocal microscopy analyses

Fifty milligrams of fresh root tissues was ground in plastic tubes with plastic pestles using liquid nitrogen and 500 ml of SDS-containing extraction buffer (60 mM Tris-HCL (pH 8.8), 2% SDS, 2.5% glycerol, 0.13 mM EDTA (pH 8.0), and 1X Protease Inhibitor Cocktail Complete (Roche)). The tissue lysates were vortexed for 30 s, heated at 70°C for 10 minutes, and then centrifuged at 13,000 g twice for 5 minutes at room temperature. The supernatants were then transferred to new tubes. For SDS-PAGE analysis, 5 µl of the extract in 1x NuPAGE LDS Sample Buffer (Invitrogen) was separated on 4-12% NuPage gel (Invitrogen) and then transferred to PVDF (polyvinyl difluoride) membrane. The membrane was incubated with 3% BSA in 1x TBST (50 mM Tris-base, 150 mM NaCl, 0.05% Tween 20, pH 8.0) overnight at 4°C, and was then probed with antibody (α-GFP, 1:20,000; Abcam) diluted in the blocking buffer (1:20,000) at room temperature for 1 h. The probed membrane was washed three times with 1x TBST for 5 min and then incubated with secondary antibody (goat anti-rabbit IgG for α-GFP, 1:20,000; Abcam) at room temperature for 1 h. Finally, the membrane was washed four times with 1x TBST for 10 min before the signals were visualized with SuperSignal® West Dura Extended Duration Substrate (Pierce Biotechnology). To

visualize YFP fluorescence, an inverted laser scanning confocal microscope Zeiss LSM510 was used to detect the DII expression.

Free IAA analysis

Approximately 20 roots were cut from 10-day-old seedlings and transferred into an Eppendorf tube containing 1 ml of methanol. Internal standard of [2H5] IAA was added to the sample at amount of 100 fmol per root.

Acknowledgements

We thank Teva Vernoux for sharing the DII-VENUS seeds and Jürgen Kleine-Vehn for sharing the *pils2-2*, *pils5-2*, and *pils2-2 pils5-2* seeds and the *Arabidopsis* Biological Resource Center (ABRC) for seed stocks. This study was supported by grants from the Chemical Sciences, Geosciences and Biosciences Division, Office of Basic Energy Sciences, Office of Science, U.S. DOE (DE-FG02-91ER20021) for the infrastructure, National Institutes of Health (R01 GM101038-01), and NASA (NNX12AN71G).

CHAPTER 5

Conclusion and Future Perspectives

The UPR maintains the integrity and dynamics of the secretory pathway in eukaryotic cells. Establishing the UPR signaling network is fundamental to illuminating molecular mechanisms underlying maintenance of the secretory pathway. This dissertation aims to identify regulators and biological roles of the UPR in *Arabidopsis*. When I started the plant UPR studies, functional roles of plant IRE1 in the UPR were not established *in vivo*. Regulatory relationships between the UPR and other cellular processes were largely unexplored.

Plant IRE1 is a Functional ER Stress Sensor and Involved in Root Growth

In Chapter 3, I present *in vivo* evidences that the two plant IRE1 homologs, IRE1A and IRE1B, are functional ER stress sensors in *Arabidopsis*. Based on the phenotypic analyses, IRE1A and IRE1B have at least partially overlapping function in ER stress tolerance and UPR activation. In addition, *ire1* displays a short-root phenotype, indicating a regulatory role of plant IRE1 in root growth. By contrast, a mutant of the splicing substrate of IRE1, *bzip60*, shows normal primary root growth. The difference of root phenotype of *ire1* and *bzip60* indicates that IRE1 mediates root growth regulation in a manner not completely dependent on the bZIP60 pathway. One possibility is that IRE1 might have additional substrate(s) other than bZIP60 and the substrate(s) has a role in the root regulation. It is also plausible that IRE1 relies on its RNA decay activity to regulate root growth. Another explanation is that IRE1 mediates root growth through protein-protein interaction. I also showed that a mutation of a component of G-protein complex, AGB1, enhances the ER stress and the short-root

phenotype in *ire1*, suggesting that the AGB1 regulation on the plant UPR does not completely rely on IRE1.

Future directions

The mutant analyses of *ire1 agb1* triple mutant demonstrate that the functional relationships between UPR transducers can be established *in vivo* in plants. To further investigate the plant UPR signaling network, future experimental approaches are presented here.

In addition of IRE1, two membrane-anchored transcription factors, bZIP17 and bZIP28, regulate the plant UPR. How these two distinct UPR signaling pathways are coordinated is not clear yet. The proteolytic cleavage of bZIP17/bZIP28 and *bZIP60* mRNA splicing are the molecular indicators of bZIP17/bZIP28 and IRE1 activation respectively. To determine whether bZIP17/bZIP28 or IRE1 has differential contributions on the UPR, their activated status can be monitored under various intensities and periods of ER stress treatment. Also, regulatory roles of bZIP17/bZIP28 and IRE1 in ER-stress triggered cell death have not been examined yet. To do so, an experimental system for a time course of prolonged ER stress treatment should be established. Once a reliable experimental setting is available, monitor of bZIP17/bZIP28 and IRE1 activation over the time course will shed lights on their involvement in regulation of cell death. Also, comparison of UPR target gene induction and cell death activation in *bzip17*/*bzip28* and *ire1* will potentially determine whether bZIP17/bZIP28 or IRE1 functions as a molecular switch of cell fate on severe ER stress. To identify mediators of ER stress-triggered cell death, transcriptomic analyses at time points covering prior and

after cell death initiation can be performed in wild-type Col-0, *bzip17*/*bzip28*, and *ire1*. The studies can also determine that whether bZIP17/bZIP28 or IRE1 transcriptionally regulates identified cell death mediators. Finally, functional relationships between the two types of plant ER stress sensors have not to be established yet. Generation of higher-order mutants of bZIP17/bZIP28 and IRE1 and perform phenotypic analyses in the above proposed experiments will define regulatory relationships between two UPR signaling arms. In case disruption of the two parallel UPR pathways leads to lethality in plants, an artificial miRNA method can be adopted to generate knock-down mutants of bZIP17/bZIP28 or IRE1.

The observation that *ire1* displays only the short-root phenotype but shows comparable shoot morphology with wild-type Col-0 indicates that IRE1 has tissue-specific role in root growth. More specifically, IRE1 is likely involved in the regulation of rapid elongation of root cells. How IRE1 senses the specialized secretory activity is unknown. One possibility is existence of cell type- or stage-specific IRE1-interacting proteins. To identify IRE1-interacting proteins in a context-specific manner, generation of epitope-tagged IRE1 under its native promoter will enable *in vivo* screening using specific tissues and growth stages. Another potential *in vivo* approach to detect IRE1-interacting proteins is to use *Arabidopsis* transgenic lines expressing IRE1 under control of an inducible promoter. After induction of IRE1 expression, blue native/SDS gel electrophoresis can be performed to detect whether IRE1 forms a protein complex. Alternatively, a yeast two-hybrid system using tissue-specific prey libraries may overcome challenges regarding potentially low expression of IRE1-interacting proteins.

In addition, how IRE1 activates the appropriate downstream response to support specific secretory activity is still unclear. One tempting model is that plant IRE1 may also process multiple types of RNA substrates according to need. To identify additional IRE1 substrates in a context-specific manner, a genome-wide screening of IRE1-interacting RNA can be performed in a tissue- or stage-specific manner. RNA-immunoprecipitation using IRE1 as bait and quantitative measurements of transcriptomes by deep RNA sequencing methods may be able to identify tissue-specific substrates of plant IRE1. Because interaction between IRE1 and its RNA substrates might be transient, an RNase inactive form of IRE1 can be used as a bait to potentially increase the duration of their physical interaction.

The Inter-regulation of UPR and Auxin Signaling

In Chapter 4, I established the inter-regulation of the UPR and auxin signaling. I found that ER stress modulates the transcription of auxin receptors and transporters. In addition, intra-cellular auxin transporters are required for the optimal induction of UPR target genes. The results support the suggestion that plants may regulate the auxin response to coordinate the growth regulation and stress adaption. Moreover, the requirement of IRE1 in the auxin homeostasis and response implies that the auxin signaling at least partially relies on the UPR-dependent secretory pathway.

Future directions

Because IRE1 and TIR1/AFBs are not essential for ER stress-triggered repression of auxin regulators, novel ER stress mediators involved in the auxin

regulation may exist. To identify genes involved in repression of auxin signaling on ER stress, ethyl methanesulfonate (EMS) mutagenesis can be performed using *Arabidopsis* expressing auxin reporters. Screening of mutants showing unaltered auxin signaling on ER stress may identify novel regulators of the UPR and auxin signaling. It is also possible that specific transcriptional regulators are responsible for down-regulation of auxin receptors and transporters on ER stress. To identify proteins that bind to promoters of auxin regulators on ER stress, a yeast one-hybrid screening system using the *PIN5* promoter and *Arabidopsis* cDNA or transcription factor libraries can be performed. Although yeast fails to survive on severe ER stress, experimental conditions allowing yeast survival and certain extent of UPR activation can be established by testing appropriate ER stress intensities.

The observation that the PIN5 is involved in the optimal induction of UPR target genes hints the possibility that ER stress regulates the PIN5 activity. ER stress may influences protein modifications, localization, or protein-protein interaction of PIN5. To monitor PIN5 protein, antibodies against PIN5 endogenous protein or epitope-tagged PIN5 under control of its native promoter can be generated. To determine whether PIN5 associates or disassociates with a protein complex *in vivo*, similar approaches mentioned above for identification of IRE1-interacting proteins can be conducted. Also, how PIN5 transmits stress signals to impact the UPR activation is not clear. One tempting hypothesis is that PIN5 induces auxin transport between subcellular compartments on ER stress. Because detection assays of auxin levels in the ER have not been established yet, an indirect but achievable approach is using a yeast efflux assay to test whether ER stress triggers auxin transport *in vitro*.

Using a strong ER stress inducer Tm, all the tested mutants of ER-localized auxin regulators show compromised UPR activation phenotype. Because the ER-localized auxin regulators differentially express, it is possible that individual ER-localized auxin regulator has a unique role in UPR-related stress adaption or growth regulation. It would be interesting to explore that whether ER-localized auxin regulators are involved in specific UPR-related regulations, such as heat and biotic stress.

To investigate molecular mechanisms how IRE1 mediates the auxin response and levels, IRE1-interacting proteins or RNA substrates under exogenous auxin treatment can be screened using the approaches mentioned above. Another possible mechanism underlying the IRE1 regulation on the auxin response is that IRE1 mediates the transcriptional reprogramming of auxin regulators. Comparison of transcriptomic profiling between wild-type Col-0 and *ire1* under exogenous auxin treatment will determine whether IRE1 controls auxin regulators at the transcriptional levels. Also, to learn whether IRE1 mediates the auxin response by regulation of mobilization of auxin regulators, fluorescently tagged auxin regulators under control of their native promoters can be introduced into *ire1*. Thus, mobilization of auxin regulators can be compared between wild-type Col-0 and *ire1*.

The Significance of Plant UPR in Cellular Function

My studies support the suggestion that the plant UPR is involved in primary root growth and auxin regulation. Because the UPR is fundamental for the secretory pathway, it is plausible that other biological processes dependent on the secretory pathway also closely associate with the UPR.

Future directions

The ER not only supports synthesis of secretory proteins, but also maintains many essential metabolic processes such as calcium storage and lipid/membrane production. As the UPR is essential for ER function, ER-dependent cellular regulation may also rely on the UPR. It would be interesting to explore functional relationships between ER-related biological processes and the plant UPR. For instance, whether lipid biosynthesis is mediated by IRE1- or bZIP17/bZIP28-dependent UPR has not reported yet. One straightforward approach is to examine the lipid compositions in mutants of UPR transducers. Also, comparison of lipid profiling between mock and ER stress-treated wild-type plants will determine that whether regulation of lipid metabolism is one of mechanisms underlying the plant UPR.

Likewise, as calcium signaling is vital for physiological and environmental responses, it would be interesting to test whether ER stress also regulates calcium homeostasis to coordinate stress adaption and growth regulation. Because calcium signaling is controlled by multiple protein kinases, one straightforward approach is to monitor the transcriptional and translational regulation of protein kinases important for calcium signaling on ER stress. If ER stress regulates components of calcium signaling pathways, phenotypic analyses of ER stress can be performed in mutants defective in calcium signaling. Likewise, calcium-signaling transmission can be monitored in mutants of UPR transducers to test whether the plant UPR is required for the calcium signaling regulation.

APPENDICES

APPENDIX A

Analysis of unfolded protein response in *Arabidopsis*

This section has been previously published in Methods in Molecular Biology

YA-NI CHEN and FEDERICA BRANDIZZI (2013)

Methods in Molecular Biology **1043**:73-80

Abstract

The unfolded protein response (UPR) is essential for development and adaption in eukaryotic cells. *Arabidopsis* has become one of the best model systems to uncover conserved regulatory mechanisms of the UPR in multicellular eukaryotes as well as unique UPR regulation in plants. Monitoring the UPR *in planta* is a fundamental approach to identifying regulatory components and to revealing molecular mechanisms of the plant UPR. In this chapter, we provide protocols for the plant UPR induction as well as the UPR activation analyses at a molecular level in *Arabidopsis*. Three kinds of ER stress treatment methods and quantitation of the plant UPR activation are described here.

Introduction

The unfolded protein response (UPR) is a collection of conserved signaling pathways aiming to maintain endoplasmic reticulum (ER) protein folding homeostasis in eukaryotic cells (UPR) [1, 2]. There is approximately one-third of protein initially folded and modified in the ER lumen. Environmental or physiological factors that cause an imbalance between ER protein folding demand and capability lead to ER stress. To relieve the ER stress, eukaryotic cells activate the UPR to increase the ER protein folding ability. Wide ranges of stimuli trigger the activation of the UPR. To experimentally examine the UPR, chemicals disturbing the ER protein folding homeostasis are applied to activate the UPR. One of the most frequently used UPR

inducers is a glycosylation inhibitor, tunicamycin (Tm). The majority of secretory proteins are glycosylated in the ER as the glycosylation is critical for protein structure formation and for protein targeting to cellular compartments. As Tm blocks the first step of *N*-linked glycosylation, it can efficiently lead to an accumulation of unfolded proteins in the ER lumen and therefore activate the UPR [163-165].

To observe the plant UPR at different plant stages, we describe three experimental approaches to perform ER stress treatment. To test long-term ER stress tolerance, seeds are directly germinated on medium containing a relatively low concentration of Tm. Tm can also been infiltrated into leaves to specifically monitor the UPR on ground tissues. Finally, to examine the early outputs of the plant UPR, a short-term Tm treatment using a liquid method is conducted to observe a more direct effect from ER stress.

To cope with dynamic ER protein folding demands, the UPR adjusts the transcription of regulators involved in assembling protein structure, degrading mis-folded protein, and determining cell fates [19, 166]. Hence, the upregulation of well-established UPR target genes, such as *BiP3* in *Arabidopsis* [39, 40, 167], is considered a molecular indicator of UPR activation. To introduce the quantitative method of reading UPR outputs, real-time reverse transcription polymerase chain reaction (qRT-PCR) analysis of UPR target genes induction is included in this chapter.

Materials

1. Basic reagents and equipment for plant sterile tissue culture and RNA work handling.

2. Plant growth medium: Linsmaier and Skoog (LS) with Buffer and Sucrose (Caisson LSP04); Phytagel (Sigma P8169).

3. Growth chamber: temperature set to 21°C, 16 h light/ 8 h dark cycle, 100 m Einstein/m2 s and 65% humidity.

4. Tunicamycin (Sigma T7765).

5. Dimethyl sulfoxide (DMSO) solvent.

6. 1 ml needleless syringes.

7. Liquid nitrogen.

8. RNeasy plant mini kit (Qiagen 74904).

9. RNase-Free DNase Set (Qiagen 79254).

10. SuperScript® VILO™ Master Mix (Invitrogen 11755500).

11. Reagents for real-time PCR: MicroAmp® Fast optical 96-well reaction plate (ABI 4346936); optical adhesive cover (ABI 4311971); FAST SYBR Master Mix (ABI 4385612).

Methods

ER stress tolerance assay

To examine the tolerant ability of plants in coping with different intensities of ER stress, seeds are directly germinated on medium containing Tm concentrations ranging from 10-50 ng/ml. Comparison of phenotype between wild-type plants and mutants of interest can reveal whether the mutants display over-sensitive or resistant growth phenotype under ER stress conditions. The Tm infiltration assay enables the observation of the plant UPR using adult plants.

1. Sterilize seeds and store at 4 ° C for two days (see Note 1).

2. Prepare ½ LS with 0.4 % Phytagel medium.

3. Autoclave the ½ LS medium on liquid cycle program for 25-40 minutes.

4. Dissolve Tm powder in DMSO to prepare 10 mg/ml Tm stock solution (see Note 2).

5. Prepare 10, 20, 30, 40 and 50 µg/ml Tm stock solutions by 1000, 500, 333, 250, and 200X dilution of 10 mg/ml Tm stock solution respectively using ½ LS liquid medium.

6. Cool the autoclaved ½ LS medium to 50 ° C.

7. Add 10, 20, 30, 40, and 50 µg/ml Tm stock solutions respectively to cooled ½ LS medium (50 ° C) by 1000X dilution to make ½ LS medium containing 10, 20, 30, 40, and 50 ng/ml Tm (see Note 3).

8. Swirl to mix and use a pipet to pour equal amount of Tm-containing medium per plate in sterile tissue culture hood. Prepare Tm-containing medium freshly right before the Tm germination assay (see Notes 4).

9. For Mock control, the same preparation procedure is carried out with the exception of replacing the Tm in the ½ LS medium with 0.0005% DMSO.

10. Germinate *Arabidopsis* seeds on ½ LS medium containing 0.0005% DMSO, 10, 20, 30, 40, and 50 ng/ml Tm. Place a single seed on the medium at similar distance between each other (see Notes 5). At least three individual plates for each Tm concentration and mock control should be used.

11. Grow the plants under these conditions: 21°C, 16 h light/8 h dark cycle, 100 mEinstein/m2 s and 65% humidity.

12. Observe the growth phenotype 7-14 days after germination. (see Note 6)

13. Using Col-0 ecotype wild-type Arabidopsis, the plants shows more pronounced growth defects starting from 30 ng/ml Tm (see Figure. A.1)

Tm infiltration into leaf tissues

1. Dissolve Tm powder in DMSO to prepare 10 mg/ml Tm stock solution (see Note2).

2. Prepare 15μg/ml Tm stock solution by 666 X dilution of 10 mg/ml Tm stock solution using ½ LS liquid medium. Prepare Tm-containing medium freshly right before the Tm infiltration assay (see Note 4).

3. Use a needleless syringe to infiltrate ½ LS liquid medium containing 15 μg/ml Tm into abaxial sides of five week-old rosette leaves (see Note 7).

4. For Mock control, the same treatment procedure is performed with the exception of replacing the Tm in the ½ LS liquid medium with 0.0015% DMSO (see Note 8).

5. Observe the leaves phenotype 1-4 days after infiltration.

Short period of ER stress treatment

While the ER stress tolerance assay can examine whether mutants of interest show plant phenotype under ER stress, even if the mutants display similar visible plant phenotype to wild-type plants, it is possible that the defects of UPR in mutants of interest do not reflect on the plant growth morphology. One of the examples is the mutant of *AtbZIP60*, a transcription factor confirmed as a UPR regulator [39, 76](10-11). To verify whether genes of interest are involved in the UPR, short-term ER stress treatment coupled with analyses of UPR target genes induction are performed to monitor the UPR phenotype at a molecular level.

1. Sterilize seeds and store at 4 ° C for two days (see Note 1).

2. Germinate seeds in vertical plates for ten days. Medium: half-strength LS with 0.4 % Phytagel. Place ten seeds, evenly spaced, per small round plate (100 X 15 mm) or square plate. Seal bottom part of plates with parafilm and upper part of plates with 3M surgical tape (see Figure A.2 and Note 9).

3. Dissolve Tm powder in DMSO to prepare 10 mg/ml Tm stock solution (see Note2).

4. Prepare 5μg/ml Tm-containing medium by 2000 X dilution of 10 mg/ml Tm stock solution using half-strength LS liquid medium. Prepare Tm-containing medium freshly right before the Tm treatment (see Note2).

5. Gently transfer ten day-old vertically grown seedlings to 5 μg/ml Tm-containing medium for an appropriate time period (see Notes 10 and 11).

6. Collect 10-20 individual Tm-treated seedlings per sample using liquid nitrogen (see Notes 12 and 13).

7. For Mock control, the same treatment procedure is performed with the exception of replacing the Tm in the half-strength LS liquid medium with 0.05% DMSO.

Quantitative measurement of UPR activation

The major output of the plant UPR identified so far is the regulation of UPR target genes transcription. Hence, measurement of UPR gene induction under ER stress is the most reliable method to quantify the plant UPR activation.

1. Extract RNA from Tm-treated seedlings using an RNeasy plant mini kit and RNase-Free DNase Set.

2. Synthesize CDNA from RNA using a SuperScript® VILO™ Master Mix.

3. Perform real-time PCR with SYBR Green detection in triplicate using the Applied Biosystems 7500 fast real-time PCR system. The primer sequence of UPR target genes is listed in Table A.1 [39].

4. Analyze Data by the DDCT method.

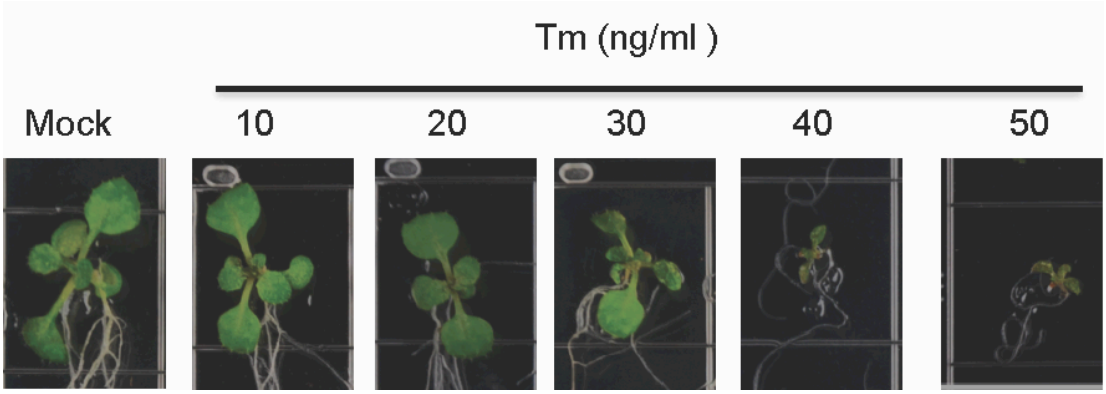

Figure A.1. Plant phenotype under tunicamycin treatments.

Wild-type Col-0 plants were germinated on half-strength LS medium containing DMSO, 10, 20, 30, 40, or 50 ng/ml Tm for 2 week.

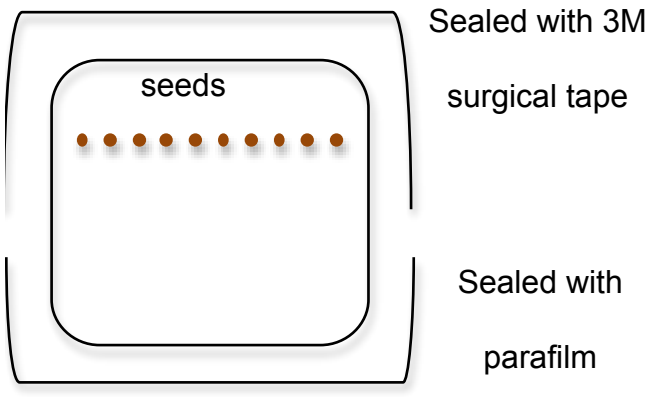

Figure A.2. Vertical growth of plant seedlings.

The 3M surgical tapes and parafilm are used respectively to seal the upper and bottom part of vertical plates.

Table A.1. DNA primers of UPR target genes

primers	Sequence (5'–3')	Gene
BiP1/2-qP For	ccaccggccccaagag	AT5G28540/AT5G42020
BiP1/2-qP Rev	ggcgtccacttcgaatgtg	AT5G28540/AT5G42020
BiP3-qP For	aaccgcgagcttggaaaat	At1g09080
BiP3-qP Rev	tcccctgggtgcaggaa	At1g09080
AtERdj3A-qP For	tcaagtggtggtggtttcaact	AT3G0890
AtERdj3A-qP Rev	cccaccgcccatattttg	AT3G0890
AtERdj3B-qP For	gaggaggcggcatgaatatg	At3g62600
AtERdj3B-qP Rev	ccatcgaacctccaccaaaa	At3g62600
PDI6-qP For	cgaagtggctttgtcattcca	AT1G77510
PDI6-qP Rev	gcggttgcgtccaatttt	AT1G77510
PDI9-qP For	ggccctgttgaagtgactgaa	AT2G32920
PDI9-qP Rev	cagcagaaccacacttcttttcc	AT2G32920
CNX1-qP For	gtgtcctcgtcgccattgt	AT5G61790
CNX1-qP Rev	ttgccaccaaagataagcttga	AT5G61790
CRT1-qP For	gatcaagaaggaggtcccatgt	AT1G56340
CRT1-qP Rev	gacggaggacgaaggtgtaca	AT1G56340
ATERDJ2A-qP For	tgggcttgtaggcgctctt	At1g79940
ATERDJ2A-qP Rev	aacccaatagttttcctccttgtg	At1g79940
ATERDJ2B-qP For	tgaaacgtcccaatggactca	At4g21180

Table A.1 (cont'd)

ATERDJ2B-qP Rev	cctctttgtggaaaggaaagtaagg	At4g21180
ATP58IPK-qP For	gcgttatagtgatgccctcgat	AT5G03160
ATP58IPK-qP Rev	gaaagcgcagggtctgctt	AT5G03160

Notes

1. The quality of seed stock is very important for ER stress related assays. Using seeds freshly harvested from healthy plants is one of key points to get reproducible and consistent results.

2. Aliquot Tm stock solution (10 mg/ml) into relatively small amount and store in a -20° C freezer. Avoid freezing and thawing.

3. High temperature destabilizes Tm.

4. Tm-containing medium is unstable if it is not freshly prepared.

5. For a fair comparison, the distance between seeds should be consistent. Square petri dish with Grid (Fisher 08-757-11A) is useful, as a single seed can be placed on the center of each small square area on the plates (see Fig1).

6. The growth phenotype can be more obvious at a relative early stage (within one week) or vice versa. To observe growth-stage-specific phenotypes, the Tm-treated seedlings should be check every day during the assay.

7. To fairly compare the ER tolerance between wild-type and mutant plants, choose the same stage, size, and condition of leaves for both varieties of plants.

8. The infiltration process needs be done carefully and should not lead to any damage of plants. Leaves infiltrated with DMSO (Mock control) should look similar to leaves without infiltration after one day.

9. To allow proper ventilation, do not wrap plates completely with parafilm.

10. If mutants of interest display normal growth phenotype as wild-type plants, choose healthy and unstressed seedlings as well as similar growth morphology for all plants to perform the treatment.

11. Using ten day-old seedlings coupled with a real time PCR system, the induction of UPR target genes can be detected from 0.5 to 16 hr. Prolong treatment is not recommended using this liquid system.

12. Using more seedlings per biological sample can reduce the standard deviation of fold change of UPR gene induction between biological replicates.

13. Sample collection should be done carefully and timely to avoid additional stress before seedlings are frozen by liquid nitrogen.

Acknowledgments

We acknowledge support by the Chemical Sciences, Geosciences and Biosciences Division, Office of Basic Energy Sciences, Office of Science, US Department of Energy (award number DE-FG02-91ER20021) and the National Aeronautics and Space Agency (NNH08ZTT003N NRA–08-FSB_Prop-0052).

APPENDIX B

Published manuscripts

1. Chen Y and Brandizzi F. IRE1: ER stress sensor and cell fate executor. *Trends in cell biology* 2013 (online preview)

2. Chen Y and Brandizzi F. Analysis of Unfolded Protein Response in Arabidopsis. *Methods in Molecular Biology* 2013; 1043:73-80

3. Chen Y, Aung K, Rolčík J, Walicki K, Friml J, and Brandizzi F. Inter-regulation of the unfolded protein response and auxin signaling. *The plant journal* 2013 (preview on line)

4. Chen Y and Brandizzi F. AtIRE1A/AtIRE1B and AGB1 independently control two essential unfolded protein response pathways in Arabidopsis. *The plant journal* 2012; 69:266-277.

5. Faso C*, Chen Y*, Tamura K*, Held M, Zemeli S, Marti L, Saravanan R, Hummel E, Kung L, Miller E, Hawes C, Brandizzi F. A missense mutation in the Arabidopsis COPII coat protein Sec24A induces the formation of clusters of the endoplasmic reticulum and Golgi apparatus. *The Plant Cell* 2009; 21:3655-3671. *These authors contributed equally to the work.

6. Chen Y*, Slabaugh E*, and Brandizzi F. Membrane-tethered transcription factors in Arabidopsis thaliana: novel regulators in stress response and development. *Current Opinion in Plant Biology* 2008; 11:695-701. *These authors contributed equally to the work.

7. Srivastava R, Chen Y, Deng Y; Brandizzi F and Howell S. Elements proximal to and within the transmembrane domain mediate the organelle-to-organelle movement of bZIP28 under ER stress conditions. *The plant journal* 2012; 6:1033-1044

8. Conger R, Chen Y, Fornaciari S, Faso C, Held M, Renna L and Brandizzi F. Evidence

for the involvement of the Arabidopsis SEC24A in male transmissions. *Journal of Experimental Botany* 201;62(14):4917-26

9. Moghe GD, Lehti-Shiu MD, Seddon AE, Yin S, Chen Y, Juntawong P, Brandizzi F, Bailey-Serres J, Shiu SH. Characteristics and significance of intergenic polyadenylated RNA transcription in Arabidopsis. *Plant Physiology* 2013; 161:210-224

10. Moreno AA, Mukhtar MS, Blanco F, Boatwright JL, Moreno I, Jordan M, Chen Y, Brandizzi F, Dong X, Orellana A, Pajerowska-Mukhtar K. IRE1/bZIP60-Mediated Unfolded Protein Response Plays Distinct Roles in Plant Immunity and Abiotic Stress Responses. *PLoS ONE* 2012; 7(2)

REFERENCES

REFERENCES

1 Kozutsumi, Y.*, et al.* (1988) The presence of malfolded proteins in the endoplasmic reticulum signals the induction of glucose-regulated proteins. *Nature* 332, 462-464

2 Schroder, M. and Kaufman, R.J. (2005) The mammalian unfolded protein response. *Annu Rev Biochem* 74, 739-789

3 Smith, M.H.*, et al.* (2011) Road to Ruin: Targeting Proteins for Degradation in the Endoplasmic Reticulum. *Science* 334, 1086-1090

4 Hoseki, J.*, et al.* (2010) Mechanism and components of endoplasmic reticulum-associated degradation. *Journal of Biochemistry* 147, 19-25

5 Feldman, M. and van der Goot, F.G. (2009) Novel ubiquitin-dependent quality control in the endoplasmic reticulum. *Trends in Cell Biology* 19, 357-363

6 Walter, P. and Ron, D. (2011) The unfolded protein response: from stress pathway to homeostatic regulation. *Science* 334, 1081-1086

7 Merksamer, P.I. and Papa, F.R. (2010) The UPR and cell fate at a glance. *Journal of cell science* 123, 1003-1006

8 Fonseca, S.G.*, et al.* (2011) Endoplasmic reticulum stress and pancreatic beta-cell death. *Trends in Endocrinology and Metabolism* 22, 266-274

9 Woehlbier, U. and Hetz, C. (2011) Modulating stress responses by the UPRosome: a matter of life and death. *Trends in biochemical sciences* 36, 329-337

10 Shore, G.C.*, et al.* (2011) Signaling cell death from the endoplasmic reticulum stress response. *Current Opinion in Cell Biology* 23, 143-149

11 Braakman, I. and Bulleid, N.J. (2011) Protein Folding and Modification in the Mammalian Endoplasmic Reticulum. In *Annual Review of Biochemistry, Vol 80* (Kornberg, R.D.*, et al.*, eds), pp. 71-99

12 Buchberger, A.*, et al.* (2010) Protein Quality Control in the Cytosol and the Endoplasmic Reticulum: Brothers in Arms. *Molecular Cell* 40, 238-252

13 Appenzeller-Herzog, C. and Hall, M.N. (2012) Bidirectional crosstalk between endoplasmic reticulum stress and mTOR signaling. *Trends in Cell Biology* 22, 274-282

14 Hetz, C. (2012) The unfolded protein response: controlling cell fate decisions under ER stress and beyond. *Nature Reviews Molecular Cell Biology* 13, 89-102

15 Jager, R.*, et al.* (2012) The unfolded protein response at the crossroads of cellular life and death during endoplasmic reticulum stress. *Biology of the Cell* 104, 259-270

16 Gardner, B.M.*, et al.* (2013) Endoplasmic reticulum stress sensing in the unfolded protein response. *Cold Spring Harb Perspect Biol* 5, a013169

17 Cox, J.S.*, et al.* (1993) Transcriptional induction of genes encoding endoplasmic reticulum resident proteins requires a transmembrane protein kinase. *Cell* 73, 1197-1206

18 Mori, K.*, et al.* (1993) A transmembrane protein with a CDC2+/CDC28-related kinase-activity is requried for signaling from the ER to the nuclues. *Cell* 74, 743-756

19 Cox, J.S. and Walter, P. (1996) A novel mechanism for regulating activity of a transcription factor that controls the unfolded protein response. *Cell* 87, 391-404

20 Shen, X.*, et al.* (2001) Complementary signaling pathways regulate the unfolded protein response and are required for *C. elegans* development. *Cell* 107, 893-903

21 Acosta-Alvear, D.*, et al.* (2007) XBP1 controls diverse cell type- and condition-specific transcriptional regulatory networks. *Molecular Cell* 27, 53-66

22 Ron, D. and Walter, P. (2007) Signal integration in the endoplasmic reticulum unfolded protein response. *Nature Reviews Molecular Cell Biology* 8, 519-529

23 Harding, H.P.*, et al.* (2000) Perk is essential for translational regulation and cell survival during the unfolded protein response. *Mol Cell* 5, 897-904

24 Haze, K.*, et al.* (1999) Mammalian transcription factor ATF6 is synthesized as a transmembrane protein and activated by proteolysis in response to endoplasmic reticulum stress. *Molecular Biology of the Cell* 10, 3787-3799

25 Koizumi, N.*, et al.* (2001) Molecular characterization of two *Arabidopsis* Ire1 homologs, endoplasmic reticulum-located transmembrane protein kinases. *Plant Physiol* 127, 949-962

26 Noh, S.J.*, et al.* (2002) Characterization of two homologs of Ire1p, a kinase/endoribonuclease in yeast, in *Arabidopsis thaliana*. *Biochimica et biophysica acta* 1575, 130-134

27 Iwata, Y. and Koizumi, N. (2012) Plant transducers of the endoplasmic reticulum unfolded protein response. *Trends in plant science* 17, 720-727

28 Wu, J. and Kaufman, R.J. (2006) From acute ER stress to physiological roles of the Unfolded Protein Response. *Cell Death Differ* 13, 374-384

29 Zhang, K.*, et al.* (2005) The unfolded protein response sensor IRE1alpha is required at 2 distinct steps in B cell lymphopoiesis. *J Clin Invest* 115, 268-281

30 Tsuru, A.*, et al.* (2013) Negative feedback by IRE1beta optimizes mucin production in goblet cells. *Proc Natl Acad Sci U S A* 110, 2864-2869

31 Scheuner, D.*, et al.* (2005) Control of mRNA translation preserves endoplasmic reticulum function in beta cells and maintains glucose homeostasis. *Nat Med* 11, 757-764

32 Ozcan, L. and Tabas, I. (2012) Role of endoplasmic reticulum stress in metabolic disease and other disorders. *Annu Rev Med* 63, 317-328

33 Minamino, T.*, et al.* (2010) Endoplasmic Reticulum Stress As a Therapeutic Target in Cardiovascular Disease. *Circulation Research* 107, 1071-1082

34 Hampton, R.Y. (2002) Proteolysis and sterol regulation. *Annu Rev Cell Dev Biol* 18, 345-378

35 Hummasti, S. and Hotamisligil, G.S. (2010) Endoplasmic Reticulum Stress and Inflammation in Obesity and Diabetes. *Circulation Research* 107, 579-591

36 Chakrabarti, A.*, et al.* (2011) A review of the mammalian unfolded protein response. *Biotechnology and bioengineering* 108, 2777-2793

37 Hetz, C. and Glimcher, L.H. (2009) Fine-Tuning of the Unfolded Protein Response: Assembling the IRE1 alpha Interactome. *Molecular Cell* 35, 551-561

38 Hetz, C.*, et al.* (2011) THE UNFOLDED PROTEIN RESPONSE: INTEGRATING STRESS SIGNALS THROUGH THE STRESS SENSOR IRE1 alpha. *Physiol Rev* 91, 1219-1243

39 Chen, Y. and Brandizzi, F. (2012) AtIRE1A/AtIRE1B and AGB1 independently control two essential unfolded protein response pathways in *Arabidopsis*. *Plant J* 69, 266-277

40 Nagashima, Y.*, et al.* (2011) *Arabidopsis* IRE1 catalyses unconventional splicing of bZIP60 mRNA to produce the active transcription factor. *Sci Rep* 1, 29

41 Ali, M.M.U.*, et al.* (2011) Structure of the Ire1 autophosphorylation complex and implications for the unfolded protein response. *Embo Journal* 30, 894-905

42 Aragon, T.*, et al.* (2009) Messenger RNA targeting to endoplasmic reticulum stress signalling sites. *Nature* 457, 736-740

43 Korennykh, A.V.*, et al.* (2009) The unfolded protein response signals through high-order assembly of Ire1. *Nature* 457, 687-693

44 Hollien, J.*, et al.* (2009) Regulated Ire1-dependent decay of messenger RNAs in mammalian cells. *The Journal of cell biology* 186, 323-331

45 So, J.S.*, et al.* (2012) Silencing of Lipid Metabolism Genes through IRE1 alpha-Mediated mRNA Decay Lowers Plasma Lipids in Mice. *Cell Metabolism* 16, 487-499

46 Sakaki, K.*, et al.* (2012) RNA surveillance is required for endoplasmic reticulum homeostasis. *Proc Natl Acad Sci U S A* 109, 8079-8084

47 Hollien, J. and Weissman, J.S. (2006) Decay of endoplasmic reticulum-localized mRNAs during the unfolded protein response. *Science* 313, 104-107

48 Moore, K.A. and Hollien, J. (2012) The unfolded protein response in secretory cell function. *Annual review of genetics* 46, 165-183

49 Vattem, K.M. and Wek, R.C. (2004) Reinitiation involving upstream ORFs regulates ATF4 mRNA translation in mammalian cells. *Proc Natl Acad Sci U S A* 101, 11269-11274

50 Raven, J.F. and Koromilas, A.E. (2008) PERK and PKR: old kinases learn new tricks. *Cell cycle* 7, 1146-1150

51 Korennykh, A. and Walter, P. (2012) Structural basis of the unfolded protein response. *Annual review of cell and developmental biology* 28, 251-277

52 Kimmig, P.*, et al.* (2012) The unfolded protein response in fission yeast modulates stability of select mRNAs to maintain protein homeostasis. *Elife* 1, e00048

53 Mishiba, K.*, et al.* (2013) Defects in IRE1 enhance cell death and fail to degrade mRNAs encoding secretory pathway proteins in the *Arabidopsis* unfolded protein response. *Proc Natl Acad Sci U S A* 110, 5713-5718

54 Sun, J.*, et al.* (2011) Neuronal GPCR controls innate immunity by regulating noncanonical unfolded protein response genes. *Science* 332, 729-732

55 Hotamisligil, G.S. (2010) Endoplasmic reticulum stress and the inflammatory basis of metabolic disease. *Cell* 140, 900-917

56 Fu, S.*, et al.* (2011) Aberrant lipid metabolism disrupts calcium homeostasis causing liver endoplasmic reticulum stress in obesity. *Nature* 473, 528-531

57 Hosoi, T. and Ozawa, K. (2010) Endoplasmic reticulum stress in disease: mechanisms and therapeutic opportunities. *Clinical Science* 118, 19-29

58 Li, X.*, et al.* (2011) Unfolded protein response in cancer: the physician's perspective. *Journal of hematology & oncology* 4, 8

59 Wang, S. and Kaufman, R.J. (2012) The impact of the unfolded protein response on human disease. *The Journal of cell biology* 197, 857-867

60 Tabas, I. and Ron, D. (2011) Integrating the mechanisms of apoptosis induced by endoplasmic reticulum stress. *Nature cell biology* 13, 184-190

61 Rodriguez, D.*, et al.* (2011) Integrating stress signals at the endoplasmic reticulum: The BCL-2 protein family rheostat. *Biochimica Et Biophysica Acta-Molecular Cell Research* 1813, 564-574

62 Cao, S.S. and Kaufman, R.J. (2012) Unfolded protein response. *Current Biology* 22, R622-R626

63 Marciniak, S.J.*, et al.* (2004) CHOP induces death by promoting protein synthesis and oxidation in the stressed endoplasmic reticulum. *Genes Dev* 18, 3066-3077

64 Crosti, P.*, et al.* (2001) Tunicamycin and Brefeldin A induce in plant cells a programmed cell death showing apoptotic features. *Protoplasma* 216, 31-38

65 Watanabe, N. and Lam, E. (2008) BAX inhibitor-1 modulates endoplasmic reticulum stress-mediated programmed cell death in *Arabidopsis*. *J Biol Chem* 283, 3200-3210

66 Iwawaki, T.*, et al.* (2009) Function of IRE1 alpha in the placenta is essential for placental development and embryonic viability. *Proc Natl Acad Sci U S A* 106, 16657-16662

67 Lin, J.H.*, et al.* (2007) IRE1 signaling affects cell fate during the unfolded protein response. *Science* 318, 944-949

68 Lin, J.H.*, et al.* (2009) Divergent effects of PERK and IRE1 signaling on cell viability. *PLoS One* 4, e4170

69 Upton, J.P.*, et al.* (2012) IRE1alpha cleaves select microRNAs during ER stress to derepress translation of proapoptotic Caspase-2. *Science* 338, 818-822

70 Han, D.*, et al.* (2009) IRE1 alpha Kinase Activation Modes Control Alternate Endoribonuclease Outputs to Determine Divergent Cell Fates. *Cell* 138, 562-575

71 Vakifahmetoglu-Norberg, H. and Zhivotovsky, B. (2010) The unpredictable caspase-2: what can it do? *Trends in Cell Biology* 20, 150-159
72 Lerner, A.G.*, et al.* (2012) IRE1alpha induces thioredoxin-interacting protein to activate the NLRP3 inflammasome and promote programmed cell death under irremediable ER stress. *Cell Metabolism* 16, 250-264

73 Menu, P.*, et al.* (2012) ER stress activates the NLRP3 inflammasome via an UPR-independent pathway. *Cell death & disease* 3, e261

74 Oikawa, D.*, et al.* (2010) Identification of a consensus element recognized and cleaved by IRE1 alpha. *Nucleic acids research* 38, 6265-6273

75 Koizumi, N.*, et al.* (2001) Molecular characterization of two *Arabidopsis* Ire1 homologs, endoplasmic reticulum-located transmembrane protein kinases. *Plant physiology* 127, 949-962

76 Lu, D.P. and Christopher, D.A. (2008) Endoplasmic reticulum stress activates the expression of a sub-group of protein disulfide isomerase genes and AtbZIP60 modulates the response in *Arabidopsis thaliana*. *Molecular genetics and genomics : MGG* 280, 199-210

77 Urano, F.*, et al.* (2000) IRE1 and efferent signaling from the endoplasmic reticulum. *J Cell Sci* 113 Pt 21, 3697-3702

78 Jwa, M. and Chang, P. (2012) PARP16 is a tail-anchored endoplasmic reticulum protein required for the PERK- and IRE1 alpha-mediated unfolded protein response. *Nature cell biology* 14, 1223-+

79 Lisbona, F.*, et al.* (2009) BAX Inhibitor-1 Is a Negative Regulator of the ER Stress Sensor IRE1 alpha. *Molecular Cell* 33, 679-691

80 Luo, D.H.*, et al.* (2008) AIP1 is critical in transducing IRE1-mediated endoplasmic reticulum stress response. *Journal of Biological Chemistry* 283, 11905-11912

81 Gu, F.*, et al.* (2004) Protein-tyrosine phosphatase 1B potentiates IRE1 signaling during endoplasmic reticulum stress. *J Biol Chem* 279, 49689-49693

82 He, Y.*, et al.* (2012) Nonmuscle myosin IIB links cytoskeleton to IRE1alpha signaling during ER stress. *Developmental cell* 23, 1141-1152

83 Oono, K.*, et al.* (2004) JAB1 participates in unfolded protein responses by association and dissociation with IRE1. *Neurochemistry international* 45, 765-772

84 Nguyen, D.T.*, et al.* (2004) Nck-dependent activation of extracellular signal-regulated kinase-1 and regulation of cell survival during endoplasmic reticulum stress. *Molecular biology of the cell* 15, 4248-4260

85 Nishitoh, H.*, et al.* (2002) ASK1 is essential for endoplasmic reticulum stress-induced neuronal cell death triggered by expanded polyglutamine repeats. *Genes Dev* 16, 1345-1355
86 Hetz, C.*, et al.* (2006) Proapoptotic BAX and BAK modulate the unfolded protein response by a direct interaction with IRE1alpha. *Science* 312, 572-576

87 Urano, F.*, et al.* (2000) Coupling of stress in the ER to activation of JNK protein kinases by transmembrane protein kinase IRE1. *Science* 287, 664-666

88 Yoneda, T.*, et al.* (2001) Activation of caspase-12, an endoplastic reticulum (ER) resident caspase, through tumor necrosis factor receptor-associated factor 2-dependent mechanism in response to the ER stress. *J Biol Chem* 276, 13935-13940

89 Gupta, S.*, et al.* (2010) HSP72 Protects Cells from ER Stress-induced Apoptosis via Enhancement of IRE1 alpha-XBP1 Signaling through a Physical Interaction. *Plos Biology* 8

90 Marcu, M.G.*, et al.* (2002) Heat shock protein 90 modulates the unfolded protein response by stabilizing IRE1alpha. *Molecular and cellular biology* 22, 8506-8513

91 Yang, Q.*, et al.* (2006) Tumour necrosis factor receptor 1 mediates endoplasmic reticulum stress-induced activation of the MAP kinase JNK. *EMBO reports* 7, 622-627

92 Gao, B.*, et al.* (2008) Synoviolin promotes IRE1 ubiquitination and degradation in synovial fibroblasts from mice with collagen-induced arthritis. *EMBO reports* 9, 480-485

93 Nagai, A.*, et al.* (2009) USP14 inhibits ER-associated degradation via interaction with IRE1 alpha. *Biochemical and Biophysical Research Communications* 379, 995-1000

94 Qiu, Y.*, et al.* (2010) A crucial role for RACK1 in the regulation of glucose-stimulated IRE1alpha activation in pancreatic beta cells. *Science signaling* 3, ra7

95 Ren, D.*, et al.* (2010) BID, BIM, and PUMA are essential for activation of the BAX- and BAK-dependent cell death program. *Science* 330, 1390-1393

96 Gardner, B.M. and Walter, P. (2011) Unfolded Proteins Are Ire1-Activating Ligands That Directly Induce the Unfolded Protein Response. *Science* 333, 1891-1894

97 Pincus, D.*, et al.* (2010) BiP binding to the ER-stress sensor Ire1 tunes the homeostatic behavior of the unfolded protein response. *Plos Biology* 8, e1000415

98 Oikawa, D.*, et al.* (2009) Activation of mammalian IRE1 alpha upon ER stress depends on dissociation of BiP rather than on direct interaction with unfolded proteins. *Experimental Cell Research* 315, 2496-2504

99 Oikawa, D.*, et al.* (2012) Direct association of unfolded proteins with mammalian ER stress sensor, IRE1beta. *PLoS One* 7, e51290

100 Cretenet, G.*, et al.* (2010) Circadian clock-coordinated 12 Hr period rhythmic activation of the IRE1alpha pathway controls lipid metabolism in mouse liver. *Cell Metabolism* 11, 47-57

101 Volmer, R.*, et al.* (2013) Membrane lipid saturation activates endoplasmic reticulum unfolded protein response transducers through their transmembrane domains. *Proc Natl Acad Sci U S A* 110, 4628-4633

102 Cox, D.J.*, et al.* (2011) Measuring signaling by the unfolded protein response. *Methods in enzymology* 491, 261-292

103 Hiramatsu, N.*, et al.* (2011) MONITORING AND MANIPULATING MAMMALIAN UNFOLDED PROTEIN RESPONSE. In *Methods in Enzymology, Vol 491: Unfolded Protein Response and Cellular Stress, Pt C* (Conn, P.M., ed), pp. 183-198

104 Teske, B.F.*, et al.* (2011) Methods for analyzing eIF2 kinases and translational control in the unfolded protein response. *Methods in enzymology* 490, 333-356

105 Oslowski, C.M. and Urano, F. (2011) MEASURING ER STRESS AND THE UNFOLDED PROTEIN RESPONSE USING MAMMALIAN TISSUE CULTURE SYSTEM. In *Methods in Enzymology: Unfolded Protein Response and Cellular Stress, Vol 490, Pt B* (Conn, P.M., ed), pp. 71-92

106 Deng, Y.*, et al.* (2011) Heat induces the splicing by IRE1 of a mRNA encoding a transcription factor involved in the unfolded protein response in *Arabidopsis*. *Proc Natl Acad Sci U S A* 108, 7247-7252

107 Moreno, A.A.*, et al.* (2012) IRE1/bZIP60-mediated unfolded protein response plays distinct roles in plant immunity and abiotic stress responses. *PLoS One* 7, e31944

108 Gao, H.B.*, et al.* (2008) A membrane-tethered transcription factor defines a branch of the heat stress response in *Arabidopsis thaliana*. *Proc Natl Acad Sci U S A* 105, 16398-16403

109 Liu, J.X.*, et al.* (2007) An endoplasmic reticulum stress response in *Arabidopsis* is mediated by proteolytic processing and nuclear relocation of a membrane-associated transcription factor, bZIP28. *Plant Cell* 19, 4111-4119

110 Noh, S.J.*, et al.* (2002) Characterization of two homologs of Ire1p, a kinase/endoribonuclease in yeast, in *Arabidopsis thaliana*. *Biochim Biophys Acta* 1575, 130-134

111 Lu, D.P. and Christopher, D.A. (2008) Endoplasmic reticulum stress activates the expression of a sub-group of protein disulfide isomerase genes and AtbZIP60 modulates the response in *Arabidopsis thaliana*. *Molecular Genetics and Genomics* 280, 199-210
112 Deng, Y.*, et al.* (2011) Heat induces the splicing by IRE1 of a mRNA encoding a transcription factor involved in the unfolded protein response in *Arabidopsis*. *Proc Natl Acad Sci U S A* 108, 7247-7252

113 Wang, S.Y.*, et al.* (2007) Heterotrimeric G protein signaling in the *Arabidopsis* unfolded protein response. *Proc Natl Acad Sci U S A* 104, 3817-3822

114 Neer, E.J. and Clapham, D.E. (1988) ROLES OF G-PROTEIN SUBUNITS IN TRANSMEMBRANE SIGNALING. *Nature* 333, 129-134

115 Lease, K.A.*, et al.* (2001) A mutant *Arabidopsis* heterotrimeric G-protein beta subunit affects leaf, flower, and fruit development. *Plant Cell* 13, 2631-2641

116 Jones, A.M.*, et al.* (2003) A reevaluation of the role of the heterotrimeric G protein in coupling light responses in arabidopsis. *Plant Physiology* 131, 1623-1627

117 Wei, Q.*, et al.* (2008) Heterotrimeric G-protein is involved in phytochrome A-mediated cell death of *Arabidopsis* hypocotyls. *Cell Research* 18, 949-960

118 Joo, J.H.*, et al.* (2005) Different signaling and cell death roles of heterotrimeric G protein alpha and beta subunits in the arabidopsis oxidative stress response to ozone. *Plant Cell* 17, 957-970

119 Iwata, Y. and Koizumi, N. (2005) An *Arabidopsis* transcription factor, AtbZIP60, regulates the endoplasmic reticulum stress response in a manner unique to plants. *Proc Natl Acad Sci U S A* 102, 5280-5285

120 Yamamoto, M.*, et al.* (2008) *Arabidopsis thaliana* Has a Set of J Proteins in the Endoplasmic Reticulum that are Conserved from Yeast to Animals and Plants. *Plant and Cell Physiology* 49, 1547-1562

121 Wang, D.*, et al.* (2005) Induction of protein secretory pathway is required for systemic acquired resistance. *Science* 308, 1036-1040

122 Yoshida, H.*, et al.* (2001) XBP1 mRNA is induced by ATF6 and spliced by IRE1 in response to ER stress to produce a highly active transcription factor. *Cell* 107, 881-891

123 Pandey, S.*, et al.* (2008) Regulation of root-wave response by extra large and conventional G proteins in *Arabidopsis thaliana*. *Plant Journal* 55, 311-322

124 Mudgil, Y.*, et al.* (2009) *Arabidopsis* N-MYC DOWNREGULATED-LIKE1, a Positive Regulator of Auxin Transport in a G Protein-Mediated Pathway. *Plant Cell* 21, 3591-3609

125 Verbelen, J.*, et al.* (2006) The Root Apex of *Arabidopsis thaliana* Consists of Four Distinct Zones of Growth Activities. *plant signaling and behavior 1,* 296–304.

126 Lerouxel, O.*, et al.* (2006) Biosynthesis of plant cell wall polysaccharides - a complex process. *Current Opinion in Plant Biology* 9, 621-630

127 Hamm, H.E. (1998) The many faces of G protein signaling. *Journal of Biological Chemistry* 273, 669-672

128 Shen, X.H.*, et al.* (2005) Genetic interactions due to constitutive and inducible gene regulation mediated by the unfolded protein response in *C-elegans*. *Plos Genetics* 1, 355-368

129 Kaufman, R.J. (1999) Stress signaling from the lumen of the endoplasmic reticulum: coordination of gene transcriptional and translational controls. *Genes & Development* 13, 1211-1233

130 Nakagawa, T.*, et al.* (2007) Development of series of gateway binary vectors, pGWBs, for realizing efficient construction of fusion genes for plant transformation. *Journal of Bioscience and Bioengineering* 104, 34-41

131 Earley, K.W.*, et al.* (2006) Gateway-compatible vectors for plant functional genomics and proteomics. *Plant Journal* 45, 616-629

132 Clough, S.J. and Bent, A.F. (1998) Floral dip: a simplified method for Agrobacterium-mediated transformation of *Arabidopsis thaliana*. *Plant J* 16, 735-743

133 Bertolotti, A.*, et al.* (2000) Dynamic interaction of BiP and ER stress transducers in the unfolded-protein response. *Nat Cell Biol* 2, 326-332

134 Kimata, Y.*, et al.* (2003) Genetic evidence for a role of BiP/Kar2 that regulates Ire1 in response to accumulation of unfolded proteins. *Mol Biol Cell* 14, 2559-2569

135 Credle, J.J.*, et al.* (2005) On the mechanism of sensing unfolded protein in the endoplasmic reticulum. *Proc Natl Acad Sci U S A* 102, 18773-18784

136 Mori, K.*, et al.* (1993) A transmembrane protein with a cdc2+/CDC28-related kinase activity is required for signaling from the ER to the nucleus. *Cell* 74, 743-756

137 Marciniak, S.J. and Ron, D. (2006) Endoplasmic reticulum stress signaling in disease. *Physiol Rev* 86, 1133-1149

138 Dharmasiri, N.*, et al.* (2005) The F-box protein TIR1 is an auxin receptor. *Nature* 435, 441-445

139 Gray, W.M.*, et al.* (1999) Identification of an SCF ubiquitin-ligase complex required for auxin response in *Arabidopsis thaliana*. *Genes Dev* 13, 1678-1691

140 Kepinski, S. and Leyser, O. (2005) The *Arabidopsis* F-box protein TIR1 is an auxin receptor. *Nature* 435, 446-451

141 Gray, W.M.*, et al.* (2001) Auxin regulates SCF(TIR1)-dependent degradation of AUX/IAA proteins. *Nature* 414, 271-276

142 Ulmasov, T.*, et al.* (1997) ARF1, a transcription factor that binds to auxin response elements. *Science* 276, 1865-1868

143 Petrasek, J.*, et al.* (2006) PIN proteins perform a rate-limiting function in cellular auxin efflux. *Science* 312, 914-918

144 Wisniewska, J.*, et al.* (2006) Polar PIN localization directs auxin flow in plants. *Science* 312, 883

145 Mravec, J.*, et al.* (2009) Subcellular homeostasis of phytohormone auxin is mediated by the ER-localized PIN5 transporter. *Nature* 459, 1136-1140

146 Ding, Z.*, et al.* (2012) ER-localized auxin transporter PIN8 regulates auxin homeostasis and male gametophyte development in *Arabidopsis*. *Nat Commun* 3, 941

147 Dal Bosco, C.*, et al.* (2012) The endoplasmic reticulum localized PIN8 is a pollen-specific auxin carrier involved in intracellular auxin homeostasis. *The Plant journal : for cell and molecular biology* 71, 860-870

148 Barbez, E.*, et al.* (2012) A novel putative auxin carrier family regulates intracellular auxin homeostasis in plants. *Nature* 485, 119-122

149 Friml, J. and Jones, A.R. (2010) Endoplasmic reticulum: the rising compartment in auxin biology. *Plant Physiol* 154, 458-462

150 Kamauchi, S.*, et al.* (2005) Gene expression in response to endoplasmic reticulum stress in *Arabidopsis thaliana*. *FEBS J* 272, 3461-3476

151 Brunoud, G.*, et al.* (2012) A novel sensor to map auxin response and distribution at high spatio-temporal resolution. *Nature* 482, 103-106

152 Chang, C.*, et al.* (1993) *Arabidopsis* ethylene-response gene ETR1: similarity of product to two-component regulators. *Science* 262, 539-544

153 Wulfetange, K.*, et al.* (2011) The cytokinin receptors of *Arabidopsis* are located mainly to the endoplasmic reticulum. *Plant physiology* 156, 1808-1818

154 Ma, L.*, et al.* (2007) Perinuclear and nuclear envelope localizations of *Arabidopsis* Ran proteins. *Plant cell reports* 26, 1373-1382

155 Kierzkowski, D.*, et al.* (2009) The *Arabidopsis* CBP20 targets the cap-binding complex to the nucleus, and is stabilized by CBP80. *The Plant journal : for cell and molecular biology* 59, 814-825

156 Kanneganti, T.D.*, et al.* (2007) A functional genetic assay for nuclear trafficking in plants. *The Plant journal : for cell and molecular biology* 50, 149-158

157 Ahmed, S.U.*, et al.* (1997) Cloning and subcellular location of an *Arabidopsis* receptor-like protein that shares common features with protein-sorting receptors of eukaryotic cells. *Plant physiology* 114, 325-336

158 Law, A.H.*, et al.* (2012) Secretory carrier membrane proteins. *Protoplasma* 249, 269-283

159 Friml, J.*, et al.* (2003) Efflux-dependent auxin gradients establish the apical-basal axis of *Arabidopsis*. *Nature* 426, 147-153

160 Xu, T.*, et al.* (2010) Cell surface- and rho GTPase-based auxin signaling controls cellular interdigitation in *Arabidopsis*. *Cell* 143, 99-110

161 Zhao, Y., *et al.* (2001) A role for flavin monooxygenase-like enzymes in auxin biosynthesis. *Science*, 291, 306–309

162 Che, P.*, et al.* (2010) Signaling from the endoplasmic reticulum activates brassinosteroid signaling and promotes acclimation to stress in *Arabidopsis*. *Science signaling* 3, ra69

163 Takatsuki, A.*, et al.* (1971) Tunicamycin, a new antibiotic. I. Isolation and characterization of tunicamycin. *The Journal of antibiotics* 24, 215-223

164 Heifetz, A.*, et al.* (1979) Mechanism of action of tunicamycin on the UDP-GlcNAc:dolichyl-phosphate Glc-NAc-1-phosphate transferase. *Biochemistry* 18, 2186-2192

165 Keller, R.K.*, et al.* (1979) N-Acetylglucosamine- 1 -phosphate transferase from hen oviduct: solubilization, characterization, and inhibition by tunicamycin. *Biochemistry* 18, 3946-3952

166 Acosta-Alvear, D.*, et al.* (2007) XBP1 controls diverse cell type- and condition-specific transcriptional regulatory networks. *Mol Cell* 27, 53-66

167 Iwata, Y. and Koizumi, N. (2005) An *Arabidopsis* transcription factor, AtbZIP60, regulates the endoplasmic reticulum stress response in a manner unique to plants. *Proc Natl Acad Sci U S A* 102, 5280-5285